Lab. v. Scheepsbouwkunde
Technische Hogeschool
Delft

Principles of propulsion and its optimization in incompressible and inviscid fluids

J.A. Sparenberg

Uitgave: september 1977

Prijs: f 9,00

Principles of propulsion and its optimization in incompressible and inviscid fluids

J.A. Sparenberg

Acknowledgement:

Ir. M. Kuipers and Ir. A.I. Wiersma read all of the manuscript, Ir. W.G. Frederiks and Dr.Ir. G.H. Schmidt parts of it. Their remarks improved substantially the presentation. Miss T.E. Stuit took care of the typing in an expert way.

Contents

1. Introduction 1
2. Mean forces and moments in relation with shed vorticity 3
3. Equations of motion with external force fields 8
4. Relation between external forces and their induced pressure fields 11
5. Relation between external forces and their induced velocity fields 15
6. The singular force in the direction of its motion 18
7. The singular force perpendicular to the direction of its motion 21
8. On the concept bound vorticity of a wing 25
9. A bound vortex "ending" at a rigid plate 28
10. The actuator surface 32
11. The circular flat actuator disk 37
12. Rotating vortex model of actuator disk 41
13. Some remarks on actuator disk theory 44
14. The ship screw, general considerations 46
15. The geometry of a ship screw 48
16. The screw blade with thickness and without loading 53
17. The velocity field induced by a rotating force 56
18. The screw blade of zero thickness with prescribed load, a) 61
19. The screw blade of zero thickness with prescribed load, b) 72
20. Some additional remarks 76
21. Unsteady propulsion 80
22. Small amplitude, two dimensional propulsion 84
23. The solution of the Hilbert problem 88
24. The simple time harmonic motion 93
25. Some additional remarks 97
26. Thrust production by energy extraction 99
27. Optimization theory, general considerations 103
28. Lifting surface systems, linear theory (regime i) 106
29. The variational problem for lifting surface systems 109
30. Necessary condition for the optimum 112
31. Optimum ducted screw propellers 115
32. The boundary value problem for the potential 119
33. Bound vorticity on blades and shroud 122
34. The efficiency of optimum ducted propellers 125
35. Numerical data, quality factor 128
36. The optimization of a sail of a yacht 132
37. Class of lifting surface systems 137

38. The ideal propeller 139
39. On a semilinear optimization theory 143
40. Two examples 146
41. Existence of optimum propellers 151

References 155

1. Introduction

In these notes we consider propulsion in an inviscid and incompressible fluid. We discuss mainly propellers which exert forces on the fluid by lift such as the screw propeller, the swimming plate and the sails of a yacht. Because we neglect viscosity this subject belongs to applied potential theory. We will direct our attention to principles, hence we do not claim the results to be applicable directly to practice.

The principle tool in the first part of the work is the velocity field induced by an external force moving in an arbitrary way through the fluid. This is from a theoretical point of view a satisfactory approach because vorticity is induced in the fluid by the rotation of the external force field, hence it is not necessary to consider the limiting case of vanishing viscosity. The concept of external force field is also useful for a description of the actuator disk model of a screw propeller. In the non linear case this model still defies a theoretical description of the flow at its edge.

The second part of these notes is concerned with optimization theory of lifting surface systems. By a simple application of the calculus of variations, necessary conditions for smallest induced resistance are found. The existence of optimum propellers in a class of admitted ones is still not quite known and further research is desirable on this subject.

In general the theories we discuss are linearized, by which we can carry on the analysis further than is possible in non linear theories. However with respect to optimization some semi-linear results are given among others about the screw propeller mounted on a large hub of finite length.

We do not discuss slender body propulsion which is important in bio-mechanical theories on the swimming of fishes. For this we refer to the survey given in [30].

It is assumed that the reader has already a working knowledge of hydrodynamics and is aquainted for instance with Bernoulli's law for instationary flow, the suction force at the leading edge of a wing, the linearization of a flow around a thin wing, the lifting line theory and other basic ideas.

The exercises given at the end of a number of sections are not meant in general to be solved by mathematics, often they are intended to stimulate thinking about the subject.

At last we remark that it is important to be conscious of the many approximations made in our considerations, we mention the linearizations and the neglect of viscosity. It is worth while to try to estimate to which extent the results are still valid in realistic situations.

2. Mean forces and moments in relation with shed vorticity.

There is a tight connection between the production of a force action on a fluid by a body and its shedding of vorticity. This will be discussed in this section.

Consider a body, possibly flexible, of finite extent moving with some mean velocity through an inviscid and incompressible fluid. The motion of the body will be periodic with respect to a reference frame translating with the mean velocity of the body. It is assumed that the motion started infinitely long ago. A well observed fact is that in general the body leaves behind vorticity in the fluid. Examples are the trailing vortex sheets behind an airplanewing or behind a screw propeller of a ship. In the first part of this section we will show that when a body exerts a non zero mean force on the fluid it inevitably has to shed vorticity. An analogous statement is proved for one of the components of the couple exerted by the body on the fluid. The addition "of finite extent" in the first sentence of this paragraph is essential as will be seen in the second part of this section where the two dimensional case is considered.

We will use a Cartesian coordinate system (x,y,z) with respect to which the undisturbed fluid at infinity is at rest. The body B will move with a mean velocity of advance U in the positive x direction and repeats its velocities after each time period τ or after each covered distance

$$b = U\,\tau \quad , \tag{2.1}$$

in the positive x direction.

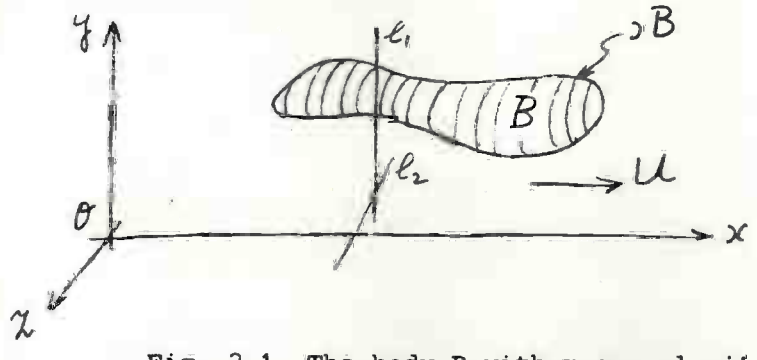

Fig. 2.1. The body B with mean velocity U.

If the fluid motion is irrotational and without divergence, its velocity field $\vec{v}$ can be derived from a potential function $\Phi=\Phi(x,y,z,t)$

$$\vec{v} = (u,v,w) = \operatorname{grad} \Phi \tag{2.2}$$

with

$$\Delta \Phi = \left(\frac{\partial^2}{\partial x^2} + \frac{\partial^2}{\partial y^2} + \frac{\partial^2}{\partial z^2}\right)\Phi = 0 \qquad (2.3)$$

We assume that no vorticity is shed by the moving body B and then show that no non zero mean forces can be exerted on the fluid by B. In this case Φ is defined in the whole space outside B. When the velocities induced by the body tend to zero sufficiently fast at large distances R of the body, the force $\vec{F}(t)$ exerted by the fluid on B, which is the opposite of the force exerted by B on the fluid, has the value ([12], page 349)

$$\vec{F}(t) = \mu \frac{d}{dt} \int_{\partial} \int_{B} \Phi \, \vec{n} \, d S \qquad (2.4)$$

where μ is the density of the fluid, ∂B is the boundary of B, d S an element of area and $\vec{n} = (n_x, n_y, n_z)$ the local outward normal on ∂B. In [12] this formula is derived for a moving rigid body, but it is easily seen to be true also for a deformable body. In the latter case also the velocities tend to zero sufficiently fast for large values of R, $|\vec{v}| \approx O(R^{-2})$, which occurs in the case of a temporarily expanding body.

The mean value of $\vec{F}(t)$ over one period τ of time becomes

$$\frac{1}{\tau} \int_{t}^{t+\tau} \vec{F}(t) dt = \frac{\mu}{\tau} \iint_{\partial B} \{\Phi(x+b,y,z,t+\tau)\vec{n}(x+b,y,z,t+\tau) +$$

$$- \Phi(x,y,z,t)\vec{n}(x,y,z,t)\} \, d S. \qquad (2.5)$$

The velocities of the fluid at times t and $t+\tau$ are the same for the points (x,y,z) and $(x+b,y,z)$. Hence the difference of the potential for the different values of place and time can be only a constant c, then

$$\frac{1}{\tau} \int_{t}^{t+\tau} \vec{F}(t) dt = \frac{\mu c}{\tau} \int_{\partial} \int_{B} \vec{n} \, d S = 0 \quad . \qquad (2.6)$$

From (2.6) we find that a body of finite extent, moving periodically cannot experience a force with a non zero mean value without shedding vorticity. Inversely, by the principle of action = reaction, such a body cannot exert a mean force on the fluid without leaving behind vorticity. Hence it cannot act as a lift producing wing or a thrust producing propeller. When voricity is shed periodically, the function Φ is not defined in the whole space and (2.4) is not valid, so that the foregoing argument does not hold. Because the velocity field belonging to the shed vorticity represents kinetic energy, we can state that when a body of finite extent exerts a mean force on the fluid this is inevitably accompagnied by energy losses.

The moment with respect to the fixed origin O, exerted by the fluid on the body B of finite extent can be written as ([12], page 350),

$$\vec{M} = \mu \frac{d}{dt} \iint_{\partial B} \Phi . \{\vec{r} * \vec{n}\} \, d S \qquad (2.7)$$

where $\vec{r}$ is the vector from O to the surface element d S. Equation (2.7) is valid when no vorticity is shed. Hence the mean value of the moment with respect to the x axis becomes

$$\frac{\vec{e}_x}{\tau} . \int_0^\tau \vec{M}(t)dt = \frac{\mu}{\tau} \vec{e}_x . \iint_{\partial B} \Phi(x+b,y,z,t+\tau)\{(\vec{r}(x,y,z,t)+b\vec{e}_x) * \vec{n}(x+b,y,z,t+\tau)\}d S - \frac{\mu}{\tau} \vec{e}_x . \iint_{\partial B} \Phi(x,y,z,t)\{\vec{r}(x,y,z,t) * \vec{n}(x,y,z,t)\}d S \qquad (2.8)$$

Because again the difference of the potentials can be only a constant c we find

$$\frac{\vec{e}_x}{\tau} . \int_0^\tau \vec{M} \, d t = \frac{\mu c}{\tau} \iint_{\partial B} (y \, n_z - z \, n_y) \, d S = 0 \quad . \qquad (2.9)$$

We can consider also moments with respect to lines ℓ_1 and ℓ_2, for instance parallel to the y and z axis respectively, which are translated in the positive x direction with a velocity U (Fig. 2.1.). It can be easily seen that moments about these lines need not have zero mean values. Indeed there seems to be an essential difference between the moment about the x axis which is parallel to the mean direction of motion and those about ℓ_1 and ℓ_2 which are perpendicular to this direction. Consider a moment about ℓ_1. A fluid particle in front of B will obtain a velocity in some direction, however when B has passed it is conceivable the same moment will try to give the particle a velocity in the oppposite direction. These effects counter act each other. The same holds for a moment about the line ℓ_2. However when a moment with a non zero mean value is exerted about the x axis, it always has the same influence on the fluid particles in front as well as behind B. This means such a moment could induce a rotational motion of the fluid around the x axis, hence vorticity would be shed. Because this was excluded such a moment with a non zero mean value is not likely to exist. An example is a thrust producing stationary rotating screw propeller advancing through a fluid at rest in a direction parallel to the axis of rotation of the propeller. Then we have both a force in the direction of the x axis and a mo-

ment around it, hence by two reasons vorticity has to be shed.

The two dimensional case is different from the three dimensional one. In fact it can be considered as a three dimensional problem in which the velocities are, for instance, independent of the z coordinate, hence they do not tend to zero at infinity as was required in the foregoing. For instance a two dimensional wing can have a lift force per unit of length without shedding vorticity. Stated otherwise the tip vortices of such a wing are at infinity, outside the field of vision.

For the time dependent force F per unit length of span (z direction) exerted by the fluid on the profile, the following formula ([12], page 282) holds

$$F(t) = i\,\mu \frac{d}{dt} \int_{\partial B} \zeta \, d\, \Phi(x,y,t) \qquad (2.10)$$

where $\zeta = x+iy$, Φ is the real velocity potential,

$$F(t) = F_x(t) + i\, F_y(t) \qquad (2.11)$$

F_x and F_y are the components of F in the x and the y direction, i is the imaginary unit and ∂B the contour of the profile, passed through in anti-clockwise direction.

Formula (2.10) is valid when the velocities tend to zero with large distances R as $O(R^{-1})$ in the two dimensional complex plane. This happens when no free vorticity is shed by the profile. From (2.10) and (2.11) we find for the mean value of F(t) over one period τ of time

$$\frac{1}{\tau} \int_t^{t+\tau} F(t)dt = \frac{1}{\tau} \int_t^{t+\tau} (F_x(t) + i\, F_y(t))\, dt =$$

$$= \frac{i\mu}{\tau} \int_{\partial B} \{(\zeta+b)\, d\, \Phi(x+b,y,t+\tau) - \zeta\, d\, \Phi(x,y,z,t)\} =$$

$$= \frac{i\,\mu\, b}{\tau} \int_{\partial B} d\, \Phi(x,y,t) = \frac{i\,\mu\, b}{\tau}\, \Gamma, \qquad (2.12)$$

where, because $\Phi(x,y,t)$ is real the circulation Γ around the profile is real. From (2.12) we find

$$\frac{1}{\tau} \int_t^{t+\tau} F_x(t)\, dt = 0 \qquad (2.13)$$

Hence we have the result, when a periodically moving two dimensional body does not leave behind free vorticity, it cannot exert a mean force in the mean direction of its motion.

Exercise.

Discuss that a body of finite extent moving periodically in the direction of the x axis with mean velocity U, can exert moments around ℓ_1 or ℓ_2 (as defined above) with non zero mean value, without shedding vorticity.

3. Equations of motion with external force fields.

We consider the equations which describe the motion of an inviscid and incompressible fluid with respect to an inertial Cartesian frame of reference (x,y,z). These read ([12], page 8)

$$\frac{d\vec{v}}{dt} = \frac{\partial \vec{v}}{\partial t} + (\vec{v}, \text{grad})\vec{v} = -\frac{1}{\mu} \text{ grad } p + \frac{1}{\mu}\vec{F} \quad , \tag{3.1}$$

$$\text{div } \vec{v} = 0 \quad , \tag{3.2}$$

where $\vec{F}(x,y,z,t)$ is an external force per unit of volume, acting on the fluid. Here and in the following we assume that the field of flow exists and is uniquely determined by suitably chosen initial or other conditions.

First consider a force field

$$\vec{F} = \text{grad } \Psi \ (x,y,z,t) \quad , \ t > 0 \quad , \tag{3.3}$$

where Ψ is some sufficiently smooth scalar function and assume at $t = 0$, $v \equiv 0$. Then we can satisfy (3.1) and (3.2) by

$$p = \Psi \ (x,y,z,t) \quad ; \ \vec{v} \equiv 0 \quad , \quad t > 0 \quad . \tag{3.4}$$

Hence such a force field does not induce any motion in the fluid. In general only force fields will be of interest for which rot $\vec{F} \neq 0$.

Next consider two force fields $\vec{F}_1(x,y,z,t)$ and $\vec{F}_2(x,y,z,t)$ to which belong the pressure fields and velocity fields $(p_1,\vec{v}_1)$ and $(p_2,\vec{v}_2)$ respectively. The velocity fields are assumed to satisfy the same initial conditions at $t = 0$. The question can be posed, when do we have

$$\vec{v}_1(x,y,z,t) = \vec{v}_2(x,y,z,t) \quad . \tag{3.5}$$

The answer is of course closely related to (3.3) and (3.4), in fact when

$$\vec{F}_1(x,y,z,t) - \vec{F}_2(x,y,z,t) = \text{grad } \Psi \ (x,y,z,t) \quad , \tag{3.6}$$

this will happen. Then by

$$p_2 = p_1 - \Psi \ , \tag{3.7}$$

the righthand side of (3.1) in both cases will be the same and hence (3.5) is valid.

With respect to theories where vorticity is created in an inviscid fluid, external force fields are very useful. Indeed in domains where the rotation of the force field is not zero, in a natural way rotation of the motion of the inviscid fluid hence vorticity, is induced. We write (3.1) in the form

$$-\frac{\partial \vec{v}}{\partial t} + \vec{v} * \vec{\omega} = -\frac{1}{\mu}\vec{F} + \text{grad}\,(\tfrac{1}{2}|\vec{v}|^2 + \frac{p}{\mu}) \ , \tag{3.8}$$

where $\vec{\omega} = \text{rot}\ \vec{v}$. Application of the operation rot to both sides, yields

$$-\frac{\partial \vec{\omega}}{\partial t} + \text{rot}\,(\vec{v} * \vec{\omega}) = -\frac{1}{\mu}\,\text{rot}\,\vec{F} \ , \tag{3.9}$$

From (3.9) it follows, when $\text{rot}\ \vec{F} \neq 0$ then $\vec{\omega} \neq 0$.

Consider a closed contour C in the fluid and coupled to the particles, hence it is transported by the velocity field. At some time instant we calculate the circulation Γ of C, defined by the integral

$$\Gamma = \int_C \vec{v} \cdot d\vec{s} \ , \tag{3.10}$$

where the integration is taken around C and $d\vec{s}$ is an element of length. We determine

$$\frac{d\Gamma}{dt} = \int_C \frac{d\vec{v}}{dt} \cdot d\vec{s} + \int_C \vec{v} \cdot \frac{d}{dt} d\vec{s} \ . \tag{3.11}$$

It is well known ([3], page 20) that the second integral vanishes. The first integral can by (3.1), be written as

$$\int_C (-\frac{1}{\mu}\,\text{grad}\ p + \frac{1}{\mu}\vec{F}) \cdot d\vec{s} = \frac{1}{\mu}\int_C \vec{F} \cdot d\vec{s} \ . \tag{3.12}$$

Hence we have the result

$$\frac{d\Gamma}{dt} = \frac{1}{\mu} \int_C \vec{F} \cdot \vec{ds} \ . \qquad (3.13)$$

Analogous results are valid with respect to the linearized version of the equation of motion (3.1), which reads

$$\frac{\partial \vec{v}}{\partial t} = - \frac{1}{\mu} \ \text{grad} \ p + \frac{1}{\mu} \vec{F} \ . \qquad (3.14)$$

Assume again that $v \equiv 0$ at $t = 0$. We suppose that the external force field $\vec{F}$ is $0(\varepsilon)$, where ε is a small parameter. By this it is reasonable to assume that also the pressure p and the components of the vlocity $\vec{v}$ and their derivatives are $0(\varepsilon)$, then in (3.14) we have neglected quantities of $0(\varepsilon^2)$ with respect to quantities of $0(\varepsilon)$.

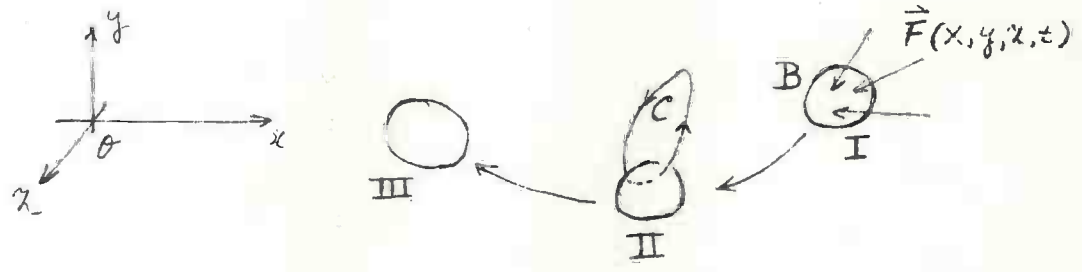

Fig. 3.1. Moving force field $\vec{F}$ and fixed contour C.

Equation (3.13) is now correct for a contour C fixed in space. It can be used to check in a linearized theory if vorticity is left behind in the fluid by a force field $\vec{F}(x,y,z,t)$, confined to a moving finite region B (figure 3.1).

Suppose that the circulation of the "probing contour" C is zero when the force field is in position I. Then in general it becomes non zero when C cuts the force region B (position II). When B moves on, it has no longer contact with C hence the circulation remains constant (position III). In this way we can check by using different kinds of contours C, if vorticity has been shed by $\vec{F}(x,y,z,t)$.

Exercise.

Use the method of the "probing contour" to show that behind an infinitely thin wing of finite span which moves stationary in an inviscid and incompressible fluid and delivers lift, trailing vorticity occurs. Replace the wing by an external force field which is concentrated on the wing and has a strength per unit area equal to the pressure jump across the wing.

4. Relation between external forces and their induced pressure fields.

We consider again the equation of motion in the form (3.8), and apply the operation div to it. The by (3,2) we find

$$\Delta\left(\frac{p}{\mu} + \tfrac{1}{2}|\vec{v}|^2\right) = \frac{1}{\mu}\,\mathrm{div}\ \vec{F}. \tag{4.1}$$

When we consider a region of space where the fluid particles have not entered or passed through any force field, for this region we have $\vec{F} = 0$ and $\vec{\omega} = 0$, then it follows from (4.1), that

$$\Delta p \leq 0. \tag{4.2}$$

Hence p is a superharmonic function outside the force region. It seems difficult to give more explicit general properties of p in this non linear case.

When we use the linearized version of the equation of motion (3.10), equation (4.1) changes into

$$\Delta p = \mathrm{div}\ \vec{F}, \tag{4.3}$$

hence there is a direct relationship between p and $\vec{F}$. Outside the force field p is a harmonic function.

We will consider the linearized case more closely for $\vec{F}$ being a singular force field concentrated in a point Q. It is clear that for such a field the linearized equations of motion do not hold in the neighbourhood of Q where the induced velocities become very large. However, the result can be used as a Green function in an integration procedure. By this the velocities can again become small so that the result will be a good approximation of the exact solution of the non-linear equations.

The point of application Q of the singular force field moves in some prescribed way

$$Q \equiv x = \xi(t),\ y = \eta(t),\ z = \zeta(t), \tag{4.4}$$

where ξ, η and ζ are sufficiently smooth functions of time. The velocity $\vec{V}$ of the point Q becomes

$$\vec{V} = (\dot{\xi}(t),\ \dot{\eta}(t),\ \dot{\zeta}(t)), \quad V = |\vec{V}| = (\dot{\xi}^2 + \dot{\eta}^2 + \dot{\zeta}^2)^{\frac{1}{2}}, \tag{4.5}$$

we assume that $V \geq \tilde{V} > 0$, where $\tilde{V}$ is some number.

The components of the singular force field are functions of time, hence

$$\vec{F}(x,y,z,t) = \vec{f}(t) \cdot \delta(x - \xi(t))\ \delta(y - \eta(t))\ \delta(z - \zeta(t)), \tag{4.6}$$

where $\delta(x)$ is the delta function of Dirac, $\vec{f}(t)$ will be called the singular force applied at Q with

$$\vec{f}(t) = (f_x(t),\ f_y(t),\ f_z(t)), \quad f = |\vec{f}| = (f_x^2 + f_y^2 + f_z^2)^{\frac{1}{2}}. \tag{4.7}$$

We consider first the pressure field at each moment t, caused by the x component of $\vec{F}$. Equation (4.3) becomes

$$\Delta p = f_x(t)\delta'(x - \xi(t))\ \delta(y - \eta(t))\ \delta(z - \zeta(t)), \tag{4.8}$$

where the Laplace operator acts on x, y and z. The solution of this equation can be derived simply from the solution of

$$\Delta q = -4\pi\ \delta(x - \xi(t))\ \delta(y - \eta(t))\ \delta(z - \zeta(t)), \tag{4.9}$$

which has the form

$$q = \{(x - \xi)^2 + (y - \eta)^2 + (z - \zeta)^2\}^{-\frac{1}{2}} \stackrel{\text{def}}{=} R^{-}. \tag{4.10}$$

By differentiation of (4.10) with respect to x we find the following solution of (4.8)

$$p = \frac{1}{4\pi} \frac{f_x(t)\ (x - \xi(t))}{R^3}, \tag{4.11}$$

where we have neglected a possible additive constant pressure p_∞. In the same way we can derive the pressure fields connected to the y and z components of $\vec{F}$. Because (4.3) is a linear equation we obtain, by superposition, for its solution

$$p = \frac{1}{4\pi} \frac{f_x(t)(x-\xi(t)) + f_y(t)(y-\eta(t)) + f_z(t)(z-\zeta(t))}{R^3} = \frac{1}{4\pi} \frac{\vec{f}(t)\cdot\vec{R}}{R^3}, \tag{4.12}$$

where

$$\vec{R} = ((x - \xi), (y - \eta), (z - \zeta)). \tag{4.13}$$

In potential theory the function (4.12) is called the field of a dipole, with its axis parallel to the force $\vec{f}$. Because here it represents a pressure field we will call it a pressure dipole field of strength $|\vec{f}|$. When we draw a picture of this field around the point Q of application at some distance from it, we obtain figure 4.1.

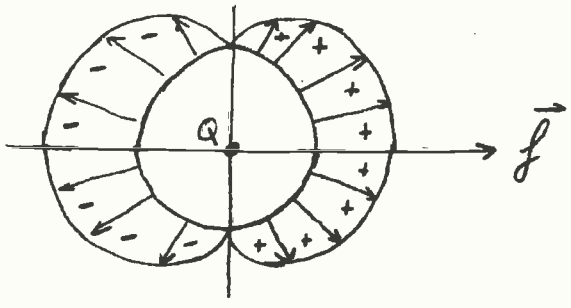

Fig. 4.1. The pressure field induced by a singular external force $\vec{f}$.

The pressures are plotted radially, the length of each radius denotes the pressure at the point of the circle.Regions indicated by a "+" ("-") have a positive (negative) disturbance pressure.

It may be remarked that as a result of our approximations (incompressibility, no viscosity, linearization) this pressure field depends only on the momentary vector $\vec{f}$ and on the point of application, hence not on the past. This means that as soon as the external force field has been switched off the pressures will have vanished everywhere, although as will become clear later on the velocities are not zero in general. In connection with (3.10) we find that when in a linearized theory the external force field has disappeared, hence also the pressure field, we have

$$\frac{\partial \vec{v}}{\partial t} = 0, \tag{4.14}$$

in words, the velocity field has become independent of time.

Exercises.

1. Show that $\Delta|\vec{v}|^2 \geq 0$, (4.1).

2. Discusss that the last paragraph of this section only applies to an unbounded fluid. When for instance a body moves freely in it or when an elastic plate is present (4.14) is no longer true when the force field has disappeared.

5. Relation between external forces and their induced velocity fields.

We consider again the linearized equations of motion and determine the velocity field belonging to a singular force moving through space. Outside the region of space through which the force has passed and where we assume rot $\vec{v} = 0$, the equation of motion (3.10) with (4.12) yields

$$\frac{\partial \vec{v}}{\partial t} = \frac{-1}{4\pi\mu} \operatorname{grad} \left(\frac{\vec{f}(t) \cdot \vec{R}}{R^3} \right) \tag{5.1}$$

Introducing for this region a velocity potential with $\vec{v} = \operatorname{grad} \Phi$ and integrating with respect to time, we find

$$\Phi(x, y, z, t) = -\frac{1}{4\pi\mu} \int_0^t \frac{\vec{f}(t) \cdot \vec{R}}{R^3} \, dt, \tag{5.2}$$

where $\vec{R}$ is given by (4,13) and (4.14). We supposed in (5.2) that

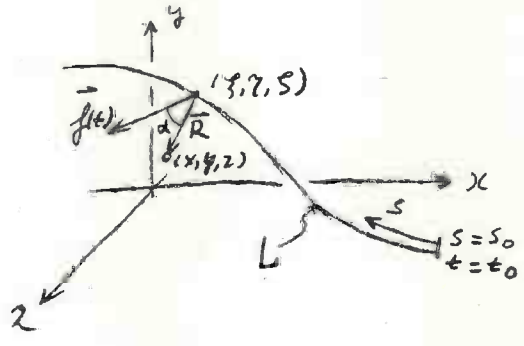

Fig. 5.1. The force $\vec{f}(t)$ moving along the line L

the velocity field is zero at $t = t_0$ and that the force has been switched on at $t = t_0$. For $t > t_0$ the force is moving along the line $L = (x = \xi(t), y = \eta(t), z = \zeta(t))$. Along L we introduce a length parameter s. Hence by our assumption $V \geq \tilde{V} > 0$ (below (4.5)) it is possible to write

$$s = s(t), \quad t = t(s), \quad s_0 = s(t_0) \tag{5.3}$$

Then (5.2) can be put into the form

$$\Phi(x, y, z, t) = -\frac{1}{4\pi\mu} \int_{s_0}^{s(t)} \frac{\vec{f}(s)}{V(s)} \cdot \frac{\vec{R}}{R^3} \, ds. \tag{5.4}$$

The velocity which follows from (5.4) is

$$\vec{v} = \text{grad } \Phi = -\frac{1}{4\pi\mu} \int_{s_o}^{s(t)} \{\frac{\vec{f}(s)}{V(s)\ R^3} - 3\ \frac{\vec{R}\ \ (\vec{f}(s)\cdot\vec{R})}{V(s)\ \ R^5}\}\, ds. \qquad (5.5)$$

This result will now be interpreted in terms of vorticity. We consider a "small" flat ring vortex of area dS and strengh Γ at the point (ξ, η, ζ). The direction of the vorticity is coupled with a

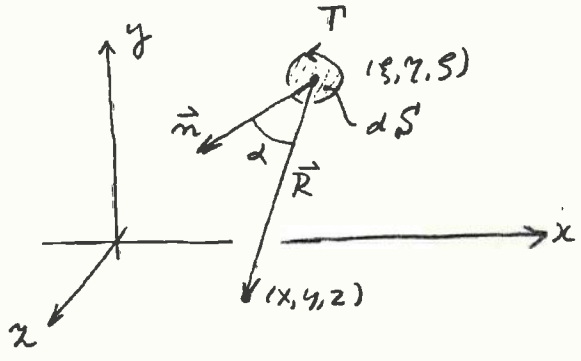

Fig. 5.2. "Small" ring vortex

right hand screw to its locally induced velocities. We erect at the centre of Γ the unit normal $\vec{n}$, related to Γ by a right hand screw (figure 5.2). It is well known ([12], page 170), that the potential $d\tilde{\Phi}(x, y, z, t)$ of this small vortex has the value

$$d\tilde{\Phi} = -\frac{\Gamma}{4\pi}\ \frac{\vec{n}\cdot\vec{R}}{R^3}\, dS = -\frac{\Gamma}{4\pi}\ \frac{\cos\alpha}{R^2}\, dS, \qquad (5.6)$$

where α is the angle between $\vec{n}$ and $\vec{R}$. From this it follows that we can consider (5.4) as a super position of ring vortices around the line L enclosing an area dS, perpendicular to $\vec{f}(s)$, connected with a right hand screw to the direction of $\vec{f}$ and of strength

$$\Gamma = \frac{1}{\mu}\ \frac{|\vec{f}|}{V(s)}\ \frac{ds}{dS}, \qquad (5.7)$$

More precisely we have to consider the limit $dS \to 0$ for the velocity potential induced by these ring vortices in order to obtain the velocity potential induced by the moving force field (4.6).

Now we can split the vector $\vec{f}$ uniquely into two parts

$$\vec{f}(t) = \vec{g}(t) + \vec{h}(t) \tag{5.8}$$

where $\vec{g}(t)$ is tangent to L and $\vec{h}(t)$ is perpendicular to L, hence

$$\vec{g}(t) = \lambda(t)\ \vec{V}(t) \tag{5.9}$$

and

$$\vec{h}(t) \cdot \vec{V}(t) = 0. \tag{5.10}$$

where $\lambda(t)$ in a scalar function.

Because our theory is linear we can add the velocities induced by these moving forces. In the next two sections we will discuss separately $\vec{g}(t)$ and $\vec{h}(t)$.

6. The singular force in the direction of its motion.

In the case of a singular force in the direction of its motion we write (5.4) as

$$\Phi(x,y,z,t) = -\frac{1}{4\pi\mu}\int_{s_o}^{s}\frac{g(s)}{V(s)}\frac{\cos\alpha}{R^2}\,ds\,, \qquad g(s) = |\vec{g}(s)|\,. \tag{6.1}$$

Because we are interested in propulsion, hence in forces exerted on the fluid in the opposite direction of the velocity $\vec{V}$ (4.5), we reckon $g(s)$ to be positive in the negative s direction. The angle α in (6.1) is defined as the angle between the tangent to L pointing in the negative s direction and $\vec{R}$.

We can now rewrite (6.1) as

$$\Phi = +\frac{1}{4\pi\mu}\int_{s_o}^{s}\frac{g(s)}{V(s)}\frac{d}{ds}\left(\frac{1}{R}\right)ds\,. \tag{6.2}$$

By partial integration we obtain

$$\Phi = \frac{1}{4\pi\mu}\left(\frac{g(s)}{V(s)}\frac{1}{R(s)} - \frac{g(s_o)}{V(s_o)R(s_o)} - \int_{s_o}^{s}\frac{1}{R}\frac{d}{ds}\left(\frac{g(s)}{V(s)}\right)ds\right). \tag{6.3}$$

This formula can be given a simple interpretation. It is known that a source placed at a point (ξ,μ,ζ), which yields a unit volume of fluid per unit of time, has the velocity potential

$$-\frac{1}{4\pi R}\,. \tag{6.4}$$

Hence (6.3) has the following meaning. On the line L we have a source distribution of strength

$$\frac{1}{\mu}\frac{d}{ds}\frac{g(s)}{V(s)} = \frac{1}{\mu V(t)}\frac{d}{dt}\frac{g(t)}{V(t)}\,. \tag{6.5}$$

At the starting point $s = s_o$ we have a starting source of strength

$$\frac{g(s_o)}{\mu V(s_o)}\,, \tag{6.6}$$

at the point where the force acts we have a source of strength

$$-\frac{g(s)}{\mu V(s)}\,. \tag{6.7}$$

hence a sink. When the force is switched off at $t = t_e$, for $s = s_e$ there remains an ending source of strength (6.7) for $s = s_e$.

The velocity follows from (6.3) by

$$\vec{v} = \text{grad } \Phi = \frac{1}{4\pi\mu}\left[\frac{g(s)}{V(s)}\frac{\vec{R}(s)}{R^3(s)} + \frac{g(s_o)}{V(s_o)}\frac{\vec{R}(s_o)}{R^3(s_o)} + \int_{s_o}^{s}\frac{\vec{R}(s)}{R^3(s)}\frac{d}{ds}\left(\frac{g(s)}{V(s)}\right)ds\right] \quad (6.8)$$

The velocity potential Φ given by (6.1) or (6.3) is only valid for points (x,y,z) not on L. It seems that by the source distribution (6.5) along L and the starting and ending sources (6.6) and (6.7) the divergence of the flow is no longer zero, hence we would not satisfy (3.2). However the total divergence in the fluid is zero. This is proved by integrating (6.5) along L and adding to the result (6.6) and (6.7). What we have left out of consideration is the local flow inside the narrow vortex tube around L, which follows from the vortex interpretation given in section 5. Because the shape of the small vortex rings around L is irrelevant we choose them circular with radius b. Then we find from (5.6)

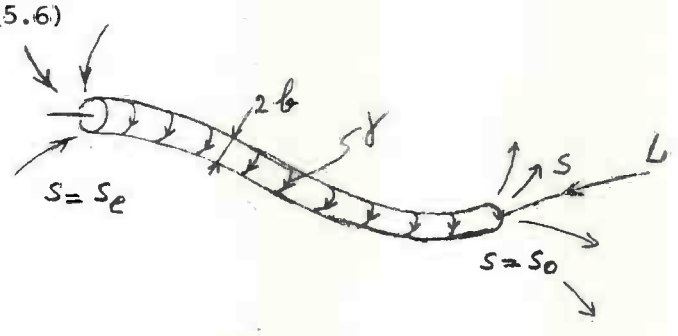

6.1 The line L surrounded by the "circular" cylinder

for the vortex strength of the tube per unit of length along L

$$\gamma(s) = \frac{1}{\pi\mu b^2}\frac{g(s)}{V(s)} \quad (6.9)$$

where $V(s) \geq \tilde{V} > 0$, (4.5). This vorticity $\gamma(s)$ is reckoned positive when it induces a flow in the negative s direction, hence when it is coupled with a right hand screw to the negative s direction. When $b \to o$ the velocities of the fluid inside the tube increase and become approximately $\tilde{v}(s) = \gamma(s)$ reckoned positive in the negative s direction. Hence the fluid transport inside the tube in the negative s direction becomes

$$\tilde{v}(s)\ \pi b^2 = \frac{g(s)}{\mu V(s)} \quad (6.10)$$

This singular mass transport along L clearly meet the sources (6.6) and (6.7) and the distribution (6.5) in such a way that no divergence of the flow occurs.

Exercise.

Show the "existence" of the "narrow" free vortex tube by the method mentioned at the end of section 3. The singular force can be spread out homogeneously over a small cylinder and the probing contour can be chosen as in figure 6.2.

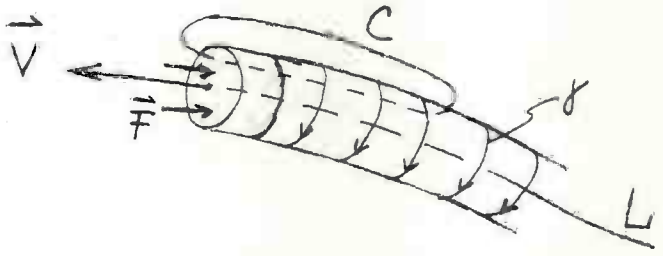

Fig. 6.2. Probing contour C and moving force field $\vec{F}$.

7. The singular force perpendicular to the direction of its motion

We now consider a singular force $\vec{h}$ perpendicular to its velocity $\vec{V}$. The induced velocity field is given by (5.5). We will also in this case discuss a different expression, which is much more complicated but gives an insight in the "vortex configuration" behind this singular force. This vortex distribution follows from the one behind a lifting line of varying intensity moving arbitrarily through space, by a limiting procedure.

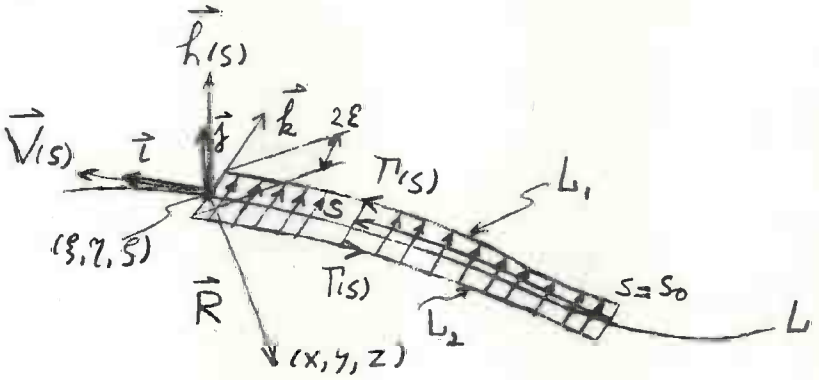

Fig. 7.1. Vortex representation of a moving force perpendicular to its velocity.

At the place where the force is acting we consider three mutual orthogonal unit vectors. The vector $\vec{i}$ tangent to L, the vector $\vec{j}$ along $\vec{h}$ and the vector $\vec{k}$ perpendicular to both, so that $\vec{i},\vec{j},\vec{h}$ form a right handed system. Then we "replace" the force $\vec{h}$ by a bound vortex of constant strength of length 2ε in the direction of $\vec{k}$. The strength of this bound vortex follows from the law of Joukowski

$$\mu \Gamma V 2\varepsilon = h = |\vec{h}|, \tag{7.1}$$

and because $\vec{h}$ is the force exerted on the fluid Γ is with a right hand screw in the negative $\vec{k}$ direction. In the neighbourhood of L we have two lines L_1 and L_2 which have the representation (4.4)

$$(\xi(s), \eta(s), \zeta(s)) \pm \varepsilon\vec{k}(s) , \tag{7.2}$$

where the + (-) sign belongs to L_1 (L_2).
Hence by the length parameter s on L we have also a parameter on L_1 and L_2, however this is no longer a length parameter.

Along L_1 we have a tip vortex of strength

$$\frac{h(s)}{\mu V(s)} \quad \frac{1}{2\varepsilon} \quad , \tag{7.3}$$

with a right hand screw in the +s direction and along L_2 we have a tip vortex of the same strength however in the -s direction. For $s = s_o$ we have a starting vortex of strength (7.3) in the $+\vec{k}$ direction. At last we have distributed vorticity along L in the $+\vec{k}$ direction of strength

$$\frac{1}{\mu} \left(\frac{d}{ds} \quad \frac{h(s)}{V(s)}\right) \quad \frac{1}{2\varepsilon} \quad , \tag{7.4}$$

per unit of length in the s direction. These four types of vorticity are such that, i) the desired force $\vec{h}(s)$ is induced and ii) the vortex field is free of divergence. We show that this vortex field in the limit $\varepsilon \to o$ induces the same velocity field as is given in (5.5).

In order to do this we need the law of Biot and Savart ([12] page 168), which states the following. Consider a line element

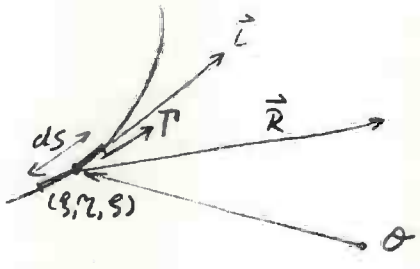

Fig. 7.2. Biot and Savarts law.

$ds\vec{i}$ around the point (ξ,η,ζ) where $\vec{i}$ is a unit vector, with a vortex of intensity Γ, coupled with a right hand screw to $\vec{i}$. This vortex element induces at the point (x,y,z) a velocity

$$\Delta\vec{v} \quad = \frac{\Gamma}{4\pi} \left(\vec{i} \times \frac{\vec{R}}{R^3}\right) ds. \tag{7.5}$$

By (7.5) the tip vortex along L_1 induces the velocity

$$\vec{v}_{L_1}(x,y,z,s_1) = \frac{1}{4\pi\mu} \quad \frac{1}{2\varepsilon} \quad \int_{s_o}^{s_1} \quad \frac{h(s)}{V(s)} \left\{ \frac{\left(\vec{i} + \varepsilon \frac{d\vec{k}}{ds}\right)}{\left|\vec{i} + \varepsilon \frac{d\vec{k}}{ds}\right|} \times \frac{\left(\vec{R} - \varepsilon\vec{k}\right)}{\left|\vec{R} - \varepsilon\vec{k}\right|^3} \right\} \left|\vec{i} + \frac{d\vec{k}}{ds}\right| ds, \tag{7.6}$$

at the point (x,y,z) while the force is at $s = s_1$. Analogously the tip vortex along L_2 induces the velocity at (x,y,z)

$$\vec{v}_{L_2}(x,y,z,s_1) = -\frac{1}{4\pi\mu}\,\frac{1}{2\varepsilon}\int_{s_0}^{s_1}\frac{h(s)}{V(s)}\left\{\frac{(\vec{i}-\varepsilon\frac{d\vec{k}}{ds})}{|i-\varepsilon\frac{d\vec{k}}{ds}|}\otimes\frac{(\vec{R}+\varepsilon\vec{k})}{|\vec{R}+\varepsilon\vec{k}|^3}\right\}\left|\vec{i}-\varepsilon\frac{d\vec{k}}{ds}\right|ds, \tag{7.7}$$

when the force is at $s = s_1$. In the limit $\varepsilon \to o$ we can write

$$\vec{v}_{L_1}+\vec{v}_{L_2}=\frac{1}{4\pi\mu}\int_{s_0}^{s_1}\frac{h(s)}{V(s)}\,\frac{d}{d\lambda}\left\{(\vec{i}+\lambda\frac{d\vec{k}}{ds})\otimes\frac{(\vec{R}-\lambda\vec{k}}{|\vec{R}-\lambda\vec{k}|^3}\right\}\Big|_{\lambda=o}ds. \tag{7.8}$$

Carrying out the differentiation yields

$$\vec{v}_{L_1}+\vec{v}_{L_2}=\frac{1}{4\pi\mu}\int_{s_0}^{s_1}\frac{h(s)}{V(s)}\left[+3\,\frac{(\vec{R}.\vec{k})}{R^5}\,\vec{i}\otimes\vec{R}+\frac{1}{R^3}\,\frac{d\vec{k}}{ds}\otimes\vec{R}-\frac{1}{R^3}\,\vec{i}\otimes\vec{k}\right]ds. \tag{7.9}$$

By partial integration we find

$$\int_{s_0}^{s_1}\frac{h(s)}{V(s)}\,\frac{1}{R^3}\,\frac{d\vec{\xi}}{ds}\otimes\vec{R}\,ds=\vec{k}\otimes\frac{\vec{R}\,h(s)}{R^3V(s)}\Big|_{s_0}^{s_1}-\int_{s_0}^{s_1}\left(\frac{d}{ds}\,\frac{h(s)}{V(s)}\right)\frac{1}{R^3}\,\vec{k}\otimes\vec{R}\,ds+$$

$$+\int_{s_0}^{s_1}\frac{h(s)}{V(s)R^3}\,\vec{k}\otimes\vec{i}\,ds-3\int_{s_0}^{s_1}\frac{h(s)}{V(s)}\,\frac{(\vec{R}.\vec{i})}{R^5}\,\vec{k}\otimes\vec{R}\,ds. \tag{7.10}$$

Hence

$$\vec{v}_{L_1}+\vec{v}_{L_2}=\frac{1}{4\pi\mu}\int_{s_0}^{s_1}\frac{h(s)}{V(s)}\left[+3\,\frac{(\vec{R}.\vec{k})}{R^5}\,\vec{i}\otimes\vec{R}-3\,\frac{(\vec{R}.\vec{i})}{R^5}\,\vec{k}\otimes\vec{R}-\frac{2}{R^3}\,\vec{i}\otimes\vec{k}\right]ds+$$

$$-\frac{1}{4\pi\mu}\int_{s_0}^{s_1}\frac{d}{ds}\left(\frac{h(s)}{V(s)}\right)\frac{1}{R^3}\,\vec{k}\otimes\vec{R}\,ds+\frac{1}{4\pi\mu}\,\frac{h(s)}{V(s)R^3}\,\vec{k}\otimes\vec{R}\Big|_{s_0}^{s_1}. \tag{7.11}$$

The contributions from the starting and the bound vortex to the velocity are

$$\left(-\frac{1}{4\pi}\cdot\frac{h(s)}{\mu V(s)}\,\frac{1}{2\varepsilon}\cdot\vec{k}\otimes\frac{\vec{R}}{R^3}\,2\varepsilon\right)\Big|_{s_0}^{s_1}=-\frac{1}{4\pi}\,\frac{h(s)}{\mu V(s)}\,\vec{k}\otimes\frac{\vec{R}}{R^3}\Big|_{s_0}^{s_1} \tag{7.12}$$

and the contribution of the distributed vorticity of strength (7.4) in the $+\vec{k}$ direction is

$$\frac{1}{4\pi\mu}\int_{s_o}^{s_1}\frac{d}{ds}\left(\frac{h(s)}{V(s)}\right)\vec{k}\otimes\frac{\vec{R}}{R^3}\,ds. \tag{7.13}$$

By adding (7.11), (7.12) and (7.13) we find for the total velocity induced by the vorticity distributions

$$\vec{v}=\frac{1}{4\pi\mu}\int_{s_o}^{s_1}\frac{h(s)}{V(s)}\left[3\frac{(\vec{R}.\vec{k})}{R^5}\vec{i}\otimes\vec{R}-3\frac{(\vec{R}.\vec{i})}{R^5}\vec{k}\otimes\vec{R}-\frac{2}{R^3}\vec{i}\otimes\vec{k}\right]ds. \tag{7.14}$$

The question is now if the velocity (7.14) is equal to the one given in (5.5) or if the following equality is true.

$$\frac{-\vec{j}}{R^3}+3\frac{\vec{R}(\vec{j}.\vec{R})}{R^5}=3\frac{(\vec{R}.\vec{k})}{R^5}\vec{i}\otimes\vec{R}-3\frac{(\vec{R}.\vec{i})}{R^5}\vec{k}\otimes\vec{R}-\frac{2}{R^3}\vec{i}\otimes\vec{k}\,. \tag{7.15}$$

This can be proved by taking inproducts of both sides of (7.15) with $\vec{i},\vec{j}$ and $\vec{k}$ respectively. In each of these three cases equality is proved easily hence (7.15) is correct and our vortex configuration can be considered as to be induced by the moving singular force perpendicular to its velocity.

Exercise.

Discuss the concept of a lifting line by a continuous distribution of external forces per unit of length along a line segment, placed in a parallel flow.

8. On the concept bound vorticity of a wing

The results of the previous section can be used after a simple Galilei transformation, for the description of a wing of zero thickness placed in a flow. We consider first the two dimensional case of a profile of zero thickness in a homogeneous flow of velocity U, hence the flow field is independent of the z coordinate. The profile is supposed to induce only small disturbance

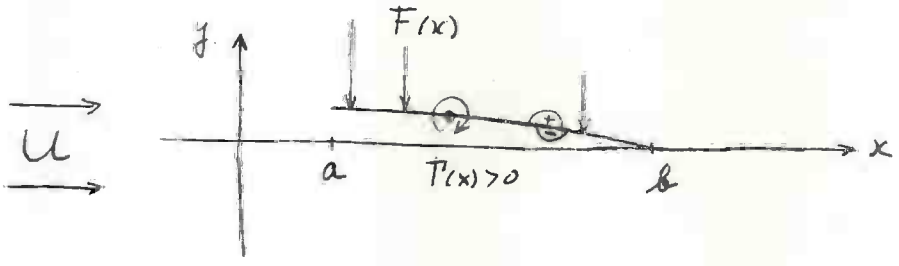

Fig. 8.1. Profile of zero thickness placed in a parallel flow.

velocities in the fluid and lies in the neighbourhood of the interval $a \leq x \leq b$ of the x axis. Because the theory is linearized we satisfy the boundary conditions for the flow not on the profile itself but on the interval (a,b).

The camber of the profile will cause pressure differences between the + and the -side of the profile

$$\Delta p(x) = p^{+}(x) - p^{-}(x). \tag{8.1}$$

From this it follows that the profile can be represented by an external force distribution F(x) per unit of length in the z direction, acting at the fluid. The force distribution is applied at the interval (a,b) and reckoned positive in the negative y direction. The strength of this field is

$$F(x) = -\Delta p(x). \tag{8.2}$$

By the previous section it is clear that we can replace this force field by a stationary bound vortex distribution along the interval (a,b) of strength per unit of length in the x direction

$$\Gamma(x) = \frac{F(x)}{\mu U}, \tag{8.3}$$

where Γ is reckoned positive in the direction denoted in figure 8.1.

The reason that here a natural "bound" vorticity can be introduced is that the velocity of the points of the profile with respect to the fluid seems to be well defined, namely U. We intuitively couple to these points the elementary forces F(x)dx, which then have the velocity U with respect to the fluid and hence can be replaced by the time independent elementary bound vortex $\Gamma(x)dx$ (8.3).

This certitude disappears when for instance the leading edge position a and the trailing edge position b become functions of time, then the identity of the points is no longer obvious. Two possible different realisations are for instance drawn in figure 8.2, where we assume that the parts of the profiles are infinitely thin and glide along each other without space inbetween.

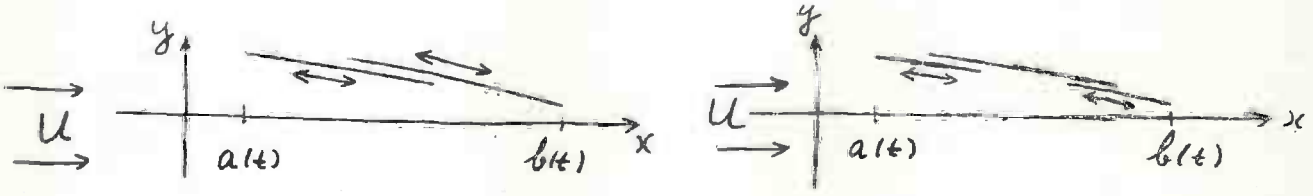

Fig. 8.2. Two different realisations of a contracting and expanding profile.

Because the fluid is inviscid the difference in construction of the profiles will not have any influence on the pressure distributions nor on the induced flow field, hence is not relevant. This means that it is not necessary to tie the bound vorticity to the material points of the profile and to give it the velocity of those points.

Even for the case of fixed a and b it is easy to show the ambiguity of the above introduced (8.3) bound vorticity concept. Consider for simplicity the case of a profile with a constant pressure jump (Δp = const.) over its whole chord. Then we can take a constant layer of bound vorticity Γ of strength per unit of length in the x direction (8.3), (8.2)

$$\Gamma = -\frac{\Delta p}{\mu U} = \text{const.}, \tag{8.4}$$

here the elements of bound vorticity $\Gamma\,dx$ are coupled to the elementary forces $F.dx = -\Delta p\,dx$ moving with velocity U with respect to the fluid.

Next we assume however that the elementary forces F.dx have a velocity V in the negative x direction, hence have with respect to the fluid, a velocity U + V. Then by (8.1) the strength of their elements of bound vorticity become

$$\tilde{\Gamma}\,dx = \frac{F\,dx}{\mu(U+V)}\,. \tag{8.5}$$

The following happens, first the elementary forces are created at the trailing edge, hence their starting vortices of strength $\tilde{\Gamma}\,dx$ remain behind and are transported downstream by the flow. This gives rise to a vortex sheet of strength per unit of length in the x direction

$$-\frac{V\tilde{\Gamma}}{U}\,. \tag{8.6}$$

Second the elementary forces move to the leading edge and create a bound vortex layer of strength

$$\tilde{\Gamma}. \tag{8.7}$$

Third the elementary forces reach the leading edge are switched off and leave behind their elementary amount of vorticity which is transported downstream from the leading edge. This creates a layer of strength.

$$\frac{V\tilde{\Gamma}}{U}\,. \tag{8.8}$$

Hence at the profile we have a layer of bound vorticity of strength (8.7) and a layer of free floating vorticity of strength(8.8). Their total strength is

$$\tilde{\Gamma}\left(\frac{U+V}{U}\right) = \frac{F}{\mu U}\,, \tag{8.9}$$

which is exactly the strength of the bound vorticity in the first case. Behind the trailing edge we have the sum of the two free floating layers of strengths (8.6) and (8.8), hence their total strength is zero, as it has to be in comparison with our first approach.

From this it follows that the flow field in both approaches is the same, because the law of Biot and Savart makes no distinction between bound and free vorticity.

This can be generalized to arbitrary moving flexible lifting surfaces which are allowed to expand or contract. The velocities of its points are of no interest and can be chosen at will, the same holds for the velocities of the time dependent elementary forces which represent the lifting surface, only the vorticity created by them has to be calculated in the way as is discussed in the previous section.

The description given here will be needed when we consider the optimization of flexible wing systems (section 28).

9. A bound vortex "ending" at a rigid plate

The following statement is sometimes heard; a bound vortex can end against a rigid wall. This kind of configuration is rather important in aero and hydrodynamics. In ship propulsion we have for instance the shrouded propeller. Here the tips of the blads with their bound vorticity, move along the inner side of the schroud which is in first approximation a cylindrical surface.

In order to focus attention we will consider the schematic case of a half infinite rigid flat plate which is infinitely thin. The plate (figure 9.1) coincides with the x,y plane of the Cartesian coordinate system x,y,z, for $x < 0$.

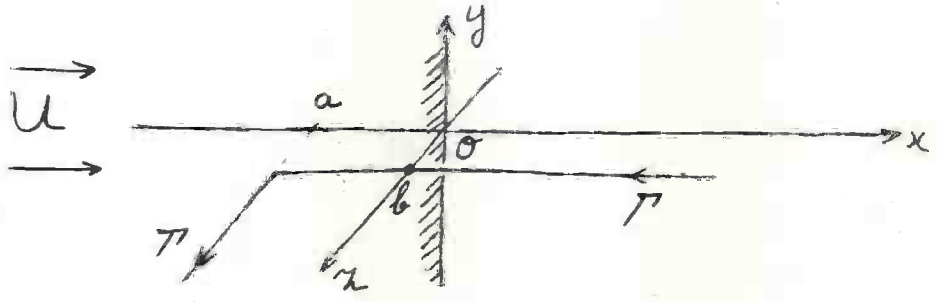

Fig. 9.1. Half infinite plate with vortex system in its neighbourhood.

The fluid in which it is embedded has a velocity U in the positive x direction.

We consider the linear theory for a half infinite bound vortex of strength Γ parallel to the z axis and coupled to the +z direction by a right hand screw. This vortex lies in x,z plane with $x = a < 0$; $z \geq b \geq 0$. The velocities induced by Γ are small of $0(\varepsilon)$ while U is assumed to be $0(\varepsilon^0)$. From the end (a,0,b) of the bound vortex starts a free vortex of the same strength which lies along a stream line of the parallel flow, hence parallel to the x axis. The question is, what happens when b tends to zero hence when the bound vortex touches the plate.

To simplify this problem we assume first that the bound vortex is far upstream of the trailing edge, hence we consider the case $a = -\infty$. Then there remains only a free vortex stretching from $x = -\infty$ along the plate at a distance b of it.

The problem of flow for this configuration can be found by assuming on the half infinite plate, a system of vortices which has to be chosen in such a way that, first, the component of the fluid velocity normal to the plate is zero and second, that the Kutta condition at the trailing edge of the half infinite plate is satisfied. This latter condition is equivalent to the statement that at both sides of the plate, when we tend to the trailing edge, the pressures must become equal for each value of y.

An exact solution to this problem is found easily in the following way. Suppose the plate is not half infinite but stretches from $x = -\infty$ towards $x = +\infty$. Then the problem is trivial.

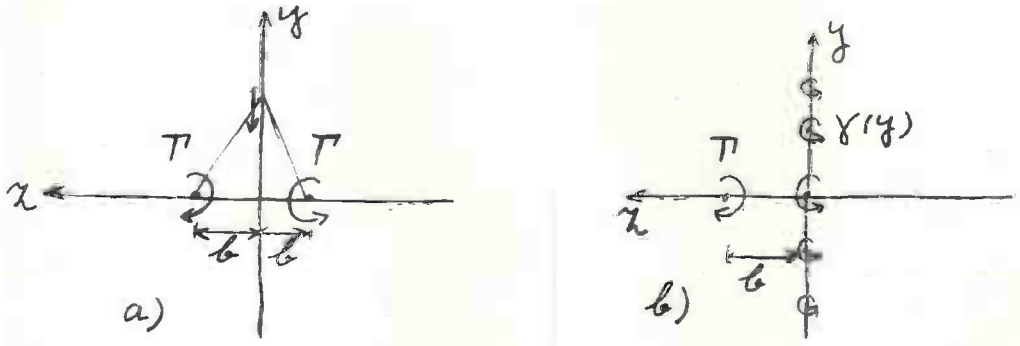

Fig. 9.2. Cross section for the case of the two sided infinite plate (y axis), a) with mirror vortex, b) with vortex layer $\gamma(y)$ on plate.

At points with $z > 0$, the influence of the plate is the same as the influence of a vortex which is the image of the free vortex under discussion (figure 9.2 a)). By this the tangential velocity at the plate is known namely $-\Gamma b/\pi(b^2 + y^2)$ in the y direction. Assuming that the flow behind the plate, hence for $z < 0$, is undisturbed, this is also the strength of the vorticity which can represent the plate

$$\gamma(y) = \frac{\Gamma b}{\pi(b^2 + y^2)} \quad , \tag{9.1}$$

coupled with a right hand screw to the positive x direction (figure 9.2 b)).

In order to take into account the two sided infinite plane we only need vortices parallel to the z axis. Then our disturbance velocities are all perpendicular to the main stream. This means that everywhere the pressure ([12], page 99)

$$p = p_\infty + \tfrac{1}{2}\mu U^2 - \tfrac{1}{2}\mu((U + u)^2 + v^2 + w^2) \approx p_\infty + O(\varepsilon^2), \tag{9.2}$$

is constant, because the x component of the disturbance velocity $\vec{v} = (u,v,w)$ is zero. Now we take away the added half plane $x > 0$, however we let intact the vortex system for $x > 0$, then we have found the solution for the half infinite plate, with a free vortex at a distance b. This is correct because first we have satisfied at the half plane $z = 0$, $x < 0$, the boundary condition of vanishing normal component of the velocity and second we satisfied the Kutta condition at the trailing edge, all pressures are equal to p_∞ within the accuracy of a linearized theory. We remark that

$$\int_{-\infty}^{+\infty} \gamma(y)\,dy = \frac{\Gamma b}{\pi} \int_{-\infty}^{+\infty} \frac{dy}{(b^2 + y^2)} = \Gamma. \tag{9.3}$$

Next we consider the limit $b \to 0$. Then from (9.1) $\gamma(y) \to 0$ for each $y \neq 0$, however as follows from (9.3) the total strength of the $\gamma(y)$ remains constant and equal to Γ. Hence for $b \to 0$ the free vortex Γ and the free vorticity $\gamma(y)$ annihilate each other and no vorticity remains for $x < 0$ as well as for $x > 0$.

The result obtained in this way describes exactly the influence of a half plane on our two sided infinite free vortex. The problem stated at the beginning however is more complicated. There we have to take into account the bound vortex parallel to the z axis and the fact that the free vortex is only half infinite $-a < x < +\infty$. These differences however cannot cause infinite induced vlocities in the neighbourhood of the trailing edge of the plate and will not give rise to concentrated free vorticity. Hence we conclude that also in this case, when $b \to 0$, the concentrated free vortex disappears and only distributed free vorticity flows from the trailing edge.

By this it is acceptable that in the case of a plate of finite extent only distributed and no concentrated free vortex will leave the trailing edge when a bound concentrated vortex ends against the plate.

Because the vector field of vorticity is without divergence it is clear that from the trailing edge free vorticity starts, with the same total strength as the bound vortex. It seems a contradiction that in the case of the two sided infinitely long concentrated free vortex and the half infinite plane when $b \to 0$ all vorticity disappeared although at $x = -\infty$ there must be a bound vortex of finite strength ending at the plate. The reason is, that because the trailing edge is infinitely long, the density of the free vorticity can become "infinitely small", hence zero, when we consider the limiting procedure $a \to -\infty$ in figure 7.1, while still it will have a finite nonzero total value.

It is also easy to describe the vorticity at the plate in the direct neighbourhood of the point Q where the concentrated bound vortex of strength Γ meets the plate. Then we can neglect the influence of the trailing edge. Hence we consider a vortex ending at an infinite plate. By r we denote the distance from a point of the plate to Q. In this case the exact solution is as follows. At the plate we will have a radially converging or diverging vortex system of strength $\Gamma/2\pi r$ per unit of length at a circle with radius r (figure 9.3).

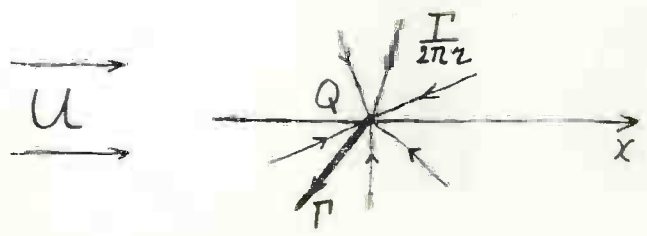

Fig. 9.3. The vorticity at the plate in the neighbourhood of the end point of the concentrated bound vortex.

Then it is seen that the total three dimensional vorticity field is without divergence and it can simply be proved that the component of the induced velocity normal to the plate, is zero. The reader can check that behind the plate the velocity of the half infinite bound vortex Γ is opposite the velocity induced by the vorticity at the plate, hence behind the plate the velocity is zero.

When the trailing edge is present it is heuristically clear that the spreading of the vorticity is qualitatively as given in figure 9.4.

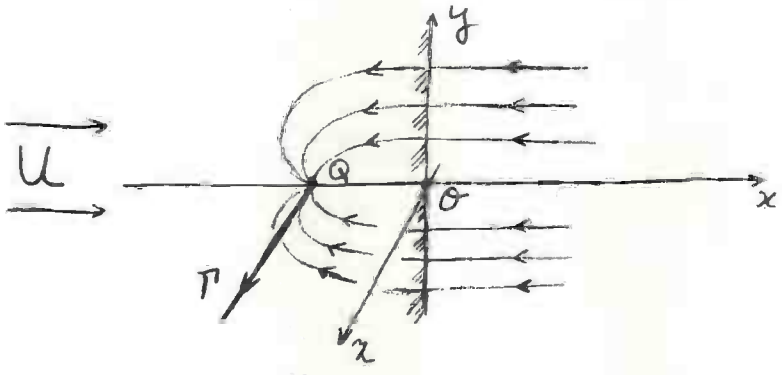

Fig. 9.4. A concentrated bound vortex ending at a flat plate in the neighbourhood of the trailing edge.

Because we have to satisfy the Kutta condition at the trailing edge, hence no pressure jump is allowed at this edge, the vorticity at the plate has to meet the edge at right angles.

Exercises.

1. Derive an integral equation for the vorticity at the plate in the case of figure 9.4.
2. Make clear by a heuristic argument that in figure 9.4 all the vorticity will leave the trailing edge.

10. The actuator surface

In general the detailed action of propulsion systems is rather complicated. Some times this detailed action is of no interest and only a more global knowledge of the induced velocities is needed. For instance when we are interested in the overall influence of a ship propeller on parts of the ship at a distance to the propeller which is large with respect to its dimensions. In these cases a simplified representation of the propulsion system can be given by some suitably chosen force field acting on the fluid. It means that in order to know the velocity field induced by the propeller we have to solve (3.1) together with (3.2) or given $\vec{F}(x,y,z,t)$. For a propulsion device we assume in general that its action is periodic with respect to time while the flow at infinity is an incoming parallel flow.

Instead of a general three dimensional force field it is simpler in many cases to represent the propeller by a force field which is concentrated on a surface

$$G(x,y,z) = 0. \tag{10.1}$$

The active part of this surface, where the force field is non zero, will be denoted by S. When the surface S is a flat circular region, the representation is generally called an actuator disk. The surface will have a + and -side, for instance the +side faces the neighbourhood of G = 0 where G > 0. For simplicity we assume that the force field and also the velocity field is independent of time. It will be represented by

$$\vec{F}(x,y,z) = \vec{f}.\delta(m) = (f_x,f_y,f_z)\ \delta(m) \tag{10.2}$$

where f_x, f_y and f_z are sufficiently smooth functions of position at the surface, m is the distance from a point in a neighbourhood of S' to G = 0, reckoned positive when the point is at the +side and $\delta(m)$ is the delta function of Dirac . The vector $\vec{f}$ at S represents the force per unit area. We do not take into account gravity which is a force field derived from a potential hence it can be included simply in p(3.4).

Consider an area A of the active region S and around it a box B_A of small width h. We apply Greens theorem to the interior of B_A and take the limit $h \to 0$. Because A has arbitrary shape, we find the following jump relation across S,

$$\vec{v}^{+} . \vec{n} - \vec{v}^{-} . \vec{n} \overset{\text{def}}{=\!=} [\vec{v} . \vec{n}]^{+}_{-} \overset{\text{def}}{=\!=} [v_n]^{+}_{-} = 0, \tag{10.3}$$

where $\vec{n}$ is the unit normal at G = 0, pointing in the direction G > 0.

Integrating the equation of motion (3.1) for the time independent case over a region B of space yields

$$\int_{\partial B} (\vec{v} \cdot \vec{n})\, \vec{v}\, d\sigma = \frac{1}{\mu} \int_{B} \vec{F}\, dV - \frac{1}{\mu} \int_{\partial B} p\, \vec{n}\, d\sigma, \tag{10.4}$$

where $d\sigma$ and dV are elements of area and volume and ∂B is the boundary of B. Choosing for B the volume B_A defined above we find by taking the limit $h \to 0$ from the component normal to G = 0 and using (10.3),

$$[p]^{+}_{-} = \vec{f} \cdot \vec{n} \underline{\underline{\text{ def }}} f_n \tag{10.5}$$

and from the component in the plane tangent to G = 0

$$\mu\, [\vec{v}_t]^{+}_{-} = \frac{\vec{f}_t}{v_n}, \tag{10.6}$$

where t denotes the tangential component.
This formula has a meaning only at places of S where it is really crossed by fluid particles hence where $v_n \neq 0$.

Introducing the head H by

$$H = \frac{p}{\mu} + \tfrac{1}{2} (u^2 + v^2 + w^2) \tag{10.7}$$

we find by (10.5) and (10.6)

$$\mu [H]^{+}_{-} = f_n + \frac{1}{v_n} \frac{\vec{v}^{+}_{t} + \vec{v}^{-}_{t}}{2} \cdot \vec{f}_t \quad . \tag{10.8}$$

We can write the equation of motion (3.1) for the time independent case as ([3] page 16),

$$\vec{v} \times \vec{\omega} = -\frac{1}{\mu} \vec{F} + \text{grad } H. \tag{10.9}$$

where $\vec{\omega} = (\omega_x, \omega_y, \omega_z)$ is the vorticity of the fluid. Outside the force free region we find for the change of H along a streamline, hence in the direction of $\vec{v}$,

$$\frac{dH}{dt} = \vec{v}.\text{grad } H = 0. \tag{10.10}$$

This represents the well known fact that outside the region of force H is a constant along the streamlines. Of course this constant can change from one streamline to another.

By equations (10.3), (10.5), (10.6) and (10.8) we can express the values of p, $\vec{v}$ and H at one side of the actuator surface in their values at the other side when $\vec{f}$ and v_n are known.

We now discuss some formulas for the vorticity induced by the external force field. From (10.6) we see that when $\vec{f}_t \neq 0$, there is concentrated vorticity at the actuator region in a direction perpendicular to $\vec{f}_t$ and of intensity Ω per unit of length in the $\vec{f}_t$ direction

$$\Omega = \frac{f_t}{\mu v_n} , \tag{10.11}$$

where $f_t = |\vec{f}_t|$. From (10.11) it follows that $\Omega = 0$ when $f_t = 0$ and $v_n \neq 0$. So normal forces do not induce a jump in $\vec{v}_t$ hence do not induce concentrated vorticity at the actuator surface, again when $v_n \neq 0$.

When $v_n = 0$ then $f_t = 0$ by (10.6) and the quotient at the right hand side of (10.11) is not determined. In this case it still can happen that a concentrated free vorticity sheet is transported by the fluid flow along S where only normal forces are acting. Then of course a jump occurs in $\vec{v}_t$ and $\Omega \neq 0$. However this Ω is, so to speak, not caused by the local force field but can be interpreted to be shed by "upstream" force fields. In this way also an infinitely thin wing can be discussed [21].

In order to discuss the free vorticity just outside the actuator surface, hence outside the force region, we translate the origin of the Cartesian coordinate system to the point under consideration at S. The x,z plane will be tangent to S and the positive y axis is at the + side of S. Outside the force region, hence for $\vec{F} = 0$, we apply (10.9), which yields two independent equations for ω_x, ω_y and ω_z for instance,

$$\omega x = \frac{1}{v_n} \{- \frac{\partial H}{\partial z} + u \omega_y\} , \tag{10.12}$$

$$\omega_z = \frac{1}{v_n} \{+ \frac{\partial H}{\partial x} + w\omega_y\} , \tag{10.13}$$

The y component (10.9) ($\vec{F} = 0$) yields an equation which is a linear combination of (10.12) and (10.13), this follows from (10.10). The value of ω_y in (10.12) and (10.13) can be computed from $\vec{v}$, since in its definition only the partial derivatives in the x,z plane occur,

$$\omega_y = \frac{\partial}{\partial z} u - \frac{\partial}{\partial x} w. \tag{10.14}$$

Hence when the force field is given and at one side of S the quantities $\vec{v}$ and H, we can calculate at the same side $\vec{\omega}$ and at the other side $\vec{v}$, H and $\vec{\omega}$ as well as the concentrated vorticity Ω at S.

From (3.5) and (3.6) we obtain interesting information with respect to changes of the velocity field $\vec{v}$ caused by a change of $\vec{F}$, hence of the actuator surface G = 0 and the force vector $\vec{f}$ per unit area of G = 0. Suppose we have two different actuator surfaces, one with an active region S_1 and another with an active region S_2 on different surfaces $G_1(x,y,z) = 0$ and $G_2(x,y,z) = 0$. A cross section with the x,y plane is drawn in figure 10.1. We assume however, that S_1 and S_2 have the same edge and the same normal load f_n, which is independent of the position on S_1 or on S_2, while $f_t = 0$. This means that the difference

$$\vec{F}_2(x,y,z) - \vec{F}_1(x,y,z), \tag{10.15}$$

of the force fields (10.2) consists of two δ functions of Dirac

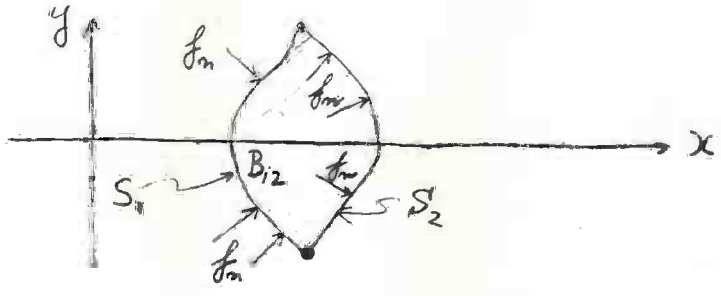

Fig. 10.1. Two different active regions S_1 and S_2 with the same edge.

one at S_1 and the other with "opposite sign" at S_2. We introduce the volume B_{12} in between S_1 and S_2.

We now put

$$p_2(x,y,z) = p_1(x,y,z) \ , \ (x,y,z) \notin B_{12} \tag{10.16}$$

and

$$p_2(x,y,z) = p_1(x,y,z) - f_n \ , \ (x,y,z) \in B_{12}. \tag{10.17}$$

Then the function $\Psi(x,y,z)$ of (3.7) is zero outside B_{12} and has the constant value $-f_n$ inside B_{12}. By this choice of Ψ we satisfy (3.6) and hence S_1 and S_2 with the same f_n induce the same velocity field.

From the foregoing we find that the shape of the inner part of an actuator surface with a constant normal load is of no importance for the induced velocities. Of course this holds only for the in viscid and incompressible fluid we consider here.

In the general equation of motion (3.1) we call the region where the three dimensional force field $\vec{F}$ is not zero, the actuator region. As is clear from this section the actuator surface theory discusses only a special case of the general equation of motion. We can go one step further by concentrating the force field $\vec{F}$ on a line, such lines could be called actuator lines. Finally we can concentrate $\vec{F}$ so that it is only non zero at a point, then a singular force (actuator point) occurs.

We mention that a singular force has no meaning in the non linear theory for inviscid fluids, it induces no velocities [21]. This is also partly true for the actuator line, although these are used as lifting lines. However when we consider for instance an infinitely long line embedded in a fluid, which is at rest at infinity, it can be shown that this line loaded by a constant force per unit of length does not induce any velocity in the fluid.

Exercise.

Show that the independence of the velocity induced by an actuator surface, from the shape of the inner part of the active region for a normal load which is independent of position, holds also when $f_n = f_n(t)$ and S is time dependent but with its edge fixed.

Summing up we find

$$\vec{v}(\tilde{x},\tilde{y},\tilde{z},t=0) = \frac{1}{4\pi\mu U} \iint_S \frac{f_{\tilde{x}}(\tilde{\eta},\tilde{\zeta})\,\vec{R}}{R^3}\, d\tilde{\eta}\, d\tilde{\zeta} + \frac{\{f_{\tilde{x}}(\tilde{y},\tilde{z})h(\tilde{x}),0,0\}}{\mu U} \quad , \tag{11.5}$$

where

$$\vec{R} = \{\tilde{x} \ , \ \tilde{y}-\tilde{\eta} \ , \ \tilde{z}-\tilde{\zeta}\} \tag{11.6}$$

and $h(x)$ is the unit step function

$$h(x) = 1 \ , \ x > 0 \quad , \quad h(x) = 0 \ , \ x < 0. \tag{11.7}$$

We still more simplify this problem by assuming that $f_{\tilde{x}}(\tilde{y},\tilde{z}) = f_n$ is independent of $\tilde{y}$ and $\tilde{z}$, hence we have a constant normal load over the disk. Using the method of section (3.1) (figure 3.1), we will give a description of the vorticity left behind by this disk. We use a rectangular probing contour C, lying in the $(\tilde{x},\tilde{y})$ plane, with corner points A_1, A_2, A_3 and A_4 (figure 11.1). We assume that the sides (A_1,A_2) and (A_3,A_4) are of length ℓ and parallel with the $\tilde{x}$ axis. The sides (A_1,A_4) and (A_2,A_3) are of length h and perpendicular to the $\tilde{x}$ axis. First we consider the case that the distance of $A_2(A_3)$ to the $\tilde{x}$ axis is smaller (greater) than b. Hence when the disk moves to the left it will be cut by the contour. After the passing of (A_2,A_3) only (A_1,A_2) pieces through the disk. From (3.12) we find

$$\frac{d\Gamma}{dt} = \frac{1}{\mu} \int_C \vec{F}\,(\tilde{x},\tilde{y},\tilde{z},t) \cdot d\vec{s} = -\frac{f_n}{\mu} \ . \tag{11.8}$$

Before the disk has met the contour its circulation Γ, (3.11) is zero. When the disk has passed entirely along C we find

$$\Gamma = -\frac{f_n}{\mu}\,\frac{\ell}{U} \ . \tag{11.9}$$

Hence per unit of length vorticity is left behind of strength

$$\gamma = \frac{\Gamma}{\ell} = -\frac{f_n}{U\mu} \ , \tag{11.10}$$

coupled with a right hand screw to the $+\tilde{z}$ direction. Because the width h of C can be made arbitrarily small, this free vorticity is concentrated at the half infinite cylinder behind the edge of the disk. Clearly (11.10) is in agreement with the second term at the right of (11.5), which causes a discontinuity in the $\tilde{x}$ component of the velocity behind the disk, hence concentrated vorticity.

11. The circular flat actuator disk

We consider now a simple example of an actuator disk, using the linearized theory. The disk is the circular region

$$\tilde{x} = -Ut \ , \ (\tilde{y}^2 + \tilde{z}^2) \leq b^2. \tag{11.1}$$

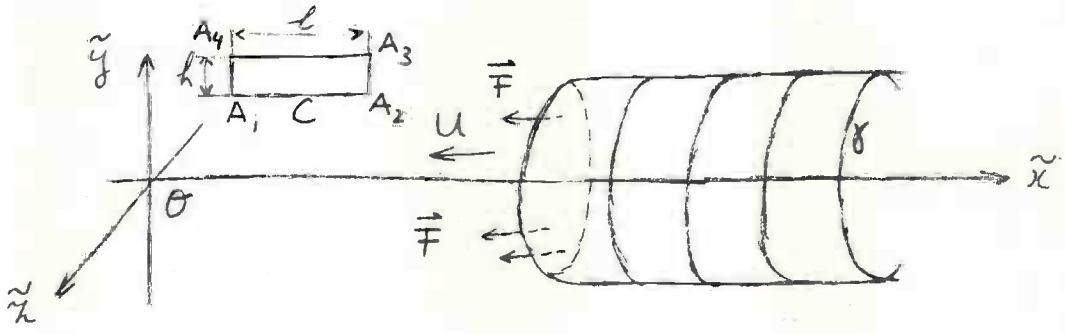

Fig. 11.1 The moving actuator disk.

It is represented by the time dependent force field

$$\vec{F}(\tilde{x},\tilde{y},\tilde{z},t) = (f_{\tilde{x}}(\tilde{y},\tilde{z}), 0,0)\ \delta(\tilde{x} + Ut), \tag{11.2}$$

where $f_{\tilde{x}}(\tilde{y},\tilde{z}) = 0$ for $\tilde{y}^2 + \tilde{z}^2 > b^2$. This force field can be considered as a set of an "infinite number" of forces $(f_{\tilde{x}}(\tilde{y},\tilde{z}),0,0)d\tilde{y}\ d\tilde{z}$. Then we can use (6.8) and (6.10) to calculate by superposition the velocity field induced by this disk. We consider the moment at which the disk just arrived at the $(\tilde{y},\tilde{z})$ plane hence $t = 0$. The length parameter s of (6.8) becomes here $-\tilde{x}$, while we assume that the motion started infinitely long ago hence $s_o = -\infty$. The force $g(s)$ in (6.8) has to be replaced by

$$g(s) = -f_{\tilde{x}}(\tilde{y},\tilde{z})\ d\tilde{y}\ d\tilde{z}, \tag{11.3}$$

and the path L of it is a line parallel to the $\tilde{x}$ axis. This force is independent of $s = -\tilde{x}$ hence the third contribution at the right of (6.8) disappears. The second contribution vanishes already because $s_o = -\infty$.

The velocity which follows from (6.10) is in this case only in the x direction, it becomes

$$\frac{1}{d\tilde{x}\ d\tilde{y}} \cdot \frac{f_{\tilde{x}}(\tilde{y},\tilde{z})}{\mu U}\ d\tilde{x}\ d\tilde{y} = + \frac{f_{\tilde{x}}(\tilde{y},\tilde{z})}{\mu U}. \tag{11.4}$$

When we take the distance of A_4 to the $\tilde{x}$ axis smaller than b, both (A_1, A_2) and (A_3, A_4) pierce through the disk and the contributions of the integrals (A_1, A_2) and (A_3, A_4) cancel each other hence $d\Gamma/dt$ remains zero. By using other probing contours parallel to the $(\tilde{y},\tilde{z})$ plane and parallel to the $(\tilde{z},\tilde{x})$ plane it is seen that no other vorticity is left behind. So (11.10) describes the only vorticity shed by this disk with a constant normal load f_n.

Because only the relative motion of the disk with respect to the undisturbed fluid is essential, we have also solved the problem of an actuator disk placed in a parallel flow of magnitude U in the positive x direction of a reference system (x,y,z) (figure 11.2). This problem is

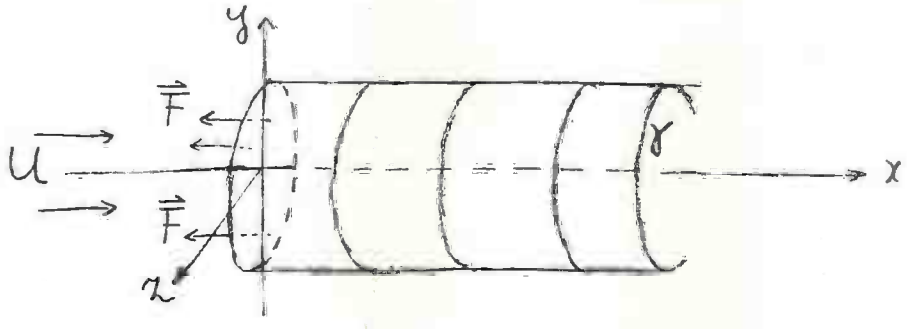

Fig. 11.2. The actuator disk placed in a parallel flow.

independent of time hence it is a special case of the type of problems discussed in the previous section, although there the theory was non linear. The velocity field in this case simply follows from (11.5) by adding the x component U

$$\vec{v}(x,y,z) = (U,0,0) + \frac{f_n}{4\pi\mu U} \iint_S \frac{\vec{R}}{R^3}\, d\eta\, d\zeta + \frac{\{f_n\, h(x),0,0\}}{\mu U} \quad . \tag{11.11}$$

Because the actuator disk is covered with a layer of pressure dipoles with their axis perpendicular to the disk, the induced pressure field will have a jump of magnitude f_n. This is in agreement with (10.5). From (10.11) it follows that no concentrated vorticity is present at the disk, $\Omega = 0$, because the load is normal in this case.

When $f_n < 0$ the disk acts as a propeller and it follows from (11.11) or (11.5) that behind the disk is a jet in which the fluid flows downstream with a larger velocity than the surrounding fluid outside the vortex cylinder. This is in agreement with the slipstream which can be expected behind a propeller.

Suppose the total thrust of an actuator disk with a constant normal load over its area A is T and the incoming velocity is U. Then by (11.11) the excess velocity far behind the disk is $T/\mu AU$. Hence the kinetic energy E_i shed per unit of time becomes

$$E_i = T^2/2\mu UA. \tag{11.12}$$

The efficiency η, which is defined as the quotient of the useful work TU and the total work which is the sum of the useful work and the lost kinetic energy, becomes

$$\eta = \left(\frac{TU}{TU + E_i}\right) = \left\{1 + \frac{T}{2\mu U^2 A}\right\}^{-1} \tag{11.13}$$

In section 38 it will be shown that this is the smallest upperbound for the efficiency of a propeller acting in an inviscid and incompressible fluid with the same total thrust T, working area A and velocity of advance U. Therefore this actuator disk is sometimes called an ideal propeller.

Exercises.

1. Discuss by the method of the probing contour the vorticity shed by the actuator disk when the normal load depends on $\tilde{y}$ and $\tilde{z}$ (11.2).
2. Show that the thrust of a normally loaded actuator disk and the impulse far behind it in the slipstream are in agreement with the momentum theorem ([12] page 54).

12. Rotating vortex model of actuator disk

The question arises if we can give a simple vortex representation of an actuator disk which resembles a screw propeller. This will be shown to be possible. For simplicity we assume a constant normal load and a linear theory.

We introduce a cylindrical coordinate system (x,r,φ) as drawn in figure 12.1. Consider a straight vortex OA of length b. The endpoint 0 coincides

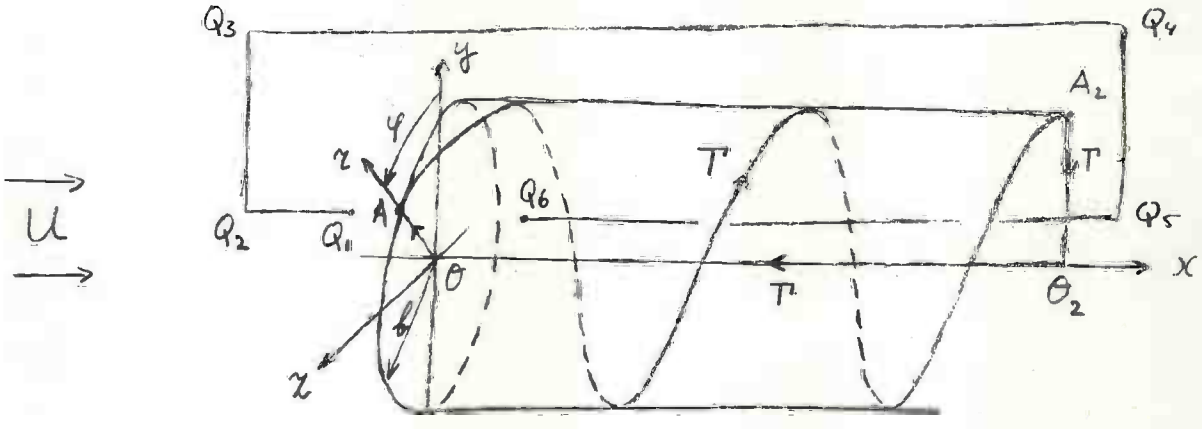

Fig. 12.1. The rotating vortex OA.

with the origin of the coordinate system and the vortex rotates with angular velocity ω in the plane $x = 0$. The strength of this vortex is Γ coupled with a right hand screw to the positive r direction. From the endpoint 0 starts a free vortex of strength Γ stretching along the x axis and from the endpoint A a free vortex of the same strength along the helicoidal line

$$\varphi - \omega t + ax = 0 \quad , \quad r = b, \tag{12.1}$$

where $a = \omega/U$. These two free vortices are connected by the starting vortex 0_2A_2, which was shed by the beginning of the proces "long ago" and which makes the vortex field free of divergence.

By the theorem of Joukowsky the force per unit of length exerted by the fluid on the vortex 0A becomes

$$\mu(U,0 - \omega r) \otimes (0,\Gamma,0) = \mu(\omega r\Gamma,0,U\Gamma), \tag{12.2}$$

where the components of the vectors are their physical components in the (x,r,φ) system. For $\Gamma < 0$ the x component of this force becomes negative hence the vortex acts as a propeller.

Now suppose that ω increases indefinitely and Γ decreases so that $\Gamma\omega$ remains constant. Then several limits have to be considered. First, the free vortex along the x axis and the starting vortex disappear. Second, the helicordal vortices become circular and their strength per unit of length

in the x direction assumes the value

$$\Gamma\omega/2\pi U \quad , \tag{12.3}$$

coupled with a right hand screw to the negative φ direction. Third, the force exerted on the vortex becomes perpendicular to the actuator disk ($x = 0,\ 0 \leq r \leq b$) and its mean value per unit of area at a radius r becomes

$$\frac{\mu\ \omega r\ \Gamma\ dr}{2\pi\ r\ dr} = \frac{\mu\ \omega\ \Gamma}{2\mu} \quad , \tag{12.4}$$

which is independent of r.

When we suppose

$$\frac{\mu\ \omega\ \Gamma}{2\pi} = f_n \tag{12.5}$$

we have the actuator disk with a constant normal load of the previous section. We will check if the characteristic features of the disk also can be recovered by the model of this section. The vorticity (12.3) on the cylinder behind the edge of the disk becomes by (12.5)

$$\Gamma\omega/2\pi U = f_n/\mu U \quad , \tag{12.6}$$

which is in agreement with (11.10), the change of sign is only due to the different definitions of positive direction in both cases.

The vorticity on the disk tends to zero because $\Gamma \to 0$, this is in agreement with $\Omega = 0$ for $f_t = 0$ in (10.11). At last we discuss the pressure jump over the disk which in the previous section followed from the force representation almost directly.

Consider in figure 12.1, the two points Q_1 and Q_6 which we suppose to be close to each other, Q_1 with a negative x coordinate and Q_6 with a positive one, hence each at a side of the "disk". We connect these points by a contour $Q_1, Q_2, Q_3, Q_4, Q_5, Q_6$, where the parts (Q_3,Q_4) and (Q_5,Q_6) are very long because we assumed that the process started long alo and the contour encircles all vorticity at the cylinder. In order to calculate the pressure difference between Q_1 and Q_6, in the limit $\omega \to \infty$, we use the instationary and linearized formulation of Bernoulli's law ([12] page 99),

$$p = -\mu\ Uu - \mu\ \frac{\partial\Phi}{\partial t} \quad , \tag{12.7}$$

where Φ is the velocity potential and a possible addition of a time dependent "constant" is neglected. The potential difference $\Phi_I - \Phi_6$ between the two points Q_1 and Q_6, can be written as

$$\Phi_6 - \Phi_1 = \left(\int_{Q_1}^{Q_2} + \ldots + \int_{Q_5}^{Q_6} \right) \vec{v} \cdot d\vec{s} \,, \tag{12.8}$$

This potential difference is equal to the total vorticity enclosed by the contour, because by (12.6) this is each unit of time increased by an amount f_n/μ, we find

$$\frac{\partial}{\partial t} (\Phi_6 - \Phi_1) = \frac{f_n}{\mu} \tag{12.9}$$

The condition of no divergence of the velocity field has as a consequence that the u component of it must be continuous across the disk, also in the case of $\omega \to \infty$. Then we find from (12.7)

$$p_6 - p_1 = - f_n \,, \tag{12.10}$$

which is the desired pressure jump.

Exercises.

1. Give also a rotating vortex model when the normal load $f_n = f_n(r)$, hence depends on r, by choosing the strength of the rotating vortex Γ to depend also on r.
2. Create a vortex model in the most general (linear) case, when the load depends arbitrarily on position and time, while the plan form of the disk is no longer circular.

13. Some remarks on actuator disk theory

We considered in sections 10, 11 and 12 the non linear and linear theory of actuator surfaces with prescribed loads. In this section we will conclude with some short remarks on these subjects and also with respect to the case that the load is not prescribed but has to be determined.

For the case of a prescribed load we refer to [28] for a method to recast the problem in an integral formulation. By this it is possible to carry out effectively numerical calculations by means of an iteration procedure. In this work an actuator disk is considered with normal and tangential components of the load, in such a way that an approximation of the loading of a ship screw is obtained. In [6] this method is used to calculate numerically the flow pattern of an actuator disk of this type. However it is not quite clear if the assumption made in [6] on the release of the vortex sheet from the edge is correct. In a linearized theory there is no problem with respect to this because the vorticity of the sheet remains at the place where it was formed, with respect to the fluid, it is not transported by its own induced velocities. In the non linear case this is no longer true. In [6] it was assumed that the sheet leaves the edge of the disk in some well defined direction. In [21] it is argued that possibly such a direction need not to exist and it is proved mathematically that in a very simple case this sheet can have the shape of a spiral encircling an infinite number of times the edge. In figure 13.1 we have drawn a picture of this phenomenon. The question is still open what happens in more realistic cases. It can be remarked that by experiments the spiralling behaviour is not to be rejected.

When the device which has to be represented by an actuator disk is very well specified it can be desirable not to assume a load but actually to calculate it. This could be done as follows.

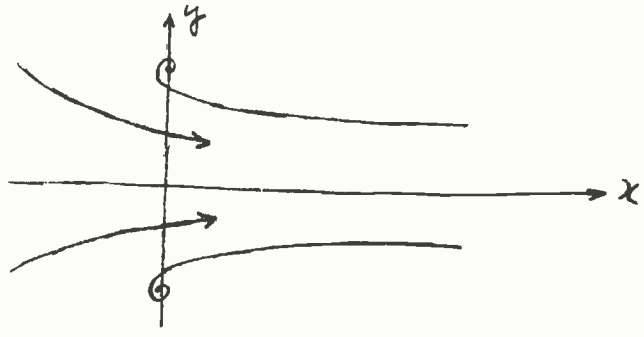

Fig. 13.1. Cross section of an actuator disk with spiralling vortex sheet.

First assume some unknown load on the actuator disk. Write down the induced velocities by this load and add these to the known incoming flow. Next we use the geometrical description of the device to find an additional relation between the velocities at the place of the disk and the force field. In this way we have two equations for the unknown velocity field as well as for the unknown force field. This has been done in [9] for a quickly rotating boomerang under the assumption of small forces and small disturbance velocities, hence in the linearized case.

Other applications of actuator disk theory are for instance in the theory of helicopter rotors we mention [19] for a more general survey we mention [10].

14. The ship screw, general considerations

Our next subject will be the ship screw which is up to now the most important device for hydrodynamic propulsion. It consists of a number of helicoidally shaped blades connected to a hub. The number of the blades can vary from two upto about six. The hub is mounted on a shaft (figure 14.1), which is rotated

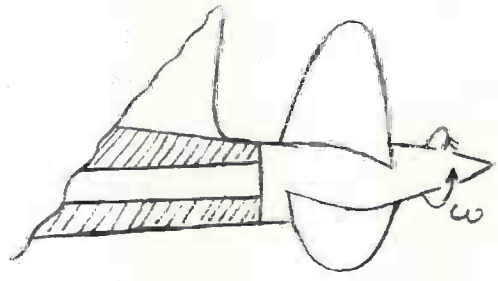

Fig. 14.1. Ship screw.

by the engine. The problem is how to shape the blades so that at a given rotational velocity, a prescribed thrust is produced which moves the ship with a desired speed. This is a very difficult problem because of the many complications which occur in a realistic situation. We now discuss, not at all in an exhaustive way, a number of these.

The ship screw is generally working behind the ship in a flow which is disturbed by the ship. This disturbance roughly proceeds from two different origins. First, the water has to follow the ship's form, hence behind it, it has to converge and by this the inflow in the propeller region is not homogeneous. Second, the water flows along the ship is dragged with it by viscosity and becomes turbulent.

The hull of the ship influences in still another way the propeller. Because it is a rigid surface it will hinder the water to be set into motion by the propeller hence the resulting pressures on the blades will be changed. The free surface of the water has an analogous effect. It is also a boundary of the domain in which the propeller is working although perhaps with an opposite effect to that of the rigid hull. The tip of the blade will experience a different inertia of the water when it is in the neighbourhood of the free surface than when it is far beneath it.

Considering such difficulties it seems wise to make simplifications in order to obtain a model which is still tractable by mathematics. However, these simplifications may not go too far, so that no conclusions about the real propeller can be obtained.

We will neglect viscosity and assume no influence of the ship hull at all

and also not of the free surface. The incoming flow will be a homogeneous one with velocity U. The thrust is mostly delivered by parts of the blades which are not too close to the hub, because the relative velocity of the water is larger at those parts which have a certain distance to the axis of rotation. This makes it acceptable to neglect in first instance the influence of the hub. Hence we consider a number of blades moving "freely" through the fluid, however along a prescribed path. The last step is to consider only one blade because this already shows all the mathematical difficulties which can be encountered.

Later on we shall discuss some possible corrections such as the influence of the other blades and the influence of an inhomogeneous inflow.

15. The geometry of a ship screw

For the description of a screw blade we use a cylindrical coordinate system x,r,φ of which the x axis is along the axis of rotation of the screw (figure 15.1). With respect to the coordinate system we have an

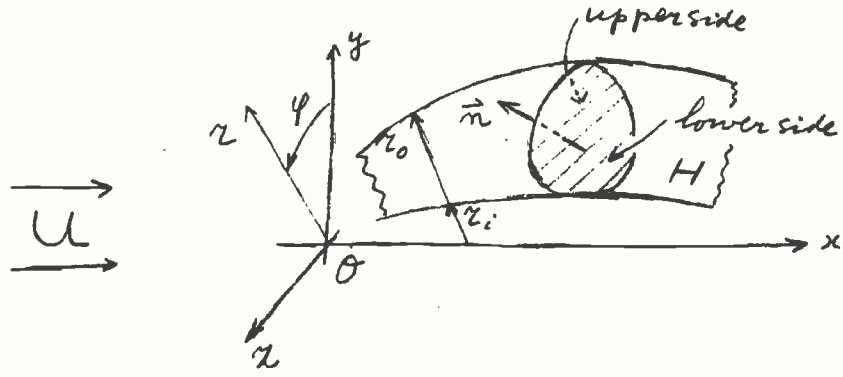

Fig. 15.1. A blade of a screw propeller.

incoming homogeneous parallel flow with its velocity U in the positive x direction. Our first aim is to find impermeable surfaces which can rotate about the x axis without disturbing the parallel flow.

Suppose we have a surface

$$G(x,r,\varphi,t) = 0 \tag{15.1}$$

moving through a fluid with a velocity field $(U + v_x, v_r, v_\varphi)$ and ask for the conditions which the velocity field has to satisfy in order that the fluid flows along this surface. Consider $G = G(x,r,\varphi,t)$ as a function defined in space. Then each moving particle of the fluid perceives at the place where it is at a certain moment, some value of G. When this particle moves on, the rate of change of this value is easily calculated as

$$\frac{dG}{dt} = \frac{\partial G}{\partial t} + (U + v_x)\frac{\partial G}{\partial x} + v_r \frac{\partial G}{\partial r} + v_\varphi \frac{\partial G}{r\partial \varphi} . \tag{15.2}$$

A particle moving along the surface (15.1) has to observe the value G = 0 during its motion. This means that the velocity $(U + v_x, v_r, v_\varphi)$ of that particle has to satisfy

$$\frac{\partial G}{\partial t} + (U + v_x)\frac{\partial G}{\partial x} + v_r \frac{\partial G}{\partial r} + v_\varphi \frac{\partial G}{r\partial \varphi} = 0 \tag{15.3}$$

This is the well known condition which the velocity field has to satisfy at the surface (15.1) in order that the fluid flows along the surface.

Now we consider a rigid surface rotating around the x axis

$$G(x,r,\varphi - wt) = 0. \tag{15.4}$$

In order that this surface does not disturb the homogeneous incoming parallel flow it has to satisfy (15.3) with $v_x = v_r = v_\varphi = 0$. At $t = 0$ we find

$$- \omega \frac{\partial G}{\partial \varphi} (x,r,\varphi) + U \frac{\partial G}{\partial x} (x,r,\varphi) = 0. \tag{15.5}$$

The general solution of this equation is

$$G = G(\varphi + ax - \omega t, r) \quad , \quad a = \omega/U, \tag{15.6}$$

where G is an arbitrary function of its arguments $(\varphi + ax - \omega t)$ and r. We restrict ourselves here to the case of the simple helicoidal surface H

$$H = \varphi + ax - \omega t = 0. \tag{15.7}$$

This surface will be called the helicoidal reference surface.

On H we choose a two dimensional coordinate system for instance x and r. Then we can define on H the planform B of a propeller blade by

$$x_\ell(r) \leq x \leq x_t(r) \quad , \quad r_i \leq r \leq r_o \ , \tag{15.8}$$

where $x_\ell(r)$ and $x_t(r)$ are given functions.

The plan form (15.7), (15.8) as an impermeable rigid surface does not disturb the incoming flow. A realistic blade however produces a thrust and because it is a body of finite extent it has to shed vorticity (section 2) and disburbs the parallel flow. Because we discuss a linear theory the disturbance velocities (v_x, v_r, v_φ) will be small. This happens when the blade is in the neighbourhood of the plan form B. We represent it by

$$\varphi - \omega t + ax + \varepsilon f_j(x,r) = 0 \quad , \quad j = 1,2, \tag{15.9}$$

$$f_1(x,r) \geq f_2(x,r), \tag{15.10}$$

where $\varepsilon f_1(x,r)$ and $\varepsilon f_2(x,r)$ describe the small deviations of respectively the upper side and the lower side of the blade from B. The number ε is a small parameter which is used to linearize the theory, we will neglect quantities of $0(\varepsilon^2)$ with respect to quantities of $0(\varepsilon)$. The leading edge and the trailing

edge of the blade correspond to the functions $x_\ell(r)$ and $x_t(r)$ used in (15.8), hence in general

$$f_1(x_\ell(r), r) = f_2(x_\ell(r), r),\ f_1(x_t(r), r) = f_2(x_t(r), r). \tag{15.11}$$

We introduced the upper-side and the lower-side of the blade. This can be done otherwise by saying, the upper-side of the blade is that side which can be approached with constant x, r and t through increasing values of φ. The other side is the lower-side. The upper-side is in general the suction side, the lower-side is in general the pressure side of the blade.

The thickness D of the blade for an arbitrary point (x,r) of the planform will now be defined. Introduce the unit normal $\vec{n}$ on the plan form, pointing in the direction of decreasing values of φ

$$\vec{n} = (n_x, n_r, n_\varphi) = \frac{-1}{(1 + a^2r^2)^{\frac{1}{2}}}\,(ar, 0, 1). \tag{15.12}$$

Determine the points of intersection of a line through the point (x,r) on the plan form and perpendicular to it, with the upper- and lower-side. Then the thickness D of the blade will be the distance of these two points of intersection

$$D(x,r) = \varepsilon\, r\, \frac{\{f_1(x,r) - f_2(x,r)\}}{(1 + a^2r^2)^{\frac{1}{2}}}. \tag{15.13}$$

At the leading and the trailing edge of the blade D = 0 (15.11).

The mean plane H_m lying in the middle of the upper- and the lower-side, has the form

$$H_m = \varphi - \omega t + ax + \varepsilon\, f_3(x,r), \tag{15.14}$$

where the camber $\varepsilon\, f_3(x,r)$ which is the deviation of H_m from the plan form B (15.8), follows from

$$f_3(x,r) = \tfrac{1}{2}\{f_1(x,r) + f_2(x,r)\}. \tag{15.15}$$

In the sequel we need the concept of the local angle of incidence α_i of H_m at some point (x,r). This is the angle which the helicoidal line at the planform hence at H = 0, through the point (x,r) forms with H_m at (x,r). This angle follows from the scalar product of the unit normal at H_m for (x,r) and the unit tangent to the helicoidal line at that point,

$$\alpha_i = -\frac{\{r(a+\varepsilon\frac{\partial}{\partial x}f_3), r\,\varepsilon\frac{\partial}{\partial r}f_3, 1\}}{\{r^2(a+\varepsilon\frac{\partial}{\partial r}f_3)^2 + (r\varepsilon\frac{\partial}{\partial r}f_3)^2 + 1\}^{\frac{1}{2}}} \cdot \frac{(1, 0, -ar)}{\{1+a^2r^2\}^{\frac{1}{2}}} + O(\varepsilon^2) =$$

$$= \frac{-\varepsilon r}{(1+a^2r^2)}\frac{\partial}{\partial x}f_3 + O(\varepsilon^2). \qquad (15.16)$$

A profile of the blade is defined as the cross section of the blade with a cylinder r = const. The profiles are symmetric with respect to the skeleton line, which is the intersection of the middle plane H_m (15.14) with the cylinder r = const.

At the upper- and lower-side of the blade we have to satisfy the boundary conditions for the flow, stating that the fluid velocities are tangent to these surfaces. Because our theory is a linearized one, these conditions will not be demanded at points of the blade itself but on the planform.

In the following we generally identify the blade of the propeller and its planform B. A chord of the blade is by definition a line r = const. at B. Chord lines can be chosen as reference lines for profiles because they lie in their neighbourhood.

We now state the problem which has to be solved by the lifting surface theory. Assume that the load Q which is defined as the pressure difference between upper and lower surface of the blade, is given as a function of position

$$Q = Q(x,r) \qquad (15.17)$$

Besides this assume that, for instance by demands on strength and stiffness, the thickness D of the blade is known at each point

$$D = D(x,r). \qquad (15.18)$$

Then the question is, how do we have to choose the middle surface H_m of the real blade so that we obtain the desired load (15.17). When H_m is found we can construct the upper- and the lower-side of the blade, because the thickness is known.

This problem can be split into two separate parts. First, what is the camber $\varepsilon f_{3D}(x,r)$ (15.14) which yields a loading $Q(x,r) \equiv 0$, while the thickness D = D(x,r) is taken into account. Second, what is the camber $\varepsilon f_{3S}(x,r)$ which yields the prescribed load Q = Q(x,r) while $D(x,r) \equiv 0$. Then the total camber needed to satisfy (15.17) under the demand (15.18) follows from

$$f_3(x,r) = f_{3D}(x,r) + f_{3S}(x,r). \tag{15.19}$$

This is allowed because our theory is linear.

The splitting of the problem into two independent parts is interesting from several points of view. By changing either the thickness D or the load Q separately, we need to take into account the changing quantity only. A simple multiplication of D or Q by a constant is reflected by a simple multiplication of f_{3D} or f_{3S} by the same constant.

16. The screw blade with thickness and without loading

We will discuss now the first part of the problem as described in the last paragraph of the previous section. How can we construct a screw blade with a prescribed thickness distribution $D(x,r)$ and without pressure differences between upper- and lower-side, $Q(x,r) \equiv 0$.

Consider a layer of sources placed at the planform B. This layer induces a disturbance potential Φ of the form ([11], page 160),

$$\Phi = -\frac{1}{4\pi} \iint_B \frac{\sigma}{R} \, dS, \tag{16.1}$$

where σ is the local strength per unit of area of the source layer and R is the distance from the point where we calculate Φ towards the place of the element of area d S. We also determine the limiting values of the normal derivative of Φ at the upper-side (1) or at the lower-side (2) respectively ([11], page 164),

$$\frac{\partial \Phi_1}{\partial n} = \frac{\sigma}{2} - \frac{1}{4\pi} \iint_B \sigma \frac{\partial}{\partial n} \frac{1}{R} \, dS, \tag{16.2}$$

$$\frac{\partial \Phi_2}{\partial n} = -\frac{\sigma}{2} - \frac{1}{4\pi} \iint_B \sigma \frac{\partial}{\partial n} \frac{1}{R} \, dS, \tag{16.3}$$

where $\frac{\partial}{\partial n}$ means differentiation in the direction of the normal $\vec{n}$ given in (15.12). Hence we find for the difference of the normal components of the disturbance velocity at both sides of the blade B

$$\frac{\partial \Phi_1}{\partial n} - \frac{\partial \Phi_2}{\partial n} = \sigma, \tag{16.4}$$

which is a well known formula in potential theory.

The condition that the fluid flows along the upper- and lower-side of the blade, follows from substitution of (15.9) into (15.3). This yields when we neglect terms of $O(\varepsilon^2)$,

$$\varepsilon U \frac{\partial f_j}{\partial x} = -\left(a v_{x,j} + \frac{v_{\varphi,j}}{r}\right), \quad j = 1,2, \tag{16.5}$$

where $v_{x,j}$ and $v_{\varphi,j}$ denote the disturbance velocity components at the upper-side ($j = 1$) or at the lower side ($j = 2$). The difference of the normal components of the disturbance velocity at both sides can now be written as

$$\frac{\partial \Phi_1}{\partial n} - \frac{\partial \Phi_2}{\partial n} = \vec{n} \cdot (v_{x,1} - v_{x,2}, v_{r,1} - v_{r,2}, v_{\varphi,1} - v_{\varphi,2}). \tag{16.6}$$

Using (15.12), (16.5), (16.4) and (16.6) we find

$$\sigma = \frac{\varepsilon\, U\, r}{(1+a^2r^2)^{\frac{1}{2}}} \cdot \left(\frac{\partial f_1}{\partial x} - \frac{\partial f_2}{\partial x}\right). \tag{16.7}$$

By the definition of the thickness D of the blade (15.13) we can write this as

$$\sigma(x,r) = U\,\frac{\partial}{\partial x}\,D(x,r) = U\,(1+a^2r^2)^{\frac{1}{2}}\,\frac{\partial D}{\partial s}\,(x,r)\ , \tag{16.8}$$

where s is a length parameter along the planform B for r = const.

This formula could have been derived more directly.
The quantity

$$U(1+a^2r^2)^{\frac{1}{2}} = (U^2+\omega^2r^2)^{\frac{1}{2}}\ , \tag{16.9}$$

is the relative velocity of the fluid with respect to B, hence the right hand side of (16.8) can be interpreted as the difference in normal velocity of the fluid at both sides of the blade, because $\partial D/\partial s$ is the difference in slope of the sides of the blade. Then in connection with (16.4) we obtain (16.8).

Now we derive a relation between the middle surface H_m (15.14) and the disturbance velocities. Consider the sum of normal components of the disturbance velocities,

$$\frac{\partial \Phi_1}{\partial n} + \frac{\partial \Phi_2}{\partial n} = \vec{n}\ .\ (v_{x,1}+v_{x,2}\ ,\ v_{r,1}+v_{r,2}\ ,\ v_{\varphi,1}+v_{\varphi,2})\ . \tag{16.10}$$

By (15.12), (16.2), (16.3), (16.4) and (15.4) we find

$$\frac{\varepsilon\, r\, U}{(1+a^2r^2)^{\frac{1}{2}}}\ \frac{\partial}{\partial x}\ f_3 = \frac{1}{2}\left(\frac{\partial \Phi_1}{\partial n} + \frac{\partial \Phi_2}{\partial n}\right) = -\frac{1}{4\pi}\iint_B \sigma\,\frac{\partial}{\partial n}\,\frac{1}{R}\ d\,S\ . \tag{16.11}$$

The physical meaning of this result can be understood in the following way. We calculate the normal component of the undisturbed parallel flow with respect to the middle plane H_m, from (15.16) we find the value

$$\alpha_i\ .\ U(1+a^2r^2)^{\frac{1}{2}} = -\frac{\varepsilon\, r\, U}{(1+a^2r^2)^{\frac{1}{2}}}\ \frac{\partial}{\partial x}\ f_3\ . \tag{16.12}$$

This however is exactly minus the left hand side of (16.11). Hence when we disturb the parallel flow only by the second term of the right hand sides of (16.2) and (16.3), there results a flow tangent to the middle surface. The first term at the right hand sides of (16.2) and (16.3) takes care of difference in slope at both sides of the blade.

The middle surface H_m is not defined uniquely by (16.11). We can choose at the planform B some line ℓ in which H_m cuts B, for instance a line x = const. Then by integration with respect to x along lines r = const., we can determine f_3, hence H_m.

We have the following result. Given the thickness distribution $D = D(x,r)$ of the blade. From (16.8) we find the source distribution (sinks when $\sigma < 0$) on the blade B. By (16.11) we construct a middle surface H_m, around which we have to build symmetrically the blade with the prescribed thickness.

One question is left, are the pressures at both sides of the blade, constructed in the way just mentioned, equal to each other so that $Q \equiv 0$. This follows directly from the fact that we have used only sources and sinks to represent the blade. The instationary linearized version of Bernoulli's law ([12], page 99) reads in our case

$$p = -\mu \left(\frac{\partial \Phi}{\partial t} + U \frac{\partial \Phi}{\partial x}\right), \tag{16.13}$$

which we apply in the neighbourhood of the blade. Because the blade rotates, we can replace the partial derivative with respect to t by a derivative with respect to φ, as follows

$$p = -\mu \left(-\frac{\partial \Phi}{r\partial \varphi} r\omega + U \frac{\partial \Phi}{\partial x}\right). \tag{16.14}$$

This is the inner product of grad Φ and $(U,0,-\omega r)$. The latter vector is the velocity of a particle of the undisturbed parallel flow with respect to the planform B. This means that (16.14) represents the rate of change of Φ by moving along the planform with r = const. with a velocity $(U^2 + \omega^2 r^2)^{\frac{1}{2}}$. Hence we can write

$$p = -\mu \left(U^2 + \omega^2 r^2\right)^{\frac{1}{2}} \frac{\partial \Phi}{\partial s}, \tag{16.16}$$

where s is a length parameter along B for r = const. It is well known ([11], page 160) that the tangential derivative of the potential of a layer of sources is continuous across the layer. Hence p has at both sides of B the same value.

17. The velocity field induced by a rotating force

After having discussed in the previous section the ship screw with prescribed thickness $D = D(x,r)$ and zero loading $Q \equiv 0$, we consider the ship screw with zero thickness $D \equiv 0$ and prescribed loading, $Q = Q(x,r)$. First determine explicitly the principal tool namely the Green function used in the integral representation of the geometry of such a screw. This Green function is the velocity field induced by a rotating force perpendicular to and rotating with the helicoidal reference surface (15.7), its point of application moves along the line $x = \xi$, $r = \rho$.

The relevant features of this velocity field are described in sections 5 and 7, however we cannot use these formulas directly because they are derived for a force moving in a fluid at rest while here we have an incoming velocity U. First we will show how we can reformulate the problem slightly so that we can apply the theory of sections 5 and 7.

The helicoidal reference surface $H = \varphi - \omega t + ax = 0$ rotates about the x asis and is placed in an incoming parallel flow with velocity U in the + x direction. On this surface we have, using cylindrical coordinates, a point $A = (\xi, \rho, \theta + \omega t)$. This point is on H when $\theta = -a\xi$.

At the point A there is a force of strength h, perpendicular to H and with a component in the $+\varphi$ direction, hence it can be represented by

$$\vec{h} = (h_\xi, h_\rho, h_\theta) = -h\vec{n} = h\,\frac{(a\rho, 0, 1)}{(1 + a^2\rho^2)^{\frac{1}{2}}}, \tag{17.1}$$

where $\vec{n}$ is given in (15.12). We remark that the components of $\vec{h}$ given in (17.1) are in the local directions of the coordinate system at the point (ξ,ρ,θ). This force is assumed to be rotating already infinitely long so that its vortex system stretches at each moment t along the helicoidal line L

$$L : \varphi - \omega t + ax = 0 \quad , \quad r = \rho = \text{const.}, \tag{17.2}$$

upto $x = +\infty$.

With respect to the coordinate system (x,r,φ), the rotating force $\vec{h}$ keeps the same value of its axial coordinate $x = \xi$. We can however also refer this force to a cylindrical coordinate system (x',r',φ') translating in the +x direction with a velocity U, $x' = x - Ut$, $r = r'$ and $\varphi = \varphi'$. With respect to the (x', r', φ') system the fluid at $r' \to \infty$ is at rest and the force $\vec{h}$ is moving along the helicoidal line L'

$$L' : \varphi' + ax' = 0 \quad , \quad r' = \rho, \tag{17.3}$$

in the $-x'$ direction with a velocity $V = U(1 + a^2\rho^2)^{\frac{1}{2}}$ along L' and is perpendicular

to its velocity. At $t = 0$ both coordinate systems coincide and at $t = 0$ the force is at the point $A = (\xi, \rho, -a\xi)$. Because the force induces at $t = 0$ in both systems the same disturbance velocity field, it is clear that we can derive the velocity field in system (x,r,φ) at $t = 0$ also in the following way. Consider a force of strength h, moving in the negative x direction along the line ((17.2), $t = 0$) $\varphi + ax = 0$, $r = \rho = \text{const.}$, with a velocity $V = U(1 + a^2r^2)^{\frac{1}{2}}$. The force is perpendicular to $\varphi + ax = 0$ and in the $+\varphi$ direction. It started to move at $x = +\infty$ and arrives at $(\zeta,\rho,-a\xi)$ exactly at $t = 0$. The advantage of this change of view point is that now we can apply the results of sections 5 and 7.

The velocity field follows from (5.5) which reads

$$\vec{v}(x,r,\varphi,\ t = 0) = (v_x, v_r, v_\varphi) = -\frac{1}{4\pi\mu} \int_{-\infty}^{s(o)} \{ \frac{\vec{h}(s)}{V(s)\ R^3} - \frac{3\ \vec{R}.(\vec{h}(s).\vec{R})}{V(s)\ R^5} \}\, ds, \quad (17.4)$$

where the integration is performed along L. The components of all vectors in (17.4) have to be taken into the directions of the coordinate system at (x,r,φ), this is denoted by the indices x, r and φ to the components of $\vec{v}$. Hence we have to transform the components of a vector at a point (ξ,ρ,Θ) which are generally given in the directions of the coordinate system at (ξ,ρ,Θ), into the components of the same vector with respect to the coordinate directions at (x,r,φ). To carry this out we have the following simple scheme. Consider a vector $\vec{g}$ written in its components at (ξ,ρ,Θ) and at (x,r,φ) hence

$$\vec{g} = (g_\xi, g_\rho, g_\Theta)\ ;\ \vec{g} = (g_x, g_r, g_\varphi) \quad (17.5)$$

then

$$g_x = g_\xi\ ;\ g_r = g_\rho \cos(\varphi - \Theta) + g_\Theta \sin(\varphi - \Theta)\ ;\ g_\varphi = -g_\rho \sin(\varphi - \Theta) + g_\Theta \cos(\varphi - \Theta). \quad (17.6)$$

In (17.1) are given $(h_\xi, h_\rho, h_\Theta)$ hence we can write also

$$\vec{h} = (h_x, h_r, h_\varphi) \equiv \frac{h}{(1 + a^2\rho^2)^{\frac{1}{2}}} (a\rho, \sin(\varphi - \tilde{\Theta}), \cos(\varphi - \tilde{\Theta})), \tilde{\Theta} = -a\tilde{\xi}\ , \quad (17.7)$$

we have given the Θ and ξ a "tilde" in order to denote that in the integral (17.4) $\tilde{\xi}$ becomes a variable with respect to which the integration is carried out. Analogously we find for the vector $\vec{R}$ from (ξ,ρ,Θ) towards (x,r,φ),

$$\vec{R} = (R_x, R_r, R_\varphi) = (x - \tilde{\xi},\ r = \rho \cos(\varphi - \tilde{\Theta}), \rho \sin(\varphi - \tilde{\Theta})), \tilde{\Theta} = -a\tilde{\xi}\ . \quad (17.8)$$

Substitution of (17.7) and (17.8) into (17.4) yields

$$\vec{v}(x,r,\varphi,t=0) = (v_x, v_r, v_\varphi) = -\frac{1}{4\pi\mu}\,\frac{h}{U(1+a^2\rho^2)^{\frac{1}{2}}}\int_{\xi}^{\infty}\Big[\frac{(a\rho,\ \sin(\varphi+a\tilde{\xi}),\ \cos(\varphi+a\tilde{\xi}))}{R^3} +$$

$$-3\,\frac{(x-\tilde{\xi},\ r-\rho\cos(\varphi+a\tilde{\xi}),\rho\sin(\varphi+a\tilde{\xi}))\ \{a\rho(x-\tilde{\xi})+\ r\sin(\varphi+a\tilde{\xi})\}}{R^5}\Big]\,d\tilde{\xi}\,, \qquad (17.9)$$

where $R = |\vec{R}|$, $V(s) = U(1+a^2\rho^2)^{\frac{1}{2}} = \text{const.}$ and $ds = (1+a^2\rho^2)^{\frac{1}{2}}\,d\tilde{\xi}$.

In order to bring this integral into a form used in literature we put $\tilde{\xi} = -\tau + x$, then

$$\vec{v}(x,r,\varphi,t=0) = (v_x,\ v_r,\ v_\varphi) = \frac{1}{4\pi\mu}\,\frac{h}{U(1+a^2\rho^2)^{\frac{1}{2}}}\int_{-\infty}^{(x-\xi)}$$

$$\Big[-\frac{(a\rho,\ \sin(\varphi+a(x-\tau)),\ \cos(\varphi+a(x-\tau)))}{R^3} +$$

$$+3\,\frac{(\tau,\ r-\rho\cos(\varphi+a(x-\tau)),\rho\sin(\varphi+a(x-\tau)))\ ,\ \{a\rho\tau+\ r\sin(\varphi+a(x-\tau))\}}{R^5}\Big]\,d\tau,$$

(17.10)

where

$$R = \{\tau^2+r^2+\rho^2-2r\rho\cos(\varphi+a(x-\tau))\}^{\frac{1}{2}}. \qquad (17.11)$$

We will give another representation of this velocity field by using the vortex model of section 7. The velocity field consists of two parts in our case. First we have a contribution $\vec{v}_1$, by the short vortex which represents the force and for which the contribution is given by the upper bound in (7.12). The relevant quantities in that formula are $V(s) = U(1+a^2\rho^2)^{\frac{1}{2}}$, the vector $\vec{k}$ pointing in the $+\rho$ direction hence by (17.6)

$$\vec{k} = (k_\xi,\ k_\rho,\ k_\Theta) = (0,1,0) \rightarrow \vec{k} = (k_x,\ k_r,\ k_\varphi) = (0,\ \cos(\varphi-\Theta),\ -\sin(\varphi-\Theta),\Theta = -a\xi\ ,$$

(17.12)

and the vector $\vec{R}$, given in (17.8) however without tilde, because here we consider the point $(\xi,\rho,-a\xi)$ where at $t = 0$ the force is acting. In this way the contribution of (7.12) becomes

$$\vec{v}_1(x,r,\varphi,t=0) = (v_{1x},v_{1r},v_{1\varphi}) = -\frac{1}{4\pi\mu}\,\frac{h}{U(1+a^2\rho^2)^{\frac{1}{2}}}$$

$$\frac{(r\sin(\varphi+a\xi),-(x-\xi)\sin(\varphi+a\xi),-(x-\xi)\cos(\varphi+a\xi))}{\{(x-\xi)^2+r^2+\rho^2-2r\rho\cos(\varphi+a\xi)\}^{3/2}}\,. \qquad (17.13)$$

Second we have to add to $\vec{v}_1$ the contribution $\vec{v}_2$ from the two tip vortices (figure 7.1), given in (7.8). This formula reads in our case

$$\vec{v}_2 = (v_{2x},v_{2r}\ v_{2\varphi}) = \frac{1}{4\pi\mu}\int_{\infty}^{\xi}\frac{h}{U\sqrt{1+a^2\rho^2}}\,\frac{d}{d\lambda}\left\{(\vec{i}+\lambda\frac{d\vec{k}}{ds})\otimes\frac{(\vec{R}-\lambda\vec{k})}{|\vec{R}-\lambda\vec{k}|^3}\right\}\Big|_{\lambda=0}\cdot -(1+a^2\rho^2)^{\frac{1}{2}}d\tilde{\xi}, \qquad (17.14)$$

where we changed from the parameter s in (7.8) to the parameter $\tilde{\xi} = -(1+a^2\rho^2)^{-\frac{1}{2}}s$. The quantities in the integrand are the following and can be determined easily, first

$$\vec{i} = (i_{\tilde{\xi}},i_{\rho},i_{\tilde{\theta}}) = \frac{(-1,0,a\rho)}{(1+a^2\rho^2)^{\frac{1}{2}}}\,,\quad \vec{i} = (i_x,i_r,i_\varphi) = \frac{(-1,\ a\rho\sin(\varphi+a\tilde{\xi}),a\rho\cos(\varphi+a\tilde{\xi})}{(1+a^2\rho^2)^{\frac{1}{2}}}\,. \qquad (17.15)$$

In (17.12) $\vec{k}$ is given, from which we find by differentiating

$$\frac{d\vec{k}}{ds} = -\frac{d\vec{k}}{d\tilde{\xi}}\,\frac{d\tilde{\xi}}{ds} = -\frac{1}{(1+a^2\rho^2)^{\frac{1}{2}}}\,(0,-a\sin(\varphi+a\tilde{\xi}),\ -a\cos(\varphi+a\tilde{\xi}))\,, \qquad (17.16)$$

which are the components "at x,r,φ". At last $\vec{R}$ is given in (17.8).

We now can carry out the vector product in (17.14) and find

$$\vec{v}_2 = \frac{1}{4\pi\mu}\,\frac{h}{U(1+a^2\rho^2)^{\frac{1}{2}}}\,\frac{d}{d\lambda}\int_{\xi}^{\infty}\Big(\frac{(a(\rho+\lambda)^2-ar(\rho+\lambda)\cos(\varphi+a\tilde{\xi}),(x-\xi)a(\rho+\lambda)\cos(\varphi+a\tilde{\xi})+$$

$$\frac{+(\rho+\lambda)\ \sin(\varphi+a\tilde{\xi}),-r+(\rho+\lambda)\ \cos(\varphi+a\tilde{\xi})-(x-\tilde{\xi})a(\rho+\lambda)\sin(\varphi+a\tilde{\xi})}{|\vec{R}-\lambda\vec{k}|^3}\Big)d\xi\Big|_{\lambda=0}\cdot \qquad (17.17)$$

In order to bring this formula in the form used in the literature we change again the integration variable into $\tau = -\tilde{\xi} + x$. Further we remark that in the integrand only the combination $(\rho + \lambda)$ occurs, hence we can put $\lambda = 0$ and change the differentiation with respect to λ into a differentiation with respect to ρ. We find

$$\vec{v}_2 = \frac{1}{4\pi\mu} \frac{h}{U(1+a^2\rho^2)^{\frac{1}{2}}} \frac{\partial}{\partial\rho} \int_{-\infty}^{x-\xi} \{ \frac{a\rho^2 - ar\rho\cos(\varphi + a(x-\tau)),}{}$$

$$\frac{\tau\, a\rho\cos(\varphi + a(x-\tau)) + \rho\sin(\varphi + a(x-\tau)), -r + \rho\cos(\varphi + a(x-\tau)) - \tau a\rho\sin(\varphi + a(x-\tau))}{(\tau^2 + r^2 + \rho^2 - 2r\rho\cos(\varphi + a(x-\tau)))^{3/2}}$$

$$d\tau. \quad (17.18)$$

The total velocity is then given by $\vec{v}_1 + \vec{v}_2$,

$$\vec{v} = (v_x, v_r, v_\varphi) = \frac{h}{4\pi\mu U(1+a^2\rho^2)^{\frac{1}{2}}} \{ \frac{(-r\sin(\varphi + a\xi), (x-\xi)\sin(\varphi + a\xi), (x-\xi)\cos(\varphi + a\xi))}{\{(x-\xi)^2 + r^2 + \rho^2 - 2r\rho\cos(\varphi + a\xi)\}^{3/2}} +$$

$$+ \frac{\partial}{\partial\rho} \int_{-\infty}^{x-\xi} \frac{(a\rho^2 - ar\rho\cos(\varphi + a(x-\tau)), \tau a\rho\cos(\varphi + a(x-\tau)) + \rho\sin(\varphi + a(x-\tau)),}{}$$

$$\frac{-r + \rho\cos(\varphi + a(x-\tau)) - \tau a\rho\sin(\varphi + a(x-\tau))}{(\tau^2 + r^2 + \rho^2 - 2r\rho\cos(\varphi + a(x-\tau)))^{3/2}} d\tau \}. \quad (17.19)$$

18. The screw blade of zero thickness with prescribed load, a.

We will discuss the screw blade of zero thickness and prescribed load $Q(x,r)$. It is only necessary to consider the blade in its position at $t = 0$ because during its rotation in a homogeneous incoming flow the pressures on it are independent of time. All positions are equivalent in the sense that the whole disturbance field of the propeller rotates with the blade and is independent of time with respect to the blade.

Two different ways can be followed. One way is by using the representation of the velocity field (17.10) for a rotating singular force, the other way is by using (17.19). We will treat both methods separately and start with the first one.

Suppose the screw blade, with zero thickness, is defined by

$$\varphi - \omega t + ax + \varepsilon f(x,r) = 0 \tag{18.1}$$

$$x_\ell(r) \leq x \leq x_t(r) \quad , \quad r_i \leq r \leq r_o. \tag{18.2}$$

The condition (15.3) for the fluid flow to be tangent to the blade, becomes

$$\varepsilon U \frac{\partial f}{\partial x} = - \left(av_x + \frac{v_\varphi}{r}\right). \tag{18.3}$$

We assume that the blade experiences a load $Q = Q(x,r)$ perpendicular to the blade as a result of the action of the fluid. This load is called positive $Q > 0$, when it has a component in the negative x direction, hence when it contributes to the thrust of the propeller. Inversely an elementary area dS of the blade exerts a force QdS on the fluid in the direction of increasing φ, by this it is allowed to replace h by QdS in formulas (17.10) and (17.19) in order to find the velocity field induced by the elementary force QdS.

We want to determine the right hand side of (18.3) at the blade, then also $\partial f/\partial x$ is known and by an integration we can find $f(x,r)$. Then by (18.1) the blade is known. First we calculate the right hand side of (18.3) for a point (x,r,φ) at a finite distance of the blade. By (17.10) we find

$$-4\pi\mu Ur\left(av_x + \frac{v_\varphi}{r}\right) = \iint_B Q(\xi,\rho) \int_{-\infty}^{(x-\xi)} \left[\frac{\{a^2 r\rho + \cos(\varphi + a(x-\tau))\}}{R^3} + \right.$$

$$\left. -3\,\frac{\{ar\tau + \rho\,\sin(\varphi + a(x-\tau))\}\{a\rho\tau + r\,\sin(\varphi + a(x-\tau))\}}{R^5}\right] d\tau d\xi d\rho \overset{\text{def}}{=\!=}$$

$$= \iint_B Q(\xi,\rho) \int_{-\infty}^{(x-\xi)} G(x,r,\varphi,\rho,\tau)\,d\tau d\xi d\rho \overset{\text{def}}{=\!=} \iint_B Q(\xi,\rho)\, K^*(x,r,\varphi,\xi,\rho)\,d\xi d\rho, \tag{18.4}$$

where we replaced the element of area dS by $(1 + a^2\rho^2)^{\frac{1}{2}}d\xi d\rho$, introduced the functions G and K* and where (17.11)

$$R = \{\tau^2 + r^2 + \rho^2 - 2r\rho\cos(\varphi + a(x-\tau))\}^{\frac{1}{2}}. \tag{18.5}$$

As has been said, we have to take the limit $(x,r,\varphi) \to (a,r,-ax)$, where x and r satisfy (18.2), then the point (x,r,φ) tends to the blade. From (18.3) we find

$$4\pi\mu\varepsilon\, U^2 r\, \frac{\partial f}{\partial x}(x,r) = \lim_{\varphi \to -ax} \iint_B Q(\xi,\rho)\, K^*(x,r,\varphi,\xi,\rho)\,d\xi d\rho. \tag{18.6}$$

First we simply try to interchange the limit procedure and the integration. Hence we have to consider the kernel function

$$K(x,r,\xi,\rho) \overset{\text{def}}{=\!=} K^*(x,r,-ax,\xi,\rho) =$$

$$= \int_{-\infty}^{(x-\xi)} \left[\frac{\{a^2r\rho + \cos a\tau\}}{\{\tau^2 + r^2 + \rho^2 - 2r\rho\cos a\tau\}^{3/2}} - \frac{3\{ar\tau - \rho\sin a\tau\}\{a\rho\tau - r\sin a\tau\}}{\{\tau^2 + r^2 + \rho^2 - 2r\rho\cos a\tau\}^{5/2}} \right] d\tau. \tag{18.7}$$

When $x - \xi > 0$ and $\rho \to r$ this function becomes infinite. The singularity arises from a small part of the range of integration in the neighbourhood of $\tau = 0$ because there the denominator tends to zero for $\tau \to 0$ and $\rho \to r$. For the study of this singular behaviour the range of integration in (18.7) can be changed into $-\alpha \leq \tau \leq \alpha$, where α is some sufficiently small but fixed positive number. Putting $\rho = r + \nu$, where $|\nu|$ is assumed to be small, we expand the numerators in (18.7) with respect to τ and ν, then we obtain integrals of the form

$$\nu^\ell \int_{-\alpha}^{+\alpha} \frac{\tau^m d\tau}{\{\tau^2 + r^2 + (r+\nu)^2 - 2r(r+\nu)\cos a\tau\}^{q/2}} \leq \nu^\ell \int_{-\alpha}^{+\alpha} \frac{\tau^m d\tau}{\{\tau^2 + \nu^2\}^{q/2}} \leq$$

$$\leq 2\nu^{\ell+m+1-q} \int_0^{+\alpha/\nu} \frac{\xi^m}{\{\xi^2+1\}^{q/2}}\, d\xi \leq \nu^{\ell+m+1-q}\{1 + \int_1^{\alpha/\nu} \xi^{m-q}\, d\xi\}, \tag{18.8}$$

where ℓ and m are 0,1,2,... and q = 3 or 5. It is seen easily that for $\ell + m \geq q - 1$ this expression remains finite or increases logarithmically when $\nu \to 0$. By this we have to expand the numerators of the first and the second term under the integral sign in (18.7), only up to and including terms of the second and the fourth order, respectively. By doing this we find after an estimation of the resulting integrals

$$K(x,r,\xi,\rho) \approx \frac{2(1+a^2r^2)^{\frac{1}{2}}}{(r-\rho)^2} - \frac{ra^2}{(1+a^2r^2)^{\frac{1}{2}}(r-\rho)} + O(\ell n\ |r-\rho|),\ \xi < x,\ \rho \to r \qquad (18.9)$$

This singularity cannot be integrated in the ρ direction. Hence the interchange of the limit $\varphi \to -ax$ and the integral in (18.6) is not allowed. A more careful method for giving a meaning to this limit will be given in the following.

We divide the area of the blade into three regions (figure 18.1). The

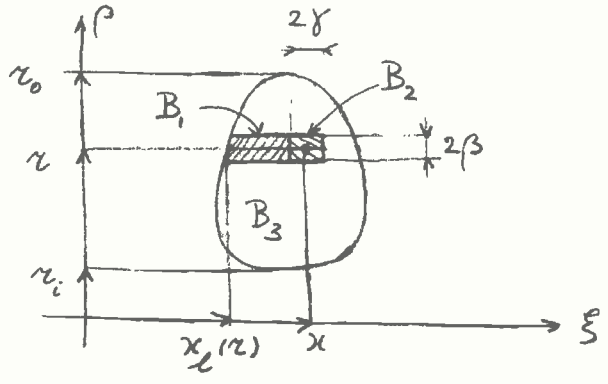

Fig. 18.1. The domain of integration $B = B_1 + B_2 + B_3$.

strip B_1 defined by $x_\ell(r) \le \xi \le x - \gamma$, $|\rho - r| \le \beta$, where $x_\ell(r)$ is the leading edge (15.8), γ and β are sufficiently small positive quantities. Next the rectangle B_2 defined by $|x - \xi| \le \gamma$, $|\rho - r| \le \beta$ and the remaining part B_3.

The domain B_3 does not yield any difficulty in the limiting process $\varphi \to -ax$, because for its points (ξ,r) the value of $(r - \rho)$ does not become zero.

The integration in (18.4) over B_1 when first $\varphi \to -ax$ and then $\beta \to 0$, can be written as

$$\lim_{\varphi \to -ax} \int_{x_\ell(r)}^{x-\gamma} \int_{r-\beta}^{r+\beta} Q(\xi,\rho) \left\{ \int_{-\alpha}^{+\alpha} G(x,r,\varphi,\rho,\tau)\, d\tau \right\} d\rho d\xi, \qquad (18.10)$$

where α is again a small, however fixed quantity. The restriction of the integration over τ to the interval $(-\alpha, +\alpha)$ is valid because only the singular part of the kernel can possibly yield a contribution to the integral over the strip of vanishing width, $\beta \to 0$. We introduce the new variables δ and ν, by

$$\delta = \varphi + ax\ ,\ \nu = \rho - r. \qquad (18.11)$$

Substitution of (18.11) into (18.10) yields

$$\lim_{\delta\to 0} \int_{x_\ell(r)}^{x-\gamma} \int_{-\beta}^{+\beta} Q(\xi, r+\nu) \left\{ \int_{-\alpha}^{+\alpha} G(x, r, -ax+\delta, r+\nu, \tau)\, d\tau \right\} d\nu\, d\xi. \tag{18.12}$$

First we consider the integrations with respect to τ and ν. When α, β and δ are sufficiently small we assume that we can expand $Q(\xi, r+\nu)$ and the two numerators in the function $G(x, r, -ax+\delta, r+\nu, \tau)$ (18.4) with respect to τ, ν and δ. Then we obtain integrals of the form

$$I(\ell, m, n, q) = \delta^{\ell} \int_{-\beta}^{+\beta} \int_{-\alpha}^{+\alpha} \frac{\tau^m \nu^n \, d\tau \, d\nu}{\{\tau^2 + r^2 + (r+\nu)^2 - 2r(r+\nu)\cos(\delta - a\tau)\}^{q/2}}, \tag{18.13}$$

where

$$\ell \geq 0, \; m \geq 0, \; n \geq 0, \; q = 3 \text{ or } 5. \tag{18.14}$$

We have to keep in mind that we consider the limiting procedure, first $\delta \to 0$ for fixed β, $0 \leq \beta \leq \beta_0$ and then $\beta \to 0$. There exists a constant $k > 0$, independent of β, such that

$$|I(\ell, m, n, q)| \leq |\delta|^{\ell} \int_{-\beta}^{+\beta} \int_{-\alpha}^{+\alpha} \frac{|\tau|^m |\nu|^n \, d\tau \, d\nu}{\{\tau^2 + \nu^2 + k\, r^2 (a\tau - \delta)^2\}^{q/2}}. \tag{18.15}$$

Next we introduce new variables of integration τ^* and ν^* by

$$\tau = |\delta| \{\tau^* (1 + ka^2 r^2)^{-\frac{1}{2}} \pm a k r^2 (1 + k a^2 r^2)^{-1}\} \overset{\text{def}}{=\!=} |\delta|(a, \tau^* \pm a_2), \quad \delta \gtrless 0, \tag{18.16}$$

$$\nu = |\delta| \nu^*, \tag{18.17}$$

where the upper signs are related to $\delta > 0$ and the lower signs to $\delta < 0$, this will be assumed also in the following. Substitution of (18.16) and (18.17) into (18.15) and neglecting the asterisks, yields

$$|I(\ell, m, n, q)| \leq a_1 |\delta|^{(\ell+m+n-q+2)} \int_{-\beta/|\delta|}^{\beta/|\delta|} |\nu|^n d\nu \int_{-a_1^{-1}(\frac{\alpha}{|\delta|} \pm a_2)}^{a_1^{-1}(\frac{\alpha}{|\delta|} \mp a_2)} \frac{|a_1 \tau \pm a_2|^m}{(\tau^2 + \nu^2 + a_3)^{q/2}} \, d\tau, \tag{18.18}$$

where

$$a_3 = \frac{k\, r^2}{(1 + ka^2 r^2)}. \tag{18.19}$$

The constant $a_3 \neq 0$ for $r \geq r_i > 0$, which will be assumed in the following.

It is clear that in (18.18) the origin $\tau = \nu = 0$ is no longer the dangerous location when $\delta \to 0$. The singular behaviour of the two dimensional integral is now determined by the behaviour of the integrand for large values of τ and ν. This means that we can replace (18.18) by

$$|I(\ell,m,n,q)| \leq C_1 |\delta|^{(\ell+m+n-q+2)} \int_0^{\beta/|\delta|} \nu^n d\nu \int_0^{a_1^{-1}(\frac{\alpha}{|\delta|} \mp a_2)} \frac{\tau^m}{(\tau^2+\nu^2+a_3)^{q/2}} d\tau, \tag{18.20}$$

where C_1 is a suitable constant independent of β

We now consider the case

$$\ell + m + n = q + 2 \geq 1. \tag{18.21}$$

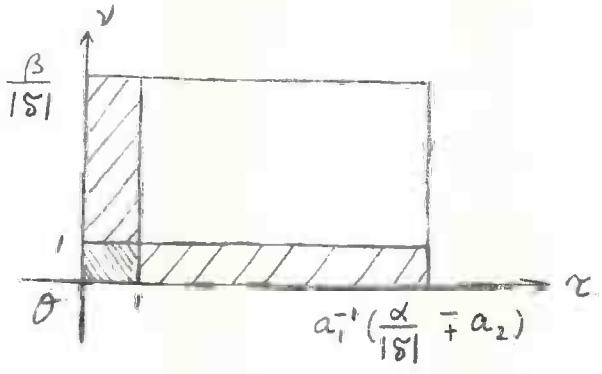

Fig. 18.2. Several parts of the domain of integration in (18.20), $|\delta| \ll \beta$.

Then it is allowed to neglect in (18.20) the area of integration $0 \leq \tau, \nu \leq 1$ (figure 18.2), of which the contribution $|I(\ell,m,n,q)|$ tends to zero with δ because $a_3 > 0$ (18.19). We consider also separately the area of integration

$$0 \leq \tau \leq 1, \quad 1 \leq \nu \leq \beta/|\delta|.$$

$$C_1 |\delta|^{(\ell+m+n-q+2)} \int_1^{\beta/|\delta|} \nu^n d\nu \int_0^1 \frac{\tau^m d\tau}{(\tau^2+\nu^2+a_3)^{q/2}} \leq C_2 |\delta|^{(\ell+m+n-q+2)} \cdot \int_1^{\beta/|\delta|} \nu^{n-q+\varepsilon} d\nu =$$

$$= C_2 |\delta|^{(\ell+m+n-q+2)} \frac{\nu^{n-q+1+\varepsilon}}{(n-q+1+\varepsilon)} \Bigg|_1^{\beta/|\delta|}, \tag{18.22}$$

where C_2 is a suitable constant independent of β and ε a sufficiently small positive fixed number, introduced to keep the denominator of the last expression away from zero. Then we find (18.22) $\to 0$ when $\delta \to 0$. Analogously we estimate the contribution of the area of integration, $0 \le \nu \le 1$, $1 \le \tau \le a_1^{-1}(\frac{\alpha}{|\delta|} + a_2)$, which also tends to zero for $\delta \to 0$.

In this way we can replace (18.20) by

$$|I(\ell,m,n,q)| \le C_1 |\delta|^{\ell+m+n-q+2} \int_1^{\beta/|\delta|} \nu^n d\nu \int_1^{a_1^{-1}(\frac{\alpha}{|\delta|} \mp a_2)} \frac{\tau^m}{(\tau^2+\nu^2+a_3)^{q/2}} d\tau + o(\delta), \tag{18.23}$$

where $o(\delta)$ is a quantity which tends to zero with δ.

We estimate the denominator of the integral as follows

$$(\tau^2+\nu^2+a_3)^{q/2} = \tau^{\frac{q}{2}(2-\varepsilon)} \nu^{\frac{q\varepsilon}{2}} \{(\frac{\tau}{\nu})^{\varepsilon} + (\frac{\nu}{\tau})^{2-\varepsilon} + \frac{a_3}{\tau^{2-\varepsilon}\nu^{\varepsilon}}\}^{q/2} \ge$$

$$\ge \tau^{\frac{q}{2}(2-\varepsilon)} \nu^{\frac{q\varepsilon}{2}}, \tag{18.24}$$

where ε is a sufficiently small positive fixed number. This holds because we have $\tau/\nu \ge 1$ or $\nu/\tau \ge 1$ in (18.23). Hence we find from (18.23)

$$|I(\ell,m,n,q)| \le C_1 |\delta|^{(\ell+m+n-q+2)} \int_1^{\beta/|\delta|} \nu^{(n-\frac{\varepsilon q}{2})} d\nu \int_1^{a_1^{-1}(\frac{\alpha}{|\delta|} \mp a_2)} \tau^{(m-q+\frac{\varepsilon q}{2})} d\tau =$$

$$= C_1 \frac{|\delta|^{(\ell+m+n-q+2)}}{(n-\frac{\varepsilon q}{2}+1)(m-q+\frac{\varepsilon q}{2}+1)} \nu^{(n-\frac{\varepsilon q}{2}+1)} \Big|_1^{\beta/|\delta|} \tau^{(m-q+\frac{\varepsilon q}{2}+1)} \Big|_1^{a_1^{-1}(\frac{\alpha}{|\delta|} \mp a_2)} + o(\delta) =$$

$$= O(|\delta|^{\ell} \beta^{(n-\frac{\varepsilon q}{2}+1)}) + o(\delta). \tag{18.25}$$

For $\ell \ge 1$ this tends to zero with $\delta \to 0$, for $\ell = 0$ it tends to zero with $\beta \to 0$.

We have found the result that under condition (18.21), the integrals (18.13) tend to zero under the limits first $\delta \to 0$, or what is the same $\varphi \to -ax$ and then $\beta \to 0$.

Next we consider more closely the expansions of the function $Q(\xi, r+\nu)$ and of the two numerators in $G(x,r,-ax+\delta, r+\nu,\tau)$ in (18.12). From the foregoing result it follows that we have to develop these functions to such an extent that (18.21),

$$\ell + m + n \leq 1 \ , \ q = 3 \ ; \quad \ell + m + n \leq 3 \ , \ q = 5, \tag{18.26}$$

higher order terms will not give a contribution in the limit procedure under consideration.

First we consider the numerators of $G(x,r,-ax+\delta, r+\nu,\tau)$ (18.4). In connection with (18.26) and the definitions of ℓ, m and ν (18.13) we take

$$\{a^2 r(r+\nu) + \cos(\delta - a\tau)\} = \{(1 + a^2 r^2) + a^2 r\,\nu + \ldots\ldots\} \ , \ q = 3, \tag{18.27}$$

$$-3\{ar\,\tau + (r+\nu)\sin(\delta - a\tau)\}\{a(r+\nu)\tau + r\sin(\delta - a\tau)\} = -3\{r^2\delta^2 + r\,\nu\,\delta^2\}, \ q = 5, \tag{18.28}$$

where ν and τ have there original meaning. In connection with (18.26) it follows that we have to expand $Q(\xi, r+\nu)$ only up to and including terms of the first order

$$Q(\xi, r+\nu) \approx Q(\xi,r) + \nu \frac{\partial Q}{\partial r}(\xi,r) + \ldots\ldots . \tag{18.29}$$

Then we find for (18.12), when we still disregard for a while the integration with respect to ξ

$$\lim_{\delta \to 0} \int_{-\beta}^{+\beta} \{Q(\xi,r) + \nu \frac{\partial Q}{\partial r}(\xi,r) + \ldots\} \cdot \int_{-\alpha}^{+\alpha} \Big[\frac{\{(1 + a^2 r^2) + a^2 r\,\nu + \ldots\}}{\{\tau^2 + r^2 + (r+\nu)^2 - 2r(r+\nu)\cos(\delta + a\tau)\}^{3/2}} +$$

$$- \frac{3\{r^2\delta^2 + r\,\nu\,\delta^2 + \ldots\}}{\{\tau^2 + r^2 + (r+\nu)^2 - 2r(r+\nu)\cos(\delta + a\tau)\}^{3/2}} \Big] d\tau d\nu \ , \tag{18.30}$$

where we replaced the variable of integration τ by $-\tau$. Next we want to expand the cosine in the denominators. We write

$$\{\tau^2 + r^2 + (r+\nu)^2 - 2r(r+\nu)\cos(\delta + a\tau)\} = \{\tau^2 + \nu^2 + r^2(\delta + a\tau)^2\}\{1 + 0((\delta + a\tau)^2$$

$$\cdot (\nu + (\delta + a\tau)^2)\} \tag{18.31}$$

which is upto and including second order quantities even in ν.

Using this property and again (18.26), we find by expanding the denominators in (18.30) that we can replace (18.30) by

$$\lim_{\delta\to 0} Q(\xi,r) \int_{-\beta}^{+\beta}\int_{-\alpha}^{+\alpha} \left[\frac{(1+a^2r^2)}{\{\tau^2+\nu^2+r^2(\delta+a\tau)^2\}^{3/2}} - \frac{3r^2\delta^2}{\{\tau^2+\nu^2+r^2(\delta+a\tau)^2\}^{3/2}}\right] d\tau d\nu, \tag{18.32}$$

We now choose new variables of integration λ and σ as follows

$$\nu = \frac{r\delta}{(1+a^2r^2)^{\frac{1}{2}}}\lambda \quad , \quad \tau = \frac{r\delta}{(1+a^2r^2)}\cdot(\sigma - ar). \tag{18.33}$$

Then (18.32) changes into

$$\frac{(1+a^2r^2)}{r} Q(\xi,r) \lim_{\delta\to 0} \frac{1}{\delta} \int_{-\frac{\beta_1}{\delta}}^{+\frac{\beta_1}{\delta}} \int_{-\frac{\alpha_1}{\delta}+\alpha_2}^{+\frac{\alpha_1}{\delta}+\alpha_2} \left\{\frac{1}{(\sigma^2+\lambda^2+1)^{3/2}} - \frac{3}{(\sigma^2+\lambda^2+1)^{5/2}}\right\} \cdot d\lambda d\sigma, \tag{18.34}$$

where

$$\beta_1 = \frac{\sqrt{1+a^2r^2}}{r}\beta \quad , \quad \alpha_1 = \frac{(1+a^2r^2)\alpha}{r} \quad , \quad \alpha_2 = ar, \tag{18.35}$$

and where we assume $\delta \to 0$ through positive values.

First we remark that

$$\int_{-\infty}^{+\infty}\int_{-\infty}^{+\infty} \left\{\frac{1}{(\sigma^2+\lambda^2+1)^{3/2}} - \frac{3}{(\sigma^2+\lambda^2+1)^{5/2}}\right\} d\lambda d\sigma = 2\pi \int_0^{+\infty} \left\{\frac{1}{(\rho^2+1)^{3/2}} - \frac{3}{(\rho^2+1)^{5/2}}\right\} \cdot \rho d\rho = 0 \tag{18.36}$$

hence a finite limit for $\delta \to 0$ is possible in (18.34). The integrals in (18.34) can be calculated in closed form ([7], I, page 48, 13) and page 49, 18a), 18b)). We do not enter in all details but state that after some calculations we can write (18.34) in the form

$$= \frac{4\sqrt{1+a^2r^2}\, Q(\xi,r)}{\beta} + 0(\beta). \tag{18.37}$$

This result substituted into (18.12) yields for the contribution of the strip B_1 (figure 18.1) to the integral (18.4)

$$\frac{-4\sqrt{1+a^2r^2}}{\beta} \int_{x_\ell(r)}^{x-\gamma} Q(\xi,r)d\xi + O(\beta). \tag{18.38}$$

The remaining part of the integration over the blade, is over the region B_2 (figure 18.1) in which the point (x,r) is situated. The contribution of B_2, when first $\varphi \to -ax$ and then $\beta \to 0$, has the form

$$\lim_{\varphi \to -ax} \int_{r-\beta}^{r+\beta} d\rho \int_{x-\gamma}^{x+\gamma} d\xi\, Q(\xi,\rho) \int_{-\infty}^{x-\xi} G(x,r,\varphi,\rho,\tau)d\tau =$$

$$= \lim_{\varphi \to -ax} \sum_{n,m=0}^{\infty} Q_{mn} \int_{r-\beta}^{r+\beta} (\rho - r)^n d\rho \int_{x-\gamma}^{x+\gamma} (\xi - x)^m d\xi \int_{-\infty}^{x-\xi} G(x,r,\varphi,\rho,\tau)d\tau , \tag{18.39}$$

where

$$Q_{mn} = \frac{1}{m!n!} \frac{\partial^{m+n}}{\partial x^m \partial r^n} Q(x,r), \tag{18.40}$$

and we assumed the expansion of Q to be valid, as well as the change of summation and integration.

Introducing again the variables $\delta = \varphi + ax$ and $\nu = \rho - r$ (18.11) and the new variable

$$\eta = \xi - x, \tag{18.41}$$

we write (18.39) as

$$\lim_{\delta \to 0} \sum_{n,m=0}^{\infty} Q_{mn} \int_{-\beta}^{+\beta} \nu^n d\nu \int_{-\gamma}^{+\gamma} \eta^m d\eta \int_{-\infty}^{-\eta} G(x,r,-ax+\delta, r+\nu,\tau)d\tau. \tag{18.42}$$

First we discuss the integrations with respect to η and τ. Partial integration with respect to η yields

$$\frac{1}{(m+1)} \{\eta^{m+1} \int_{-\infty}^{-\eta} G(x,r,-ax+\delta,r+\nu,\tau)d\tau \Big|_{-\gamma}^{+\gamma} + \int_{-\gamma}^{+\gamma} \eta^{m+1} G(x,r,-ax+\delta,r+\nu,-\eta) d\eta\}. \tag{18.43}$$

The value of the first term of (18.43) for the upper bound $+\gamma$ is finite because γ is fixed and positive, hence it yields no contribution to (18.42) in the limit $\delta \to 0$. Then the relevant part of (18.43) can be written as

$$\frac{1}{(m+1)}\{-(-\gamma)^{m+1}\int_{-\infty}^{+\gamma} G(x,r,-ax+\delta,r+\nu,\tau)d\tau + \int_{-\gamma}^{+\gamma}(-\tau)^{m+1}G(x,r,-ax+\delta,r+\nu,\tau)d\tau\}. \tag{18.44}$$

We consider separately the two terms in (18.44). We find for the contribution of the first one to (18.42)

$$\lim_{\delta\to 0} -\sum_{n,m=0}^{\infty}\frac{(-\gamma)^{m+1}}{(m+1)}\,Q_{mn}\int_{-\beta}^{+\beta}\int_{-\infty}^{+\gamma}\nu^n G(x,r,-ax+\delta,r+\nu,\tau)d\tau d\nu, \tag{18.45}$$

Analogous to our previous reasoning we can show that only for an interval of τ enclosing $\tau = 0$ and for $n = 0$, we have a contribution in the case $\beta \to 0$. Hence instead of (18.45) we consider

$$\lim_{\delta\to 0} -\sum_{m=0}^{\infty}\frac{(-\gamma)^{m+1}}{(m+1)!}\,\frac{\partial^m Q(x,r)}{\partial x^m}\int_{-\beta}^{+\beta}\int_{-\gamma}^{+\gamma} G(x,r,-ax+\delta,r+\nu,\tau)d\tau d\nu. \tag{18.46}$$

We compare this expression with (18.12). When we replace there $Q(\xi,r+\nu)$ by the constant

$$-\sum_{m=0}^{\infty}\frac{(-\gamma)^{m+1}}{(m+1)!}\,\frac{\partial^m Q(x,r)}{\partial x^m} \tag{18.47}$$

and replace the fixed constant α by the fixed constant γ, we can use the result (18.37). In this way we find for (18.46)

$$+\frac{4\sqrt{1+a^2r^2}}{\beta}\cdot\sum_{m=0}^{\infty}\frac{(-\gamma)^{m+1}}{(m+1)!}\,\frac{\partial^m Q(x,r)}{\partial x^m} = -\frac{4\sqrt{1+a^2r^2}}{\beta}\int_{x-\gamma}^{x} Q(\xi,r)d\xi. \tag{18.48}$$

This is the extension upto x of the integral in (18.38).

It can be proved that the second term in (18.43) gives no contribution when first $\delta\to 0$ and second $\beta\to 0$. In this way we give the following meaning to (18.6).

$$4\pi\mu\varepsilon\, U^2 r\,\frac{\partial f}{\partial x}(x,r) = \lim_{\beta\to 0}\{(\int_{r_i}^{r-\beta} + \int_{r+\beta}^{r_o})\int_{x_\ell(\rho)}^{x_t(\rho)} Q(\xi,\rho)K(x,r,\xi,\rho)d\xi d\rho +$$

$$-\frac{4\sqrt{1+a^2r^2}}{\beta}\int_{x_\ell(r)}^{x} Q(\xi,r)\,d\xi\}, \tag{18.49}$$

where $K(x,r,\xi,\rho)$ is defined in (18.7) and the first two terms of its singular behaviour are given in (18.9).

The limit procedure defined in (18.49) is called the Hadamard principal value of the integration with respect to ρ. In the one dimensional

case the Hadamard principal value of the "non existing" integral

$$\int_a^b \frac{f(\rho)}{(\rho - r)^2}\, d\rho \quad , \quad a < r < b, \tag{18.50}$$

is defined by

$$\lim_{\varepsilon \to 0} \{ (\int_a^{r-\varepsilon} + \int_{r+\varepsilon}^b) \frac{f(\rho)}{(\rho - r)^2}\, d\rho - \frac{2f(r)}{\varepsilon} \}, \tag{18.51}$$

which corresponds to (18.49) for a fixed value of $\xi < x$.

19. The screw blade of zero thickness with prescribed load, b

In this section we will discuss again the screw blade of zero thickness with prescribed load, however we will start from the representation (17.17) of the velocity induced by a rotating force. The basic expression at the right hand side of (18.3) now has to be calculated using (17.17). We find

$$-4\pi\mu Ur\left(a v_x + \frac{v_\varphi}{r}\right) = \iint_B Q(\xi,\rho)\left[\frac{\{+ar^2\sin(\varphi+a\xi) - (x-\xi)\cos(\varphi+a\xi)\}}{\{(x-\xi)^2 + r^2 + \rho^2 - 2r\rho\cos(\varphi+a\xi)\}^{3/2}} + \right.$$

$$\left. + \frac{\partial}{\partial\rho} M(x,r,\varphi,\xi,\rho)\right] d\xi d\rho \ , \qquad (19.1)$$

where

$$M(x,r,\varphi,\xi,\rho) = \int_{-\infty}^{x-\xi} \frac{\{\rho(a^2r^2-1)\cos(\varphi+a(x-\tau))+r(1-a^2\rho^2)+\tau a\rho\sin(\varphi+a(x-\tau))\}}{\{\tau^2 + r^2 + \rho^2 - 2r\rho\cos(\varphi+a(x-\tau))\}^{3/2}} d\tau, \qquad (19.2)$$

and (x,r,φ) is still an arbitrary point in space. By partial integration we can write (19.1) in the form

$$-4\pi\mu Ur\left(a v_x + \frac{v_\varphi}{r}\right) = \iint_B Q(\xi,\rho)\frac{\{ar^2\sin(\varphi+a\xi) - (x-\xi)\cos(\varphi+a\xi)\}}{\{(x-\xi)^2 + r^2 + \rho^2 - 2r\rho\cos(\varphi+a\xi)\}^{3/2}} d\xi d\rho +$$

$$- \iint_B \frac{\partial Q(\xi,\rho)}{\partial\rho} \cdot M(x,r,\varphi,\xi,\rho)\, d\xi d\rho + \int_{x_f}^{x_b} Q(\xi,\rho_u(\xi))\, M(x,r,\varphi,\xi,\rho_u(\xi))\, d\xi +$$

$$- \int_{x_f}^{x_b} Q(\xi,\rho_d(\xi))\, M(x,r,\varphi,\xi,\rho_d(\xi))\, d\xi \ , \qquad (19.3)$$

where (figure 19.1) x_f and x_b denote the smallest and the largest value of the ξ coordinate on the screw blade and $\rho_u(\xi)$ and $\rho_d(\xi)$ describe the upper and lower edge of the blade as a function of ξ. The above is correct in the case that the blade in the (ξ,ρ)plane is a convex domain, which we assume to be true. Otherwise the integration boundaries have to be specified somewhat more carefully.

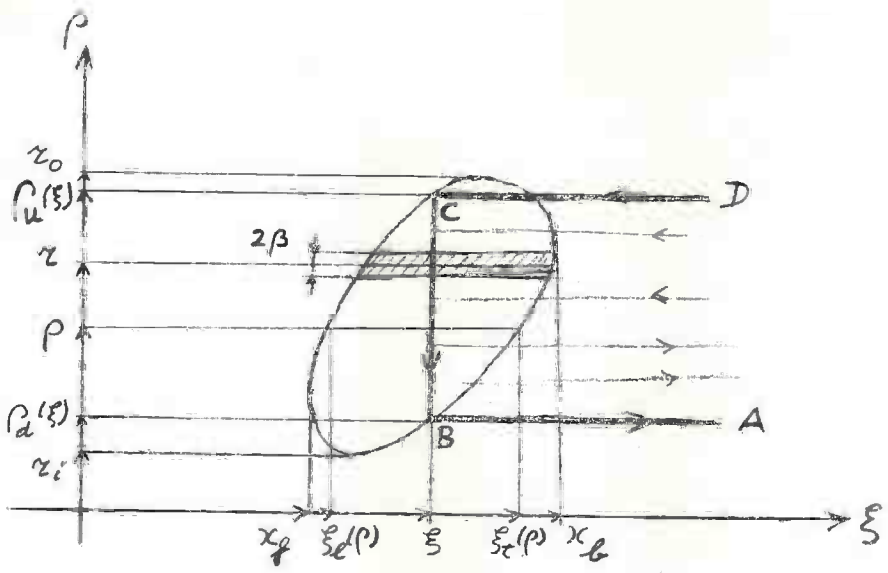

Fig. 19.1. A typical vortex system on the blade of the screw.

We again want to obtain information about the local angle of incidence of the screw blade, hence we have to consider the limit $\varphi \to -ax$. When we consider the case $\varphi = -ax$ the kernels in (19.3) possess singularities which can easily be estimated. We find for the kernel of the first integral

$$\lim_{\substack{\xi\to x \\ \rho\to r}} \frac{\{ar^2\sin(a(\xi-x)) - (x-\xi)\cos(a(\xi-x))\}}{\{(x-\xi)^2 + r^2 + \rho^2 - 2r\rho\cos(a(\xi-x))\}^{3/2}} \approx$$

$$\approx \frac{-(1+a^2r^2)(x-\xi)}{\{(1+a^2r^2)(x-\xi)^2 + (r-\rho)^2\}^{3/2}} \quad . \tag{19.4}$$

The singular behaviour of the function $M(x,r,\varphi,\xi,\rho)$ is given by

$$\lim_{\rho\to r} M(x,r,-ax,\xi,\rho) \approx \frac{2(1+a^2r^2)}{(r-\rho)} \quad , \quad x > \xi \tag{19.5}$$

By excluding a strip $|r-\rho| < \beta$ from the domain of integration we exclude the singularity and it is possible to carry out the integrations in (19.3). From (19.4) and (19.5) it follows that the limit $\beta \to 0$ exists. However when the integrals can be interpreted in this way, we are not sure that the result is correct. There remains a possibility of contributions of functions which for $\varphi = ax$ are zero everywhere except for $\rho = r$ (δ functions of Dirac or its derivatives). That this does not happen follows from a more careful passing to the limit first $\varphi \to ax$ and then $\beta \to 0$.

The last two integrals in (19.3) are one dimensional with ξ as the variable of integration. It is more natural to introduce ρ instead of ξ because then for $r_i \leq \rho \leq r_o$ the whole leading edge and the whole trailing edge are covered separately. Using (18.3) we obtain

$$4\pi\varepsilon\mu U^2 r \frac{\partial f}{\partial x} = \lim_{\beta\to 0} \Big[\int_{x_f}^{x_b} \Big(\int_{\rho_d(\xi)}^{r-\beta} + \int_{r+\beta}^{\rho_u(\xi)} \Big) \frac{Q(\xi,\rho)\{-ar^2 \sin a(x-\xi) - (x-\xi)\cos a(x-\xi)\}}{\{(x-\xi)^2 + r^2 + \rho^2 - 2r\rho\cos a(x-\xi)\}^{3/2}} \cdot d\rho d\xi +$$

$$- \int_{x_f}^{x_b} \Big(\int_{\rho_d(\xi)}^{r-\beta} + \int_{r+\beta}^{\rho_u(\xi)} \Big) \frac{\partial Q(\xi,\rho)}{\partial\rho} M(x,r,-ax,\xi,\rho) d\rho d\xi +$$

$$+ \Big(\int_{r_i}^{r-\beta} + \int_{r+\beta}^{r_o} \Big) Q(\xi_\ell(\rho),\rho)\, M(x,r,-ax,\xi_\ell(\rho),\rho) \frac{d\xi_\ell(\rho)}{d\rho} d\rho +$$

$$- \Big(\int_{r_i}^{r-\beta} + \int_{r+\beta}^{r_o} \Big) Q(\xi_t(\rho),\rho)\, M(x,r,-ax,\xi_t(\rho),\rho) \frac{d\xi_t(\rho)}{d\rho} d\rho \Big]. \qquad (19.6)$$

We now discuss the physical meaning of the different parts of the right hand side of equation (19.6). The first integral represents the velocity induced by the bound vortices of which in figure 19.1 a typical one is drawn, the thick line BC. The second integral provides the velocities induced by the variation of the bound vorticity in the ρ direction. In the figure the vortices are drawn as horizontal lines starting at BC and stretching to the right. The last two equations in (19.6) give the velocities induced by the free vortices which arise by the ending of the bound vortices at the circumference of the blade. Typical ones are CD and BA.

Possible directions of the rotation of these vortices (right hand screw) are indicated by arrows. In figure (19.1) it is clear that the bound vortex BC attains its maximum value at about its middle, at the place where the free vortices of the second integral (19.6) change their direction. Although we have used the word vortex in this description it is clear that in fact we have vortex densities.

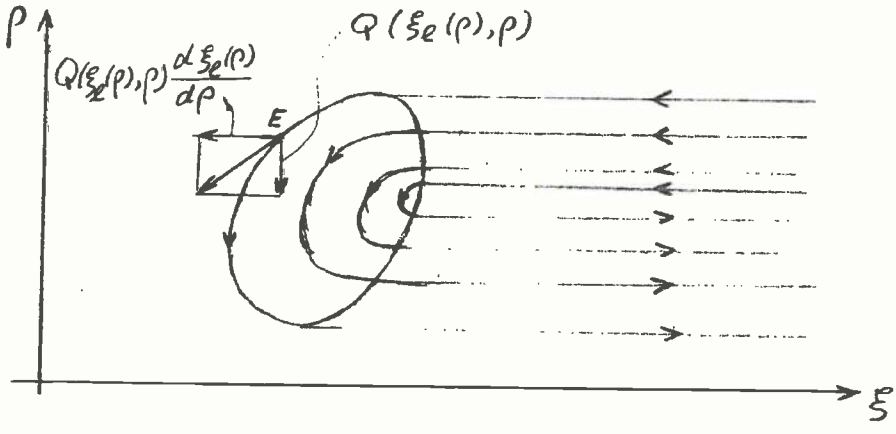

Fig. 19.2. Another picture of the vorticity on the blade of the screw.

It is well known that

$$\operatorname{div}\left(\operatorname{rot}.\ (U + v_x,\ v_r,\ v_\varphi)\right) \equiv 0. \tag{19.7}$$

This means that when we consider lines on the blade of the screw, which are everywhere tangent to the direction of vorticity (figure 19.2) we get a picture which represents the flow of a two dimensional incompressible fluid on the curved surface consisting of the blade and the helicoidal surface behind it. However then the vorticity in the neighbourhood of the leading edge will be tangent to it. That this happens follows from (19.6). The vorticity component $Q(\xi,\rho)/\mu U(1 + a^2r^2)^{\frac{1}{2}}$ is the density of the bound vorticity in the ρ direction per unit of length in the ξ direction. The density of the free vorticity in the ξ direction, per unit of length in the ρ direction, at the point E in figure 19.2 has the value

$$Q(\xi_\ell(\rho),\rho)\ \frac{d\xi_\ell(\rho)}{d\rho}\ , \tag{19.8}$$

which follows from the third integral in (19.6). Hence the tangent of the angle which the resultant vorticity forms with the ρ axis at the point E is

$$Q(\xi_\ell(\rho),\ \rho)\ \frac{d\xi_\ell(\rho)}{d\rho}\ \cdot\ Q(\xi_\ell(\rho),\rho)^{-1} = \frac{d\xi_\ell(\rho)}{d\rho}\ , \tag{19.9}$$

which has to be proved.

20. Some additional remarks

In lifting surface theory, as treated in sections 18 and 19, there are two main types of problems. First the problem of determining the shape of the surface for a given load distribution. Second, the inverse problem where the surface is given and it is asked to determine the pressures exerted by the fluid. The first problem is more interesting from the point of view of the design of ship screws. Mathematically it means that in our integral equations (18.49) and (19.6) the function $Q(\xi,\rho)$ is known. In order to calculate the function $f(x,r)$ which determines the angle of attack and the camber of the blade sections, we have to carry out the indicated integrations. This is rather cumbersome owing to the complicated nature of the kernels. In practical calculations (18.49) seems to be more adequate, for the origin of this method we refer to [18].

Another point which has to be discussed is the extension of the theory to more blade screws. Here we have to consider also the velocities induced by the other blades. We assume that the pressure distributions on the N equally spaced blades are identical. Then we can simply replace (18.6) for instance by

$$4\pi\mu\varepsilon U^2 r \frac{\partial f}{\partial x} = \lim_{\varphi \to -\infty} \iint_B Q(\xi,\rho) \sum_{n=0}^{N-1} K^*\left(x,r,\varphi + \frac{2\pi n}{N},\xi,\rho\right) d\xi d\rho . \tag{20.1}$$

The added part of the kernel has no singularities, because the points of one blade are at a finite distance of the points of the other blades. From this it follows that all our limit considerations and statements about integrability remain valid. The same can be done with respect to the vortex theory. For applications of this theory we refer to [5] where also some non linear effects of the flow have been taken into account.

Next we discuss shortly the screw behind a ship, in which case the inflow is no longer homogeneous. The presence of the hull induces perturbation velocities at the screw disk. These perturbations depend in general on the angular coordinate φ of our cylindrical coordinate system. Then the load of the screw will possess a periodic character. In order that the phenomenon can be described by a linear theory the deviations of the homogeneous flow at the place of the screw must remain sufficiently small. Hence we have to make the assumption that the total velocity $\vec{U}_o$ behind the ship when the screw is absent, can be written as

$$\vec{U}_o = (U + v_{ox}, v_{or}, v_{o\varphi}) , \tag{20.2}$$

where v_{ox}, v_{or} and $v_{o\varphi}$ which are induced by the hull, satisfy the relation

$$\left|\frac{v_x}{U}\right|, \left|\frac{v_r}{U}\right|, \left|\frac{v_\varphi}{U}\right| \ll 1 . \tag{20.3}$$

We can assume further, that because of the short distance covered by the screw in the x direction these components are independent of x. In practice the condition (20.3) can be relieved to a certain extent by comparing the disturbance velocities not with the incoming velocity U, but with the relative velocity $U(1+\omega^2 r^2)$ at some place r. Of course the velocity v_o does not enter into this theory (18.3) when a single helicoidal reference surface (15.7) is used.

In order to calculate the fluctuations of the loading during each revolution of the screw, we can consider N blades which are parts of exactly helicordal surfaces

$$\varphi + \frac{2\pi n}{N} - \omega t + ax = 0 \quad , \quad n = 0, \ldots, N-1. \tag{20.4}$$

Having found, in one way or another, the fluctuating pressures in this case we can simply add them to the pressures of the screw with thickness and load, working in an undisturbed parallel flow. This is allowed because our theory is linear. We refer for instance to [25].

Next we mention the very important combination of a propeller with an annular "airfoil" (figure 20.1). This annular airfoil is also called a duct, a shroud or a nozzle. We distinguish between the accelarating duct and the decelarating duct. The first one is often used in the case of a heavily loaded screw, it can improve the efficiency of the propulsion system. The second one is used to increase the pressure inside the duct, hence it can be used for retardation of cavitation. We do not enter here into the hydrodynamical problems connected

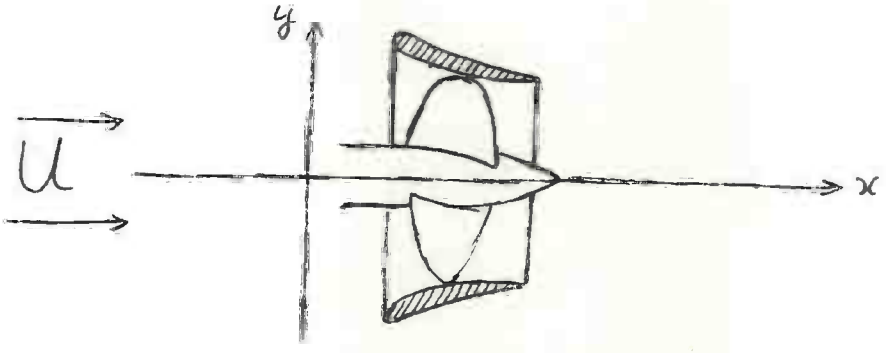

Fig. 20.1. A ducted propeller.

with this configuration but refer to [17]. In connection with the optimization

of propulsion systems we will discuss some of the properties of a duct with respect to its ability of spreading vorticity which is shed by the screw blade tips.

At last we make a remark on the concept of thrust deduction. When a propeller is placed behind a body (figure 20.2), we can measure the force transmitted by the propeller shaft. This force T which is exerted by the propeller on the fluid is in general, also in inviscid potantial flow as is considered here, not equal to the total thrust on body and propeller together. The reason is that

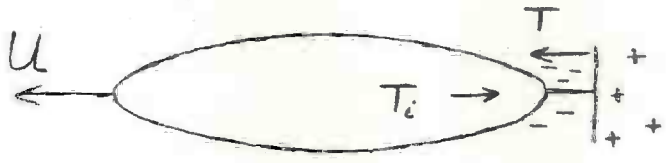

Fig. 20.2. Thrust deduction.

the body is in the influence region of the pressures induced by the propeller. By the negative pressures in front of the propeller a force T_i is exerted on the aft in the direction opposite to the thrust. Both the thrust T and the counteracting T_i are $0(\varepsilon)$.

When the propulsion system is placed besides the body it can happen that the

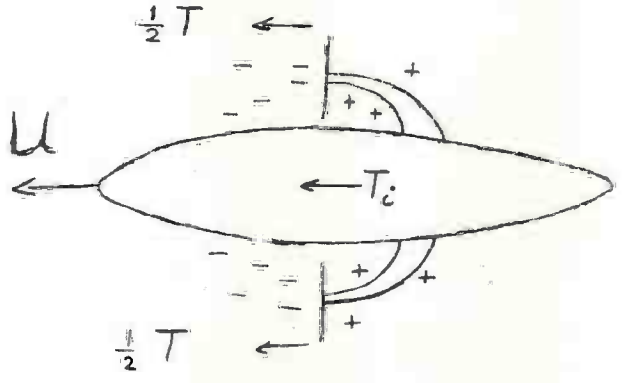

Figure 20.3. Increase of thrust.

thrust is increased by the interaction. The body is then with its front in a region of lower pressure and with its aft in a region of higher pressure, hence a force T_i is exerted on the body which is a propulsive one.

Exercise.

Discuss that the thrust deduction and the increase of thrust is in agreement with the work done by the propellers in the two cases considered in figures 20.2 and 20.3. In the first one the mean value of the velocity of the fluid at the place of the propeller is lower, in the second one it is

larger than the velocity of advance U of the body, where in both cases we assume that the disturbance velocities induced by the body are $O(\varepsilon^0)$.

21. Unsteady propulsion

It is the intention to discuss in this section and in a number of following ones some aspects of unsteady propulsion. First we will give a meaning to the expression "unsteady propeller". The most simple one seems to be: a propeller is unsteady when no inertial reference system exists with respect to which the induced flow is time independent. This however is not appropriate, we probably exclude from the conceivable propulsion systems only the sails of a yacht in steady motion, even the free running propeller becomes unsteady. A better definition seems, a propeller is unsteady when the relative fluid flow is time dependent while this time dependency is essential for its functioning. The second part of this definition is vague in some degree, it is intended to exclude for instance the screw propeller in a wake. Essential unsteady propulsion occurs in the case of Voith-Schneider propellers, contrarotating propellers, the propulsion wheels of a paddle boat, the fish tail, the flagella of bacteria, etc.

The type of unsteady propulsion we will consider here belongs to a more restricted class. We assume that the fluid is incompressible and inviscid and that propulsion occurs by lift and suctionforces. The last two assumptions exclude the flagella of bacteria and the paddle wheel. We also demand that the propulsion device will be lightly loaded, hence its shed free vorticity is small of $O(\varepsilon)$ and is not transported by its own induced velocities.

What is left are propulsion systems consisting of possibly flexible lifting surfaces making flapping motions which are assumed to be periodic and which are still allowed to have a small or a large amplitude of $O(\varepsilon)$ or of $O(\varepsilon^0)$ respectively. For the propellers of this type we admit three different regimes of working,which we will discuss now.

Regime i. finite amplitude motion, the flexible wing W moves in an ε neighbourhood of a periodically curved reference strip H (figure 21.1) which is at rest with respect to the undisturbed fluid. When W moves exactly along H it does not disturb the fluid at all and hence does not shed free vorticity, this motion will be called the base motion. Small deviations of $O(\varepsilon)$ of this base motion

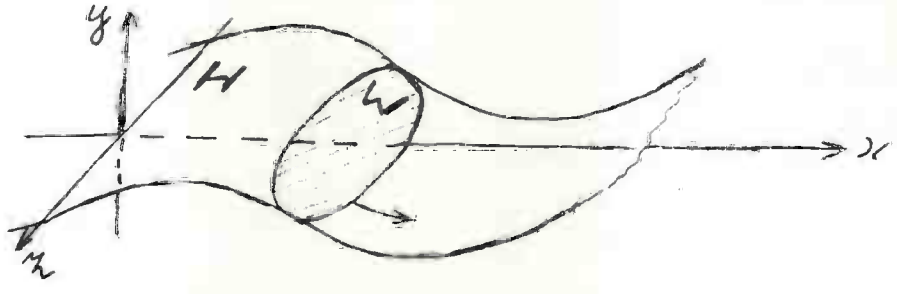

Fig. 21.1. Large amplitude flexible wing, regime i.

which induce velocities and vorticity and by which thrust can be generated, will be called the added motion. The boundary conditions related to W as well as its bound and free vorticity of $0(\varepsilon)$ are assumed to be at H.

The pressure differences between the two sides are $0(\varepsilon)$, the angles of W with the x axis which can be replaced by the angles of H with the x axis, are $0(\varepsilon^0)$, hence the thrust will be $0(\varepsilon)$.

$$T(t) = 0(\varepsilon) \tag{21.1}$$

Regime ii, finite amplitude motion of a wing which induces finite disturbances, however which sheds free vorticity of $0(\varepsilon)$. We restrict ourselves to the two

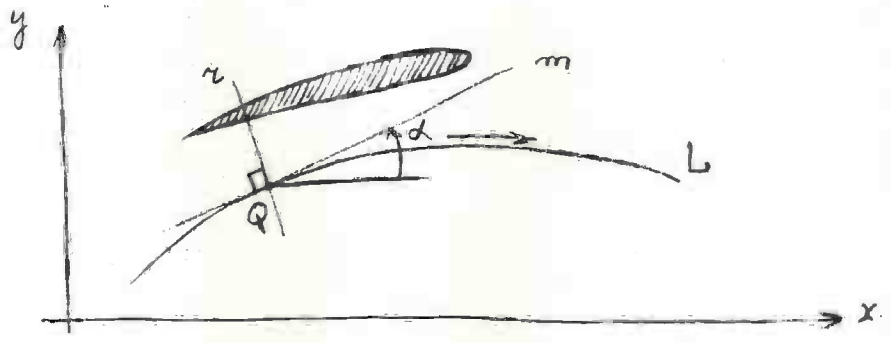

Fig. 21.2. Rigid profile moving along L, regime ii.

dimensional case in which the phenomenae are independent of the z coordinate (figure 21.2). We first describe a way to obtain a two dimensional base motion for a conventional profile. This is again a motion which does not shed free vorticity, hence the circulation of the profile has to be constant. For simplicity we take this constant equal to zero. In the sequel we assume that the Kutta condition is satisfied at the sharp trailing edge of the profile.

Consider a point Q(figure 21.2) fixed with respect to the profile such that when we rotate the profile around it the circulation of the profile is zero. The existence of such a point is easily demonstrated as follows. First consider a point Q_1 with coordinates $(-\frac{1}{3}\lambda, -\lambda)$ for sufficiently large values of λ. A clockwise rotation about Q_1 will induce a positive circulation around the profile. The value $\frac{1}{3}$ is chosen because it seems realistic, it has no exact significance. Next we take a point Q_2 with coordinates $(\frac{1}{3}\lambda, -\lambda)$. A clockwise rotation about Q_2 will induce a negative circulation around the profile,

Hence when we connect Q_1 and Q_2 by a line, there will be, by continuity, a point $\tilde{Q}$ on this line such that the circulation is zero when the profile rotates clockwise about it.

For each profile we can also find a direction of translation so that the circulation is zero, this direction is denoted by the line m. When we have found a line m and one point $\tilde{Q}$, we can find a straight line of such points, namely like the line r through $\tilde{Q}$ perpendicular to m. This is correct because a rotation around any point Q of r can be represented by a rotation around $\tilde{Q}$ and a translation in the direction m, hence the circulation is zero. Now we let the profile move in the following way. Choose any curved line L and a point Q on r. Let Q move along L and keep the line m drawn through Q tangent to L. Then the profile moves in a well defined way in the neighbourhood of L. During this motion the circulation of the profile is zero, because at each instant the motion can be described as a rotation about Q and a translation in the direction of m.

In the neighbourhood of the base motion described above, we can carry out the added motion, which deviates from it by quantities of $0(\varepsilon)$. This added motion causes free vorticity shedding and can procure a thrust of $0(\varepsilon)$ as in regime i.

Of course we can also consider motions of $0(\varepsilon^0)$ which yield a thrust of $0(\varepsilon^0)$. Because the theory of these is non linear in every respect, it is difficult to give an analytical treatment which reveals general trends.

Regime iii, small amplitude propulsion, including propulsion of fishes by tail and fins. For a survey we refer to [30] and for later work to [20].

We consider a lifting surface W which moves in an ε neighbourhood of a flat strip H, while also the local angles of incidence of W are assumed to be of $0(\varepsilon)$. The strip is part of the plane $y = 0$ (figure 21.3) and

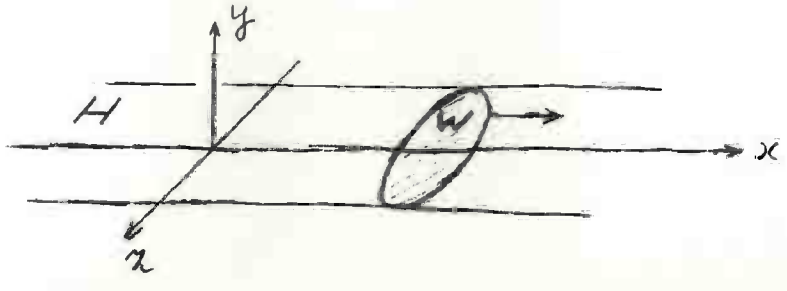

Fig. 21.3. Small amplitude flexible wing, regime iii.

stretches along the x axis. W moves in the positive x direction with a velocity U of $0(\varepsilon^0)$. When W moves exactly along H, it does not cause any fluid flow and hence does not shed any free vorticity. This motion is the base motion. Small deviations of the base motion, which are $0(\varepsilon)$ and by which thrust can be generated, form the added motion. The boundary conditions related to this lifting surface as well as its bound and free vorticity are assumed to be at the reference strip H.

Because the pressure differences between the two sides of W are $0(\varepsilon)$ and also the angles of incidence are $0(\varepsilon)$, the time dependent thrust, which is the force component in the positive x direction, will be $0(\varepsilon^2)$,

$$T(t) = 0(\varepsilon^2). \tag{21.2}$$

In the next sections we will discuss the two dimensional case of regime iii.

22. Small amplitude, two dimensional propulsion

We consider now the two dimensional case of regime i). The fluid is as always in these notes, inviscid and incompressible. In figure 22.1 is drawn the profile stretching from $x = -\ell$ towards $x = +\ell$. The motion of the profile

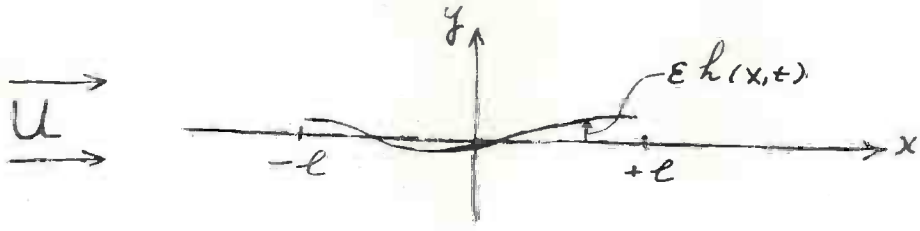

Fig. 22.1. Two dimensional small amplitude swimming motion

which we assume to be of zero thickness, is given by

$$y = h(x,t) \quad , \quad |x| \leq \ell \tag{22.1}$$

The real valued function $h(x,t)$ and its derivatives with respect to x and t are assumed to be $O(\varepsilon)$. The profile is placed in a parallel flow of velocity $U = O(\varepsilon^0)$.

The thickness of the profile is neglected because in linearized theory for a nearly flat profile it does not influence the thrust or lift production of the profile. Its flow field, described by a source and sink distribution at the x axis from $x = -\ell$ to $x = +\ell$, can simply be added to the flow described here. It has neither an influence on the pressure differences between the two sides of the profile nor on the leading edge suction force, which together determine the thrust. We remark that this is not true for the ship screw (section 16), because of the finite curvature of the blades. Also it is not true in theories for profiles of finite thickness of $O(\varepsilon^0)$, for instance [24].

The velocity of the fluid is denoted by $(U + u, v)$ where u and v are the disturbance velocities. These satisfy the linearized equations of motion

$$\frac{\partial u}{\partial t} + U \frac{\partial u}{\partial x} = - \frac{1}{\mu} \frac{\partial p}{\partial x} \quad , \tag{22.2}$$

$$\frac{\partial v}{\partial t} + U \frac{\partial v}{\partial x} = - \frac{1}{\mu} \frac{\partial p}{\partial y} \quad , \tag{22.3}$$

and

$$\operatorname{div}(u,v) = \frac{\partial u}{\partial x} + \frac{\partial v}{\partial y} = 0 \ , \tag{22.4}$$

We introduce the function

$$\varphi(x,y,t) = -\frac{1}{\mu}\, p(x,y,t) . \tag{22.5}$$

Differentiation of (22.2) with respect to x and (22.3) with respect to y and using (22.4) yields

$$\frac{\partial^2 \varphi}{\partial x^2} + \frac{\partial^2 \varphi}{\partial y^2} = 0 \tag{22.6}$$

The function $\varphi(x,y,t)$ is called the acceleration potential because its gradient yields the components of the acceleration of a particle, given in the left hand sides of (22.2) and (22.3). Next we introduce the complex variable $z = x + iy$ and the analytic function

$$f(z,t) = \varphi(x,y,t) + i\psi(x,y,t) , \tag{22.7}$$

where ψ is the complex conjugate of φ, hence φ and ψ are connected by the well known Cauchy-Riemann relations. The complex velocity vector is denoted by

$$w(z,t) = u(x,y,t) - iv(x,y,t) , \tag{22.8}$$

hence

$$\frac{\partial f}{\partial z} = \frac{\partial f}{\partial x} = \frac{\partial \varphi}{\partial x} + i\,\frac{\partial \psi}{\partial x} = \frac{\partial \varphi}{\partial x} - i\,\frac{\partial \varphi}{\partial y} = \frac{\partial w}{\partial t} + U\,\frac{\partial w}{\partial z} . \tag{22.9}$$

where we used one of the Cauchy-Riemann relations.

At the profile we have by (15.3) the boundary condition

$$v(x,+0,t) = v(x,-0,t) = \left(\frac{\partial}{\partial t} + U\frac{\partial}{\partial x}\right) h(x,t) \overset{\text{def}}{=\!=} V(x,t), \quad |x| \leq \ell . \tag{22.10}$$

From the equations of motion (22.2) and (22.3) it follows by (22.10)

$$-\frac{\partial \psi}{\partial x}(x,0,t) = \frac{\partial \varphi}{\partial y}(x,0,t) = -\frac{1}{\mu}\,\frac{\partial p}{\partial y}(x,0,t) = \left(\frac{\partial}{\partial t} + U\,\frac{\partial}{\partial x}\right) V(x,t), \tag{22.11}$$

hence this expression is known for $-\ell \leq x \leq +\ell$. Because we can represent the profile by a distribution of line forces at $y = 0$ parallel to the y axis it follows from section 4 that

$$\varphi(x,0,t) = 0 \quad , \quad \ell < |x| . \tag{22.12}$$

and that

$$\varphi(x,-0,t) = -\varphi(x,+0,t) \quad , \quad |x| < \ell \quad . \tag{22.13}$$

Because $\frac{\partial \psi}{\partial x}$ is continuous at the x axis (22.11) we have

$$\psi(x,-0,t) = \psi(x,+0,t) \quad , \quad |x| < \infty \quad . \tag{22.14}$$

As $w(z,t) \to 0$ for $z \to -\infty$(real), we find by integration of (21.9)

$$f(z,t) = U\, w(z,t) + \int_{-\infty}^{z} \frac{\partial w}{\partial t} (\zeta,t)\, d\zeta \quad . \tag{22.15}$$

Comparing imaginary parts in (22.15)

$$\psi(x,y,t) = -U\, v(x,y,t) - \int_{-\infty}^{x} \frac{\partial v}{\partial t} (\xi,y,t)\, d\xi . \tag{22.16}$$

Again from (22.9), by solving for w(z,t) we have

$$w(z,t) = \frac{1}{U} f(z,t) - \frac{1}{U^2} \int_{-\infty}^{z} \frac{\partial f}{\partial t} (\zeta, t + \frac{\zeta - z}{U}) d\zeta \quad . \tag{22.17}$$

Comparing imaginary parts in (22.17)

$$v(x,y,t) = -\frac{1}{U} \psi(x,y,t) + \frac{1}{U^2} \int_{-\infty}^{x} \frac{\partial \psi}{\partial t} (\xi,y,t + \frac{\xi - x}{U}) d\xi . \tag{22.18}$$

By substituting (22.10) into (22.16) for $y = 0$, $|x| \leq \ell$, hence on the profile we find

$$\psi(x,\pm 0,t) = -(U \frac{\partial}{\partial x} + \frac{\partial}{\partial t}) \int_{-\ell}^{x} V(\xi,t)\, d\xi - \int_{-\infty}^{-\ell} \frac{\partial v}{\partial t} (\xi,0,t)\, d\xi =$$

$$= \psi_1(x,t) + A(t) \quad , \quad |x| < \ell, \tag{22.19}$$

where

$$\psi_1(x,t) = -(U \frac{\partial}{\partial x} + \frac{\partial}{\partial t}) \int_{-\ell}^{x} V(\xi,t)\, d\xi \quad , \tag{22.20}$$

is a known function for $y = 0$, $|x| < \ell$, the remaining part of (22.19) denoted by A(t) is an unknown real function of time.

We will derive still another expression for A(t) which will be used in following sections, from (22.16) we have

$$\psi(-\ell,0,t) = -U\, v(-\ell,0,t) - \int_{+\infty}^{-\ell} \frac{\partial v}{\partial t} (\xi,0,t)\, d\xi \quad , \tag{22.21}$$

and from (22.18)

$$\psi(-\ell,0,t) = -U\, v(-\ell,0,t) + \frac{1}{U}\int_{-\infty}^{-\ell}\frac{\partial\psi}{\partial t}\left(\xi,y,t+\frac{\xi-x}{U}\right)d\xi. \tag{22.22}$$

Combination of (22.21) and (22.22) yields with the definition of A(t) (22.19)

$$A(t) = \frac{1}{U}\int_{-\infty}^{-\ell}\frac{\partial\psi}{\partial t}\left(x,0,t+\frac{x+\ell}{U}\right)dx\ . \tag{22.23}$$

With respect to the unknown function f(z,t) (22.7) we have the following data. For its real part φ we have equations (22.12) and (22.13) and for its imaginary part ψ, holds (22.19). From this it follows

$$f^{+}(z,t) + f^{-}(z,t) = 2i(\psi_1(x,t) + A(t)), \quad |x| < \ell\ , \tag{22.24}$$

$$f^{+}(z,t) - f^{-}(z,t) = 0 \qquad , \qquad |x| > \ell\ , \tag{22.25}$$

where " $^{+}$ " and " $^{-}$ " denotes the limit of (z,t) for $y \to 0$ through positive and negative values respectively. The type of problem stated in (22.24) and (22.25) is called a Hilbert problem for the function f(z,t) [16]. We remark that the complex function f(z,t) will be analytic in the whole complex plane with the exception of the line $|x| < \ell$, $y = 0$, where it exhibits a jump discontinuity. Such a function is called sectionally holomorfic.

23. The solution of the Hilbert problem

We first consider the homogeneous part of (22.24)

$$X^{+}(z) + X^{-}(z) = 0. \tag{23.1}$$

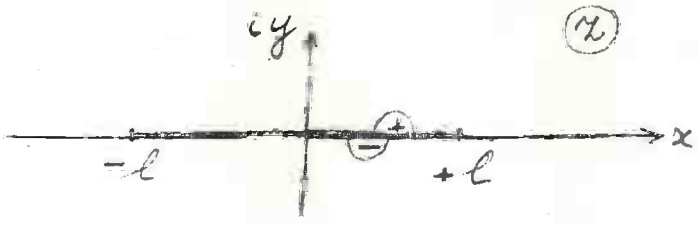

Fig. 23.1. The complex domain with the line of discontinuity of $f(z,t)$.

A simple non trivial solution which satisfies (23.1) is

$$X(z) = \sqrt{z-\ell}\ \sqrt{z+\ell} = \sqrt{z^2-\ell^2}\ , \tag{23.2}$$

where we define the square roots by assuming that we start with the value

$$\sqrt{z-\ell} \approx \sqrt{z+\ell} \approx \sqrt{x}\ , \tag{23.3}$$

for large real positive values of x and then continue the function values, the segment $|x| \leq \ell$, $y = 0$ is a cut in the complex z plane.

We now can write the solution of the inhomogeneous equation (22.24) as

$$f(z,t) = \frac{\sqrt{z^2-\ell^2}}{\pi i} \int_{-\ell}^{+\ell} \frac{(\psi_1(\xi,t) + A(t))}{\sqrt{\ell^2-\xi^2}\,(\xi - z)}\, d\xi + C(t)\ \left(\frac{z-\ell}{z+\ell}\right)^{\frac{1}{2}}, \tag{23.4}$$

where $\ell(t)$ is still an unknown function of t only. It is easily seen by the calculus of residues that the first term at the right hand side of (23.4) satisfies (22.24). The second term is another solution of the homogeneous part. We now choose $C(t)$ in such a way that the disturbances tend to zero at infinity or

$$\lim_{|z|\to\infty} f(z,t) = 0. \tag{23.5}$$

Using the following integrals

$$\int_{-\ell}^{+\ell} \frac{d\xi}{\sqrt{\ell^2 - \xi^2}} = \pi \quad , \quad \int_{-\ell}^{+\ell} \frac{d\xi}{\sqrt{\ell^2 - \xi^2}\,(\xi - z)} = -\frac{\pi}{\sqrt{z^2 - \ell^2}} \, , \tag{23.6}$$

where in the second one we assume a cut along the real axis from $x = -\ell$ to $x = +\ell$, we find from (23.4) and (23.5) for $z \to +\infty$ (real),

$$C(t) = -\frac{i}{\pi} \int_{-\ell}^{+\ell} \frac{\psi_1(\xi,t)\,d\xi}{\sqrt{\ell^2 - \xi^2}} - iA(t). \tag{23.7}$$

Substitution of this value of C(t) in (23.4) yields

$$f(z,t) = iA(t)\left\{1 - \left(\frac{z-\ell}{z+\ell}\right)^{\frac{1}{2}}\right\} - \frac{i}{\pi} \int_{-\ell}^{+\ell} \frac{\psi_1(\xi,t)}{\sqrt{\ell^2 - \xi^2}} \left\{\frac{\sqrt{z^2 - \ell^2}}{(\xi - z)} + \left(\frac{z-\ell}{z+\ell}\right)^{\frac{1}{2}}\right\} d\xi. \tag{23.8}$$

We have now to determine the still unknown function A(t). For $x < -\ell$ we obtain from (23.8)

$$\psi(x,0,t) = A(t)\left\{1 - \left(\frac{\ell - x}{-\ell - x}\right)^{\frac{1}{2}}\right\} - \frac{1}{\pi} \int_{-\ell}^{+\ell} \frac{\psi_1(\xi,t)}{\sqrt{\ell^2 - \xi^2}} \left\{\frac{-\sqrt{x^2 - \ell^2}}{(\xi - x)} + \left(\frac{x-\ell}{x+\ell}\right)^{\frac{1}{2}}\right\} d\xi. \tag{23.9}$$

Substitution of (23.9) into (22.23) yields

$$A(t) = \frac{1}{U} \int_{-\infty}^{-\ell} \left[A'\left(t + \frac{x+\ell}{U}\right)\left\{1 - \left(\frac{x-\ell}{x+\ell}\right)^{\frac{1}{2}}\right\} - \frac{1}{\pi} \int_{-\ell}^{+\ell} \frac{\frac{\partial}{\partial t}\psi_1\left(\xi, t + \frac{x+\ell}{U}\right)}{\sqrt{\ell^2 - \xi^2}} \cdot \right.$$

$$\left. \cdot \left\{-\frac{\sqrt{x^2 - \ell^2}}{(\xi - x)} + \left(\frac{x-\ell}{x+\ell}\right)^{\frac{1}{2}}\right\} d\xi\right] dx. \tag{23.10}$$

We assume that the profile is at rest for $t < T$,

$$y = h(x,t) \equiv 0 \quad , \quad (t < T), \tag{23.11}$$

and that the motion starts smoothly at $t = T$. It is assumed that the homogeneous incoming parallel flow of velocity U is present also for $t < T$. Then for $t \geq T$, we find from (23.10)

$$\int_{-(t-T)U-\ell}^{-\ell} \left[A'\left(t + \frac{x+\ell}{U}\right)\left(\frac{x-\ell}{x+\ell}\right)^{\frac{1}{2}}\right] dx = -\frac{1}{\pi} \int_{-(t-\bar{T})U-\ell}^{-\ell}$$

$$\left[\int_{-\ell}^{+\ell} \frac{\frac{\partial}{\partial t}\psi_1\left(\xi, t + \frac{x+\ell}{U}\right)}{\sqrt{\ell^2 - \xi^2}} \left\{\left(\frac{x-\ell}{x+\ell}\right)^{\frac{1}{2}} - \frac{\sqrt{x^2 - \ell^2}}{(\xi - x)}\right\} d\xi\right] dx. \tag{23.12}$$

When we replace x in (23.12) by $U(\xi - t) - \ell$ and ξ in (23.12) by x, we obtain

$$\int_T^t A'(\xi)\left\{\frac{U(\xi - t)-2\ell}{U(\xi - t)}\right\}^{\frac{1}{2}} d\xi = -\frac{1}{\pi}\int_T^t \left[\int_{-\ell}^{+\ell} \frac{\frac{\partial}{\partial \xi}\psi_1(x,\xi)}{\sqrt{\ell^2 - x^2}}\left\{\left(\frac{U(\xi - t)-2\ell}{U(\xi - t)}\right)^{\frac{1}{2}} + \right.\right.$$

$$\left.\left. - \frac{\sqrt{(U(\xi - t) - \ell)^2 - \ell^2}}{(x - U(\xi - t) + \ell)}\right\} dx\right] d\xi, \qquad (23.13)$$

from which the right hand side is a known function (22.19). We write this equation as follows.

$$\int_T^t A'(\xi)\, K(t - \xi)\, d\xi = \Psi(t), \qquad (23.14)$$

where

$$K(t) = \left(\frac{Ut + 2\ell}{Ut}\right)^{\frac{1}{2}}, \qquad (23.15)$$

and

$$\Psi(t) = -\frac{1}{\pi}\int_{-\ell}^{+\ell}\left[\int_T^t \frac{\partial}{\partial x}\psi_1(\xi,x)\, G(U(x - t) - \ell,\xi)dx\right] d\xi, \qquad (23.16)$$

with

$$G(x,\xi) \equiv \frac{1}{\sqrt{\ell^2 - \xi^2}}\left\{\left(\frac{x - \ell}{x + \ell}\right)^{\frac{1}{2}} - \frac{\sqrt{x^2 - \ell^2}}{(\xi - x)}\right\}, \quad (x < -\ell). \qquad (23.17)$$

Equation (23.14) is a Volterra type integral equation of the first kind for the unknown function A'(t). The kernel depends on $(t - \xi)$ hence the equation can be solved by the Laplace transform method [4]. Having found A'(t) we can find A(t) by a simple integration

$$A(t) = \int_T^t A'(\xi)\, d\xi, \qquad (23.18)$$

because for $t < T$ we have $A(t) \equiv 0$.

When A(t) is determined from equations (23.14) and (23.18), the complex acceleration potential f(x,t) (23.8) is known. Then the forces on the profile can be determined by simple integrations. The thrust delivered by the profile consists of two parts. First, the physically most important part is caused by the pressure differences between the two sides of the profile, then by the

slope of the profile a force in the x direction, hence a thrust, is induced. Second, we have a leading edge suction force ([12] page 251) which is proportional to the square of the factor of the leading edge singularity of the vorticity. When the vorticity of the profile in the neighbourhood of the leading edge behaves as

$$\frac{S(t)}{\sqrt{\ell + x}} \,, \tag{23.19}$$

then the leading edge suction force per unit of span has the magnitude

$$\frac{\pi}{4}\,\mu\, S^2(t). \tag{23.20}$$

The reason that the suction force can be physically less important is that it depends critically on the flow following the strongly curved surface of the nose of the profile. If the flow separates the suction force will become much smaller than its theoretical value.

The thrust reckoned positive in the negative x direction, can be written as

$$T(t) = \int_{-\ell}^{+\ell} (p^-(x,t) - p^+(x,t))\, \frac{\partial h}{\partial x}\,(x,t)\,dx + \frac{\pi}{4}\,\mu\, S^2(t) \tag{23.21}$$

where

$$p^{\pm}(x,t) = -\mu\, \varphi(x, \pm 0, t) = \mathrm{Re}\, f^{\pm}(z,t) \,, \quad |\mathrm{Re}\, z| < \ell, \tag{23.22}$$

and $f(z,t)$ is given in (23.8). The value of $S(t)$ follows also from (23.8). We consider the singularity of the pressure difference at the leading edge

$$\mathrm{Re}\left[\{-i\, A(t) - \frac{i}{\pi} \int_{-\ell}^{+\ell} \frac{\psi_1(\xi,t)}{\sqrt{\ell^2 - \xi^2}}\, d\xi\}\, \left(\frac{z-\ell}{z+\ell}\right)^{\frac{1}{2}}\right]^{\pm} \,, \quad |\mathrm{Re}\, z| < \ell, \tag{23.23}$$

where we remind that $A(t)$ and $\psi_1(\xi,t)$ are real functions. When z tends to the segment of the real x axis $|x| < \ell$ from above or from below we have to take

$$\left(\left(\frac{z-\ell}{z+\ell}\right)^{\frac{1}{2}}\right)^{\pm} = \pm\, i\, \left(\frac{\ell - x}{\ell + x}\right)^{\frac{1}{2}}. \tag{23.24}$$

Hence in the neighbourhood of $x = -\ell$ we find as the principal contribution to φ

$$\lim_{x \to -\ell} \varphi(x,t) \approx \pm \{A(t) + \frac{1}{\pi} \int_{-\ell}^{+\ell} \frac{\psi_1(\xi,t)}{\sqrt{\ell^2 - \xi^2}}\, d\xi\}\, \left(\frac{2\ell}{\ell + x}\right)^{\frac{1}{2}}. \tag{23.25}$$

From (23.25) and (23.19) it follows

$$S(t) \equiv -\frac{1}{\mu U} \lim_{x \to -l} \Delta p \equiv \frac{1}{\mu U} \lim_{x \to -l} \varphi^{+}(x,t) \equiv \frac{2\sqrt{2}l^{\frac{1}{2}}}{\mu U} \{A(t) + \frac{1}{\pi} \int_{-l}^{+l} \frac{\psi_1(\xi,t)d\xi}{\sqrt{l^2-\xi^2}}\}, \tag{23.26}$$

where Δp is the pressure difference between the + and the - side of the profile and φ^{+} the limiting value of φ at the + side of the profile. By (23.21) and (23.26) we can calculate the thrust $T(t)$.

24. The simple time harmonic motion

We now discuss the function A(t) for the simple time periodic case, hence when the motion of the profile (22.1) is given by

$$y = h(x,t) = h(x)\, e^{j\omega t} \quad , \quad |x| \leq \ell, \tag{24.1}$$

where ω is the angular frequency and j is the imaginary unit used in the time domain, which is distinguished by its notation from the imaginary unit i in flow domain. We remark that here h(x,t) is a complex valued function with respect to j. Hence in order to calculate "realistic" values of pressures or other physical quantities we have to take real parts of these quantities with respect to j. In order to assure convergence of our integrals we assume that ω has a small negative imaginary part

$$\omega = \omega_1 - j\omega_2 \quad , \quad \omega_2 > 0 \ , \tag{24.2}$$

hence the motion started long ago very smoothly with a steadily increasing amplitude. Afterwards we can take the limit $\omega_2 \to 0$.

Because the problem is linear we take A(t) as

$$A(t) = A\, e^{j\omega t} \ , \tag{24.3}$$

where A is an unknown constant which we have to determine. Substitution of (24.3) in the left hand side of (23.14) and taking $T = -\infty$, yields

$$\int_{-\infty}^{t} A'(\xi)\, K(t-\xi)\,d\xi = j\omega\, A \int_{-\infty}^{t} e^{j\omega\xi}\, K(t-\xi)\,d\xi = j\omega\, Ae^{j\omega t} \int_{0}^{\infty} e^{-j\omega\eta}\, K(\eta)\,d\eta, \tag{24.4}$$

where obvious change of integration variable is performed. By (23.15) we find

$$j\omega\, Ae^{j\omega t} \int_{0}^{\infty} e^{-j\omega\eta} \left(\frac{U\eta + 2\ell}{U\eta}\right)^{\frac{1}{2}} d\eta. \tag{24.5}$$

Introducing the variable $\xi = (U\eta/\ell) + 1$ we obtain

$$j\omega\, Ae^{j\omega t}\, \frac{\ell}{U} \int_{1}^{\infty} e^{-\frac{j\omega\ell}{U}(\xi-1)} \left(\frac{1}{\sqrt{\xi^2-1}} + \frac{\xi}{\sqrt{\xi^2-1}}\right) d\xi. \tag{24.6}$$

The integration of the first part of the integrand is well known ([26], page 170), the second part can be rewritten as the derivative with respect to ω of the first one, we find

$$j\omega\, Ae^{j\omega t}\, \frac{\ell}{U}\, e^{\frac{j\omega\ell}{U}} \left\{ \int_{1}^{\infty} e^{-\frac{j\omega\ell}{U}\xi} \frac{d\xi}{\sqrt{\xi^2-1}} + \frac{jU}{\ell}\, \frac{d}{d\omega} \int_{1}^{\infty} e^{-\frac{j\omega\ell}{U}\xi} \frac{d\xi}{\sqrt{\xi^2-1}}\, d\xi \right\} =$$

$$= j\omega\, Ae^{j\omega t}\, \frac{\ell}{U}\, e^{\frac{j\omega\ell}{U}} \left\{1 + \frac{jU}{\ell}\, \frac{d}{d\omega}\right\} \cdot -\frac{j\pi}{2}\, H_0^{(2)}\left(\frac{\omega\ell}{U}\right) =$$

$$= \frac{\pi\omega}{2}\, Ae^{j\omega\left(t + \frac{\ell}{U}\right)}\, \frac{\ell}{U} \left\{H_0^{(2)}\left(\frac{\omega\ell}{U}\right) - j\, H_1^{(2)}\left(\frac{\omega\ell}{U}\right)\right\} \ , \tag{24.7}$$

where $H_\nu^{(2)}(x) = J_\nu(x) - j\, Y_\nu(x)$, $\nu = 1,2$, are Bessel functions.

Next we determine the right hand side of (23.14) for the motion (24.1). We first consider $V(x,t)$ and $\psi_1(x,t)$ in this case, by (22.10) and (22.20)

$$V(x,t) \overset{\text{def}}{=\!=} V(x)\, e^{j\omega t} = (j\omega + U\frac{\partial}{\partial x})\, h(x)\, e^{j\omega t}\,, \tag{24.8}$$

and

$$\psi_1(x,t) \overset{\text{def}}{=\!=} \psi_1(x)\, e^{j\omega t} = (UV(x) + j\omega \int_{-\ell}^{x} V(\xi)d\xi)e^{j\omega t}. \tag{24.9}$$

Substitution of (24.9) in (23.16) and taking $T = -\infty$ yields

$$\Psi(t) = -\frac{1}{\pi}\int_{-\ell}^{+\ell}\int_{-\infty}^{t} j\omega\, \psi_1(\xi)\, e^{j\omega x}\frac{1}{\sqrt{\ell^2-\xi^2}}\{(\frac{U(x-t)-2\ell}{U(x-t)})^{\frac{1}{2}} - \frac{\sqrt{(U(x-t)-\ell)^2-\ell^2}}{(\xi - U(x-t)+\ell)}\}\,dxd\xi. \tag{24.10}$$

We now introduce the new variable of integration $\eta = \frac{U}{\ell}(x-t) - 1$, then (24.10) changes into

$$\Psi(t) = -\frac{j\omega\ell}{\pi U}\, e^{j\omega(\frac{\ell}{U}+t)}\int_{-\ell}^{+\ell}\frac{\psi_1(\xi)}{\sqrt{\ell^2-\xi^2}}\int_{-\infty}^{-} e^{\frac{j\omega\ell}{U}\eta}\{(\frac{\eta-1}{\eta+1})^{\frac{1}{2}} - \ell\frac{\sqrt{\eta^2-1}}{(\xi-\eta\ell)}\}\,d\eta d\xi. \tag{24.11}$$

We introduce the two constants G_1 and G_2 by

$$\frac{j\pi U}{\omega\ell}\, e^{-j\omega(\frac{\ell}{U}+t)}\Psi(t) = G_1 + G_2 \tag{24.12}$$

where

$$G_1 = \int_{-\ell}^{+\ell}\frac{\psi_1(\xi)}{\sqrt{\ell^2-\xi^2}}\int_{-\infty}^{-1} e^{\frac{j\omega\ell}{U}\eta}(\frac{\eta-1}{\eta+1})^{\frac{1}{2}}\,d\eta d\xi. \tag{24.13}$$

Replacing η by $-\zeta$, the integral with respect to η in (24.13) becomes of the type of the integral in (24.6), by this we find

$$G_1 = -\frac{\pi j}{2}\{H_o^{(2)}(\frac{\omega\ell}{U}) - j\, H_1^{(2)}(\frac{\omega\ell}{U})\}\int_{-\ell}^{+\ell}\frac{\psi_1(\xi)}{\sqrt{\ell^2-\xi^2}}\,d\xi. \tag{24.14}$$

The integral over $\psi_1(\xi)$ in (24.4) can be reduced to an integral over $V(\xi)$ by a partial integration, we find

$$G_1 = -\frac{\pi j}{2}\{H_o^{(2)}(\frac{\omega\ell}{U}) - j\, H_1^{(2)}(\frac{\omega\ell}{U})\}\int_{-\ell}^{+\ell}\{j\omega(\frac{\pi}{2} - \arcsin\frac{\xi}{\ell}) - \frac{U}{\sqrt{\ell^2-\xi^2}}\}V(\xi)d\xi. \tag{24.15}$$

Next we come to the part G_2 of $\Psi(t)$ (24.12), which is more complicated.

$$G_2 = -\ell\int_{-\ell}^{+\ell}\frac{\psi_1(\xi)}{\sqrt{\ell^2-\xi^2}}\int_{-\infty}^{-1} e^{\frac{j\omega\ell}{U}\eta}\frac{\sqrt{\eta^2-1}}{(\xi-\eta\ell)}\,d\eta d\xi. \tag{24.16}$$

Because $\psi_1(\xi)$ consists of two parts (24.9) we split again G_2 into two parts

$$G_2 = G_{21} + G_{22}\,, \tag{24.17}$$

where

$$G_{21} = +U\ell \int_{-\ell}^{+\ell} \frac{V(\xi)}{\sqrt{\ell^2 - \xi^2}} \int_{-\infty}^{-1} e^{\frac{j\omega\ell}{U}\eta} \frac{\sqrt{\eta^2 - 1}}{(\xi - \eta\ell)} \, d\eta d\xi. \tag{24.18}$$

and

$$G_{22} = + j\omega\ell \int_{-\ell}^{+\ell} \frac{\int_{\ell}^{\xi} V(\zeta)d\zeta}{\sqrt{\ell^2 - \xi^2}} \int_{-\infty}^{-1} e^{\frac{j\omega\ell}{U}\eta} \frac{\sqrt{\eta^2 - 1}}{(\xi - \eta\ell)} \, d\eta d\xi. \tag{24.19}$$

We go on with G_{22}, which we write as

$$G_{22} = U \int_{-\ell}^{+\ell} \frac{(\int_{\ell}^{\xi} V(\zeta)d\zeta)}{\sqrt{\ell^2 - \xi^2}} \int_{-\infty}^{-1} \frac{\sqrt{\eta^2 - 1}}{(\xi - \eta\ell)} \, de^{\frac{j\omega\ell}{U}\eta} \, d\xi =$$

$$= U \int_{-\ell}^{+\ell} \frac{(\int_{-\ell}^{+\xi} V(\zeta)d\zeta)}{\sqrt{\ell^2 - \xi^2}} \left[\frac{\sqrt{\eta^2 - 1}}{(\xi - \eta\ell)} e^{\frac{j\omega\ell}{U}\eta}\right]_{\eta = -\infty}^{-1} - \int_{-\infty}^{-1} e^{\frac{j\omega\ell}{U}\eta} \frac{\partial}{\partial\eta} \frac{\sqrt{\eta^2 - 1}}{(\xi - \eta\ell)} \, d\eta\right] d\xi. \tag{24.20}$$

The first term between square brackets vanishes as well for $\eta = -\infty$ on behalf of the imaginary part of ω(24.2), as for $\eta = -1$. We now use the following identity [29]

$$\frac{\ell}{\sqrt{\ell^2 - \xi^2}} \frac{\partial}{\partial\eta} \frac{\sqrt{\eta^2 - 1}}{(\xi - \eta\ell)} = \frac{1}{\sqrt{\eta^2 - 1}} \frac{\partial}{\partial\xi} \frac{\sqrt{\ell^2 - \xi^2}}{(\xi - \eta\ell)} \, , \tag{24.21}$$

then

$$G_{22} = \frac{-U}{\ell} \int_{-\ell}^{+\ell} (\int_{-\ell}^{+\xi} V(\zeta)d\zeta) \int_{-\infty}^{-1} e^{\frac{j\omega\ell}{U}\eta} \frac{1}{\sqrt{\eta^2 - 1}} \frac{\partial}{\partial\xi} \frac{\sqrt{\ell^2 - \xi^2}}{(\xi - \eta\ell)} \, d\eta d\xi. \tag{24.22}$$

Integration by parts with respect to the ξ coordinate yields

$$G_{22} = +\frac{U}{\ell} \int_{-\infty}^{-1} \frac{\ell}{\sqrt{\eta^2 - 1}} e^{\frac{j\omega\ell}{U}\eta} \int_{-\ell}^{+\ell} V(\xi) \frac{\sqrt{\ell^2 - \xi^2}}{(\xi - \eta\ell)} \, d\xi d\eta \, . \tag{24.23}$$

By (24.17), (24.18) and (24.23) we find

$$G_2(t) = U\ell \int_{-\ell}^{+\ell} \frac{V(\xi)}{\sqrt{\ell^2 - \xi^2}} \int_{-\infty}^{-1} \frac{e^{\frac{j\omega\ell}{U}\eta}}{(\xi - \eta\ell)} \{\sqrt{\eta^2 - 1} + \frac{1}{\ell^2} \frac{(\ell^2 - \xi^2)}{\sqrt{\eta^2 - 1}}\} \, d\eta d\xi =$$

$$= \frac{-U}{\ell} \int_{-\ell}^{+\ell} \frac{V(\xi)}{\sqrt{\ell^2 - \xi^2}} \int_{-\infty}^{-1} e^{\frac{j\omega\ell}{U}\eta} \frac{(\xi + \eta\ell)}{\sqrt{\eta^2 - 1}} \, d\eta d\xi =$$

$$= \frac{\pi j U}{2\ell} \int_{-\ell}^{+\ell} \frac{V(\xi)}{\sqrt{\ell^2 - \xi^2}} \{\xi H_0^{(2)}(\frac{\omega\ell}{U}) - j\ell H_1^{(2)}(\frac{\omega\ell}{U})\} \, d\xi \, . \tag{24.24}$$

From (24.12), (24.15) and (24.24) it follows that

$$\Psi(t) = -\frac{\omega\ell}{2U}\, e^{j\omega(\frac{\ell}{U}+t)} \left[\{H_o^{(2)}(\tfrac{\omega\ell}{U}) - jH_1^{(2)}(\tfrac{\omega\ell}{U})\} \int_{-\ell}^{+\ell} \{j\omega(\tfrac{\pi}{2} - \arcsin\tfrac{\xi}{\ell}) + \right.$$

$$\left. - \frac{U}{\sqrt{\ell^2-\xi^2}} \right\} V(\xi)\, d\xi - \frac{U}{\ell} \int_{-\ell}^{+\ell} \frac{V(\xi)}{\sqrt{\ell^2-\xi^2}}\, \xi\, H_o^{(2)}(\tfrac{\omega\ell}{U}) + j\ell\, H_1^{(2)}(\tfrac{\omega\ell}{U}) \}\, d\xi \Big]. \tag{24.25}$$

Comparing the left hand side (24.7) of (23.14) with the right hand side (24.25), we can calculate A(t) (24.3) as

$$A(t) = A e^{j\omega t} = -\frac{\ell}{\pi U} \left[\int_{-\ell}^{+\ell} \{j\omega(\tfrac{\pi}{2} - \arcsin\tfrac{\xi}{\ell}) - \frac{U}{\sqrt{\ell^2-\xi^2}}\} V(\xi)\, d\xi + \right.$$

$$\left. - \frac{U}{\ell} \int_{-\ell}^{+\ell} \frac{V(\xi)}{\sqrt{\ell^2-\xi^2}} \left\{ \frac{H_o^{(2)}(\tfrac{\omega\ell}{U}) - j\ell H_1^{(2)}(\tfrac{\omega\ell}{U})}{H_o^{(2)}(\tfrac{\omega\ell}{U}) - jH_1^{(2)}(\tfrac{\omega\ell}{U})} \right\} d\xi \right], \tag{24.26}$$

the function between brackets in the second integral can be called Theodorsen's function.

It is now possible to calculate by the formulas (23.21) - (23.26) the thrust of the swimming profile. Of course we have to take care to use only real parts, both with respect to i as well as with respect to j, of the relevant functions in these formulas, because otherwise we could get products of imaginary quantities which become real again. We remark that the product ij cannot be reduced to a real quantity.

25. Some additional remarks

In technics is one important realization of unsteady propulsion namely the Voith-Schneider propeller, of which a scheme is drawn in figure 25.1.

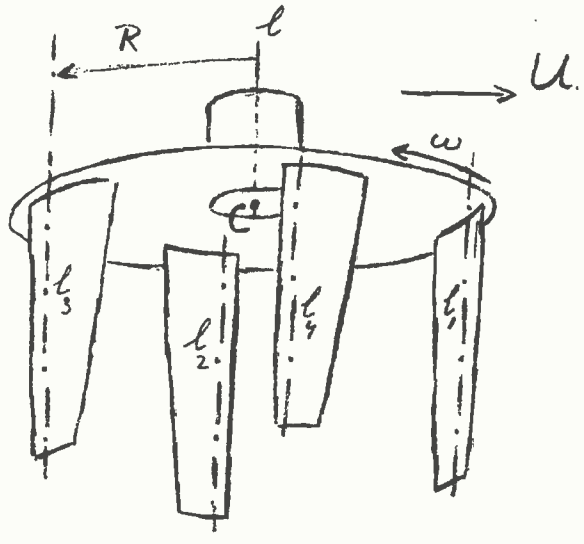

Fig. 25.1. Scheme of a four bladed Voith-Schneider propeller.

Under a ship we imagine a horizontal circular disk which rotates about a vertical axis ℓ, through its centre C. The rotational velocity of the disk is ω. On the disk are mounted several vertical wing like blades. These blades can perform oscillatory motions about vertical axes, which we call pivotal axes and which are denoted in figure 25.1 by $\ell_1, \ldots, \ell_4$.

We now discuss the cylindrical surfaces described by the pivotal axes. As a reference system we take a right handed Cartesian coordinate system x,y,z in rest with respect to the fluid. At time t = 0 the y axis coincides with the axis of rotation ℓ of the propeller which has a translational velocity U in the direction of the positive x axis. The points in which the axes $\ell_1, \ldots, \ell_4$ cut the (x,z) plane are called the pivotal points. We will consider the path of one of these points, denoted by Q, in the (x,z) plane. Assuming that at t = 0, Q is on the z axis we find

$$x = R(\nu\ \omega t + \sin \omega t),\quad z = R \cos \omega t,\quad \nu = \frac{U}{\omega R}, \tag{25.1}$$

where R is the distance from the pivotal axes $\ell_1, \ldots, \ell_4$ to ℓ. The path given by (25.1) is a cycloid of which the character is drawn in figure 25.2 for two values of ν. When $\nu > 1$ a fish tail like motion occurs, when

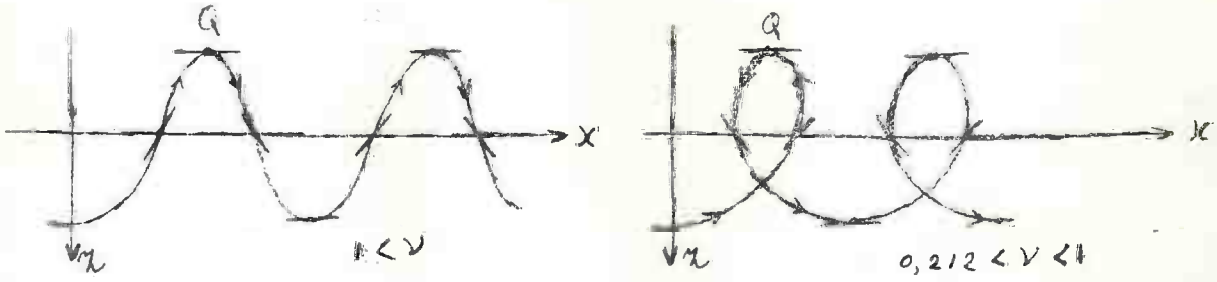

Fig. 25.2. Two types of cycloids.

$0 < \nu < 1$ the cycloid intersects itself. When $\nu < 0{,}212$ more intersections occur. In practice we have $\nu < 1$. In order that the propeller provides a mean force in the +x direction it is necessary that the blades have an appropriate angle of incidence during their motion. This is accomplished by having them execute a periodic motion about their pivotal axes, as is drawn in figure 25.2. The way in which the motion of the blades about their axes $\ell_1, \ldots, \ell_4$ is controlled mechanically will not be discussed here. We refer to [15]. We only mention that when it is possible to create a thrust in a certain direction we can, by turning the whole machinery over an angle, turn also the thrust. By this it is possible to steer a ship, which is provided with this type of propeller, hence a rudder becomes superfluous.

When the length of the chords of the wings are not too large with respect to the radii of curvature of their paths it is probably possible to describe the working of the Voith-Schneider propeller by regime i of section 21. Instead of one wing W and one surface H, we have in this case 4 wings each moving along its own surface, however this is not essential. In order to take into account the bottom of the ship, we can in figure 21.1 take the span of W two times the span of the wings of the propeller. Then the plane through the midspan points, is a plane which by symmetry is not passed through by fluid particles, hence it can represent the bottom.

Exercise.

Discuss a lifting surface theory for the blades of the Voith-Schneider propeller on the assumption that regime i of section 21 is valid.

26. Thrust production by energy extraction

We now will make some remarks on propulsion systems moving in an incompressible and inviscid fluid which in some sense is not homogeneous. First we mention a number of examples.

An unbounded fluid can have been disturbed before by the passing of some device which has shed vorticity which is equivalent to the existence of non homogeneous velocity fields. Hence in this fluid there are regions where kinetic energy is present.

Also it is possible that by viscosity in a real fluid a boundary layer has been formed because the fluid has passed along a body, for instance when air is flowing over land or water. With respect to our idealized fluid this boundary layer can be represented by vortex layers.

The fluid can be disturbed in a more or less inviscid way by flowing along a fixed object. Under a free water surface we can have nearly inviscid disturbances by a train of waves moving along the surface.

When we consider the air flowing over a water surface we can look at both media together. Then we have first an inhomogeneity of density because the water is much heavier, while also we can have a relative velocity of both components. In an idealized model we can neglect boundary layers or surface waves, and consider the two homogeneously moving half infinite media.

Of course many other inhomogeneities can be thought of and all kinds of combinations of the above mentioned ones can be made. We next show how energy can be extracted.

First consider an unbounded inviscid and incompressible fluid in which a disturbance velocity field $(\tilde{u}_0, \tilde{v}_0, \tilde{w}_0)$ is present. These velocities are assumed to be small of $0(\varepsilon)$, independent of time. Through this fluid moves a flexible wing W along some prescribed reference strip H which may be curved in a sufficiently smooth way. The velocity V with which the wing W moves along H will be $0(\varepsilon^0)$ and may be time dependent. Because we consider a linearized theory the wing W will deviate from H by distances of $0(\varepsilon)$. The question

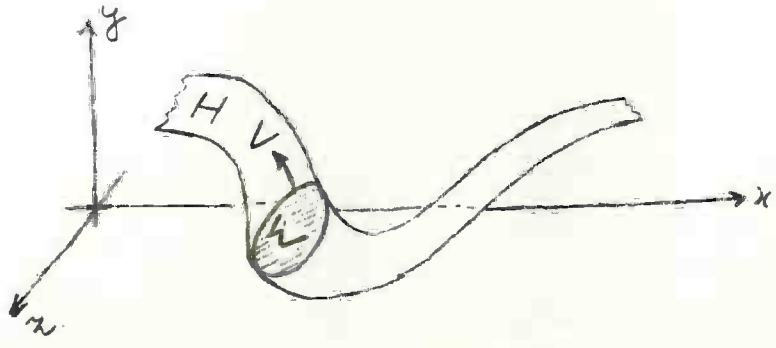

Fig. 26.1. Energy extraction by a flexible wing W.

of interest is which amount of energy can be extracted out of the kinetic energy in the fluid by the wing W.

The only possibility in a linearized theory for a lifting surface W to sense the velocity field $(\tilde{u}_o,\tilde{v}_o,\tilde{w}_o)$ in space is by its normal component at H. Hence we can replace the velocity field $(\tilde{u}_o,\tilde{v}_o,\tilde{w}_o)$ by any other (u_o,v_o,w_o) which has the same normal component at H, without altering the situation for W. We choose for (u_o,v_o,w_o) a velocity field which is induced by a vortex layer $\vec{\gamma}_o$ on H. This layer is uniquely determined by the normal component of the velocity field when we add the condition that its total circulation about H is zero. It can be found numerically by solving a Neumann problem for H, where the normal component of the unknown new velocity potential is prescribed.

Now the kinetic energy in the fluid is altered because in general the velocity field (u_o,v_o,w_o) is quite different from $(\tilde{u}_o,\tilde{v}_o,\tilde{w}_o)$. It is this new kinetic energy which can be extracted by W. The only thing W has to do is to deform, while gliding "along" H, in such a way that it sheds free vorticity of strength $-\vec{\gamma}_o$. Then it sweeps clean the strip H and no kinetic energy is left in the fluid.

The reason that we assumed the total circulation around the ship to be zero is that we want to replace the original kinetic energy by kinetic energy which can be entirely extracted by the wing, while the conditions at H remained the same. Because a wing can leave behind only free vorticity with zero total circulation this is in agreement with our reformulation of the problem. In case of a technical device the extracted energy can be stored in one way or another for instance in a flywheel and can be used to lower the power needed for propulsion. In case of animals using muscles the question remains which part of the extractable energy can be used effectively.

Another example is the thrust production by sails and keel of a sailing boat. Here we use essentially the different velocities of the two media water and air with respect to some inertial reference frame. The boat is extracting energy from these media by protruding one wing, the sail, into the air and another wing, the keel, into the water. When we suppose the boat to be upright, we have figure 26.2,

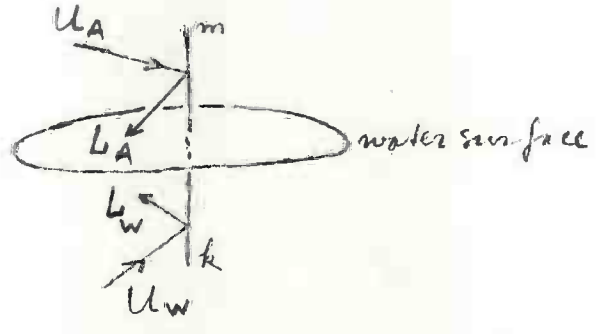

Fig. 26.2. Forces L_A and L_W on upright sailing boat.

where we have replaced the mast and the keel by lifting lines m and k respectively. The relative velocities of air and water with respect to the boat are denoted by U_A and U_W which make an angle with each other. This is possible by giving the boat a suitable course direction with respect to the inertial frame mentioned before. Then also the lift forces L_A and L_W induced by U_A and U_W make an angle with each other, hence they produce besides a moment also a thrust. The moment has to be balanced in the upright position by the crew and in more general conditions also by the weight in the keel and the stability of the boat. The thrust is balanced by the resistance of hull and rig when moving with respect to air and water.

We return to this subject in section 36, where we will discuss the optimization of a sail in a simplified case.

At last we mention a possibility of extracting energy by means of a body which does not shed vorticity itself. When a body of finite dimensions ($0(\varepsilon^0)$) moves in an inviscid and incompressible fluid it will in general have altered the relative position of fluid particles when they come to rest again after the body has passed. Suppose that vorticity of $0(\varepsilon)$ is present in the fluid, of which we neglect as usual the transportation by the velocities induced by itself. Then after the passing of the body the relative position of the vorticity will have changed and also the kinetic energy of the fluid. In the case the kinetic energy, which is of $0(\varepsilon^2)$, has been lowered the body must have experienced a mean thrust of $0(\varepsilon^2)$ in the direction of its motion, by which the energy is extracted. We give a simple example of this.

Consider the two dimensional case of a circular cylinder moving through the

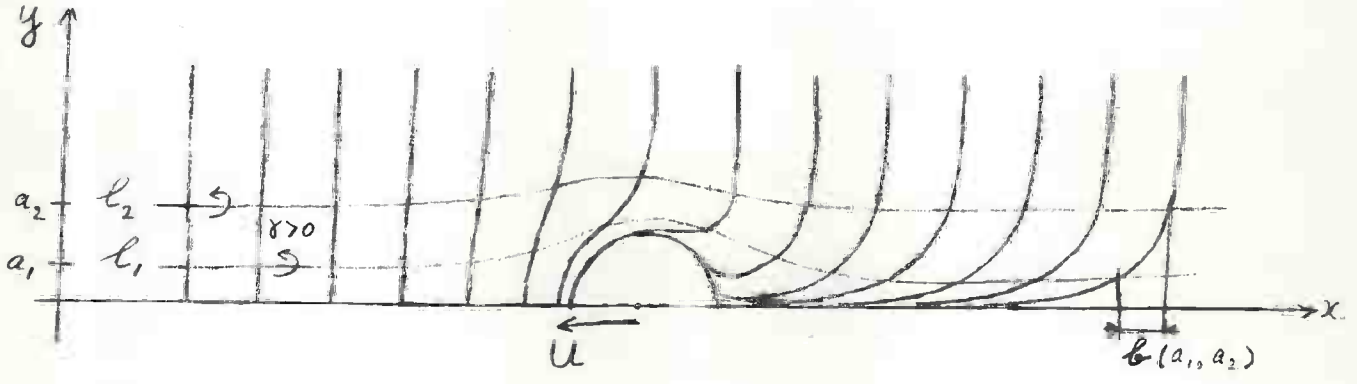

Fig. 26.3. Deformation of straight lines by the passing of a circle cylinder.

fluid, the velocity field will be independent of the z coordinate. In the fluid we have marked a number of straight lines, hence lines coupled to the

fluid particles. When the circle moves through the fluid the lines will deform and remain deformed after the circle has passed(figure 26.3). Now we assume that we have two vortex layers ℓ_1 and ℓ_2 defined by $y = a_1$ and $y = a_2$, $a_2 > a_1 > 0$ sufficiently far ahead of the circle. There the vorticity on each layer has the strength

$$\gamma = A \cos \omega x \quad , \quad \omega > 0, \tag{26.1}$$

where A is $O(\varepsilon)$ and $\gamma > 0$ is coupled with a right hand screw to the positive z direction. The kinetic energy E_b per length period $\frac{2\pi}{\omega}$ in the x direction of these layers can be calculated explicitly as

$$E_b = \sum_{j=1}^{2} \int_0^{\frac{2\pi}{\omega}} \frac{\partial \Phi}{\partial y}(x,a_j)\,[\Phi(x,a_j)]_-^+ \,dx = \frac{2\pi^2 A^2}{\omega^2}\,(1 + e^{-\omega(a_2 - a_1)}). \tag{26.2}$$

Far behind the moving cylinder the layers assume again their previous position however they have been translated with respect to each other in the x direction over some distance $b = b(a_1,a_2)$. By this the kinetic energy which we now denote by E_A is different in general,

$$E_a = \frac{2\pi^2 A^2}{\omega^2}\,(1 + \cos(\omega b) e^{-\omega(a_2 - a_1)}). \tag{26.3}$$

The difference $E_a - E_b$ can be extracted out of the fluid only by the work done by the mean value T of the thrust when it is displaced over one length period $\frac{2\pi}{\omega}$, hence

$$T = \frac{\omega}{2\pi}(E_b - E_a) = \frac{\pi}{\omega} A^2 (1 - \cos \omega b) e^{-\omega(a_2 - a_1)}. \tag{26.4}$$

When a_1, a_2, A and ω are given the value b has to be calculated by numerical means or "measured" from figure 26.3.

We remark that the model discussed above is not at all reliable when the vorticity passes to close along a body because then viscosity effects become important.

More information about energy extraction is given in the optimization theory in sections 27 - 30.

27. Optimization theory, general considerations

The optimization theory we will discuss here is intended to give insight in the best way of working of a lift, thrust or any other prescribed force action producing device, in an inviscid and incompressible fluid. First of course we have to define what will be called the best way of working. We restrict ourselves to the minimization of a simple cost function, namely the kinetic energy losses per unit of time in the fluid. For instance consider the well known problem solved already long ago [2] of the screw propeller with a given diameter, velocity of advance and rotational velocity, which has to yield a prescribed thrust. The question is what has to be its circulation distribution in spanwise direction along the blades in order that the kinetic energy left behind is as small as possible. This energy is put into the fluid by the engines which have to deliver the useful work but also have to overcome the induced resistance of the blades. This trailing vorticity in the case of an optimum screw propeller can be characterized as follows. Consider the two sided infinite helicoidal surfaces passed through by the blades when the screw, while rotating with its prescribed rotational velocity, has moved along a straight infinitely long line from one "end" to the other. Assume these surfaces to be rigid and impermeable and translate them, without rotating, with a suitable velocity in the direction of the line just mentioned. The vorticity needed to let the fluid move around the helicoidal surfaces happens to be the free vorticity shed by the optimum propeller.

In the following we will derive conditions for the optimum working of more general devices, including unsteady ones. We assume that the motion of the propulsion systems we consider will be periodic with respect to a reference frame translating with the mean velocity of the system. We have to demand a non zero mean value with respect to time of the force action, otherwise the kinetic energy left behind can be made zero and we have a trivial optimum. The constraints on the force actions can be rather general. For instance it can be demanded that a wing carrying out a flapping motion delivers lift as well as thrust. Then we can ask for the optimum motion which yields both force actions at the same time. Again it will turn out that also in these more complicated cases the shed vorticity of the optimum system can be characterized by moving the surfaces passed through by the blades or wings, in a certain way through the fluid.

It can be allowed that the fluid through which the device is moving is disturbed before, hence it has a non homogeneous velocity field. From this energy can be extracted by our system which then needs less energy from outside to perform its task, as is discussed in the previous section.

We shall discuss two types of optimization theories, a linear one and a semi linear one. To the sphere of the linear theory belongs the sculling propulsion of regime i) section 21, which in fact includes as a special case the lightly loaded screw propeller when the hub is neglected, sections 18 and 19. The semilinear theory is necessary for the optimization of the sculling propulsion of regime ii) section 21. Here we have a base motion which induces finite disturbances on which is superimposed a small added motion which can produce non zero mean values of $0(\varepsilon)$ of thrust, lift, etc. This theory also describes the lightly loaded screw propeller with a hub of finite dimensions.

The question of the existence of optimum motions yields rather delicate problems. In certain circumstances which seem physically not unrealistic, no optimum motions exist.

The theory developed here leaves out of consideration many aspects of real fluids. An important property of a fluid with respect to optimization in the sense as defined here, is its viscosity. When viscosity is neglected it will be seen that by increasing the size of propulsion systems the efficiency of it can be increased. This is the reason that in our theory based on inviscid fluids, we have to make a choice of the working area of the propeller. This restriction generally does not occur in real optimization problems because there viscosity puts a natural bound on the dimensions of the propeller. In that case the diameter of a screw propeller has to be chosen so that the potential theoretical increase in the efficiency caused by an increase in diameter will be annihilated by the decrease caused by friction losses. Although we agree that viscosity is very important in optimization theory, we will in order to avoid mixing difficulties first give a consistent linearized theory for inviscid fluids.

In the linear optimization theory we will in first instance neglect forces of $0(\varepsilon^2)$. These are forces due to leading edge suction, forces in the direction of motion of the blade caused by small local angles of incidence and second order errors of the first order forces caused by the assumption that the blade vorticity as well as the trailing vorticity lie on the reference planes. For a lightly loaded ordinary screw propeller the leading edge suction forces are not too important because these forces are nearly perpendicular to the direction of the thrust. When however we have a shrouded propeller or a ring propeller, the suction forces acting at the leading edge of shroud or ring point in the direction of the thrust and will be in practice a non neglicible part of it.

In case of the sculling propulsion described by regime iii) section 21, the second order forces are the only propulsive forces. This means that the non linear effects are dominant and have to be discussed separately.

The objection can be made that in the case of a prescribed mean value $T(\varepsilon)$ of the thrust with respect to time of $0(\varepsilon)$, errors $\tilde{T}(\varepsilon^2)$ of $0(\varepsilon^2)$ are present. These are of the same order as the kinetic energy $E(\varepsilon^2)$ left behind per period. So it seems that the efficiency η cannot be calculated at all. However we find

$$\eta = \frac{U(T(\varepsilon) + \tilde{T}(\varepsilon^2))}{U(T(\varepsilon) + \tilde{T}(\varepsilon^2)) + E(\varepsilon^2)} = \frac{U\,T(\varepsilon)}{U\,T(\varepsilon) + E(\varepsilon^2)} + 0(\varepsilon^2), \tag{27.1}$$

where U is the velocity of advance of the propelled body. From (27.1) it follows that η is accurate up to and including $0(\varepsilon)$.

First as has been said, we direct out attention to the strictly linear theory, valid for propulsion systems which induce small disturbance velocities of $0(\varepsilon)$ and which have force actions of which the mean values with respect to time are also $0(\varepsilon)$.

28. Lifting surface systems, linear theory (regime i)

We have a Cartesian reference system x,y,z, embedded in an inviscid and incompressible fluid. The reference system is at rest with respect to undisturbed parts of the fluid. Consider in this fluid m sufficiently smooth reference surfaces H_k,

$$H_k(x,y,z) = 0 \quad , \quad k = 1, \ldots, m \tag{28.1}$$

with

$$H_k(x + b,y,z) = H_k(x,y,z), \tag{28.2}$$

hence these surfaces are periodic with period b in the x direction. On each surface we have an orthogonal coordinate system ξ_k, η_k (figure 28.1) in such a way

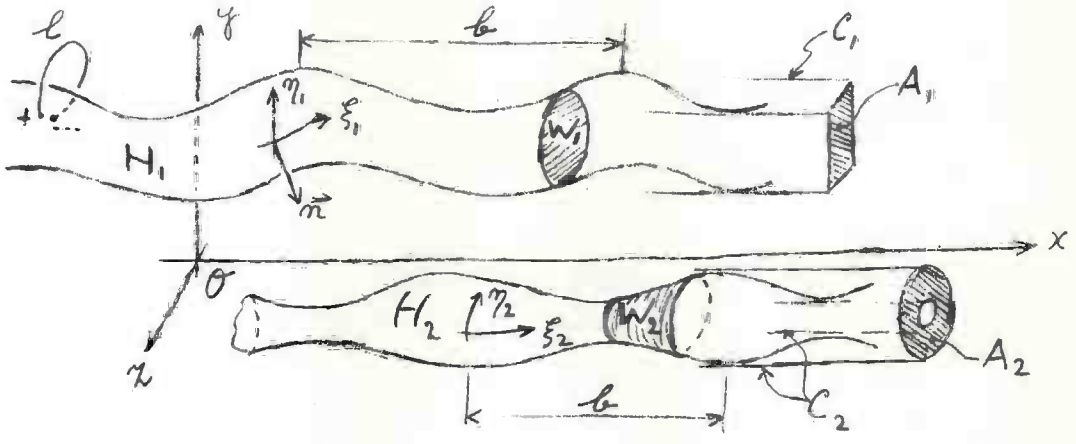

Fig. 28.1. A lifting surface system, m = 2.

that an increase in ξ_k by a number b_k, while η_k remains constant makes that we obtain an equivalent point of H_k with respect to its periodicity. The regions of ξ_k and η_k are given by

$$-\infty < \xi_k < +\infty \quad , \quad \eta_{o,k} \leq \eta_k \leq \eta_{1,k} \quad , \quad k = 1, \ldots, j, \tag{28.3}$$

$$\eta_{o,k} \leq \eta_k \leq \eta_{1,k} \quad , \quad k = j+1, \ldots, m, \tag{28.4}$$

where the half open intervals in (28.4) belong to closed surfaces as for instance H_2 in figure 28.1. The lines

$$\eta_k = \text{const.}, \tag{28.5}$$

will form a one parameter family of curves on H_k, such that through each point of H_k passes one and only one such a line.

In order to introduce a + and a-side on H_k we consider the unit vectors $\vec{e}_\xi$ and $\vec{e}_\eta$, tangent to H_k and in the positive directions of ξ_k and η_ξ. Then we construct the vector $\vec{e}_\xi * \vec{e}_\eta$. Now we agree that this vector points from the negative side H_k^- to the positive side H_k^+ of H_k (figure 28.1).

Next we have lifting surfaces W_k moving along the reference surfaces H_k. We assume that the velocity of the points of the W_k can be described by functions $V_k(\xi_k, \eta_k, t)$, $k = 1,\ldots,m$, with

$$V_k(\xi_k + b_k, \eta_k, t_k + \tau) = V_k(\xi_k, \eta_\xi, t), \tag{28.6}$$

where b_k is the period of H_k with respect to the ξ_k coordinate and τ is the time period of the system under consideration. These velocities are assumed to be tangential to the lines (28.5) and are reckoned positive in the direction of increasing values of ξ_k. This choice of the velocities of the points of the lifting surfaces W_k is not a restriction of generality as is discussed in section 8.

At last we have functions $\Gamma_k(\xi_k, \eta_k, t)$, $k = 1,\ldots,m$, which are of $0(\varepsilon)$ with

$$\Gamma_k(\xi_k + b_k, \eta_k, t + \tau) = \Gamma_k(\xi_k, \eta_k, t), \tag{28.7}$$

and which represent the bound vorticity of the lifting surfaces W_k moving along the H_k, with the velocity V_k. This vorticity is reckoned positive when it has a positive component (right hand screw) in the positive η_k direction. It is assumed that when $\Gamma_k(\xi_k, \eta_k, t) \neq 0$ for some values of ξ_k η_ξ and t then

$$\Gamma_k(\tilde{\xi}_k, \tilde{\eta}_\xi, t) = 0, \qquad |\xi_k - \tilde{\xi}_k| > C, \tag{28.8}$$

where C is some constant, for all $\tilde{\eta}_k$. This means that we consider lifting surfaces W_k of finite dimensions, gliding along the H_k.

Bound vorticity was introduced in section 7 (figure 7.1, along $\vec{k}$) as vorticity which is perpendicular to the local relative velocity of the fluid, hence to the lines (28.5) and which gives rise to pressure differences Δp_k between the + and the -side of the H_k, of magnitude

$$(p^+ - p^-) = \Delta p_k = \mu \Gamma_k V_k. \tag{28.9}$$

We define a lifting surface system, denoted by $\{H_k, V_k, \Gamma_k\}$, as the periodic surfaces H_k, together with the velocity distributions V_k and the bound vorticity distributions Γ_b.

Because our theory will be linear, the free vorticity γ_k which is shed by the bound vorticity Γ_k, remains where it is formed, hence at the surfaces H_k.

Finally we introduce the working region of a lifting surface system $\{H_k, V_k, \Gamma_k\}$. We agree that it is the region of space enclosed by the most narrow cylinders with generators parallel to the x axis which enclose the H_k. The cross section of these cylinders will be called the working area of the system. In figure 28.1 these cylinders are denoted by C_1 and C_2. The working area is allowed to consist of disconnected regions denoted by A_1 and A_2, which themselves can be multiply connected.

29. The variational problem for lifting surface systems

Our next subject is the optimization of lifting surface systems $\{H_k, V_t, \Gamma_k\}$ defined in the previous section of which the reference surfaces H_k are prescribed and V_k and Γ_k may be varied. For simplicity we assume that we have only one reference surface denoted by H, along which one lifting surface W is moving. The case of more reference surfaces can be discussed essentially in the same way.

The fluid is allowed to have a time independent velocity field $(\tilde{u},\tilde{v},\tilde{w})$ of $O(\varepsilon)$ which is periodic with period b in the x direction. As has been discussed in section 26 we replace this velocity field by another one (u_o,v_o,w_o) caused by a vorticity layer $\vec{\gamma}_o$ of $O(\varepsilon)$ at H of total circulation zero around H and which has on H the same normal component as $(\tilde{u},\tilde{v},\tilde{w})$.

When the wing has passed along, it has left behind free vorticity $\vec{\gamma}$ at H by which it alters the kinetic energy which before passing belonged to $\vec{\gamma}_o$ alone. The resulting kinetic energy E due to $\vec{\gamma}_o$ and $\vec{\gamma}$ together is wasted and should be made as small as possible. We introduce the velocity potential $\Phi_o(x,y,z)$ which belongs to the velocity induced by $\vec{\gamma}_o$ and the potential $\Phi(x,y,z)$ which belongs $\vec{\gamma}$. These potentials are independent of time because the wing is assumed to be already at a large distance. The kinetic energy left behind per period can be written as

$$E = \tfrac{1}{2}\mu \int_{-\infty}^{+\infty}\int_{-\infty}^{+\infty}\int_{0}^{b} \{(\frac{\partial}{\partial x}(\Phi_o+\Phi))^2 + (\frac{\partial}{\partial y}(\Phi_o+\Phi)^2 + (\frac{\partial}{\partial r}(\Phi_o+\Phi)^2\}\, dxdydz. \qquad (29.1)$$

The energy E has to be minimized under some constraints. For instance we demand that the mean value T with respect to time of the thrust (force in the positive x direction), must have some prescribed value. This can be written as

$$-\frac{1}{\tau}\int_0^\tau \iint_H \Delta p(\xi,\eta,t)\cos_{n,x}(\xi,\eta)\, dSdt = T, \qquad (29.2)$$

where Δp is given in (28.9), $\cos_{nx}$ is the cosine of the angle between the normal at H and the positive x direction and dS is an element of area of H. The coordinates at the surface H are denoted by ξ and η, the period of length of the ξ coordinate will be b_1. Substitution of (28.9) into (29.2) yields

$$-\frac{\mu}{\tau}\int_0^\tau \iint_H \Gamma(\xi,\eta,t)\, V(\xi,\eta,t)\cos_{n,x}(\xi,\eta)\, dSdt = T. \qquad (29.3)$$

only the lifting surface W which is a finite part of H, contributes to the integral. By the periodicity of the problem with respect to the ξ coordinate and the time we can write instead of (29.3)

$$-\frac{\mu}{\tau}\int_0^{\tau}\sum_{n=-\infty}^{+\infty}\iint_{H_b}\Gamma(\xi,\eta,t+n\tau)\,V(\xi,\eta,t+n\tau)\cos_{n,x}(\xi,\eta)\,dSdt = T, \tag{29.4}$$

where H_b is a fixed period of H stretching over the interval $0 \leq x \leq b$. Hence

$$-\frac{\mu}{\tau}\int_{-\infty}^{+\infty}\iint_{H_b}\Gamma(\xi,\eta,\,t+s)\,V(\xi,\eta,\,t+s)\cos_{n,x}(\xi,\eta)\,dSdt = T, \tag{29.5}$$

only a finite region of time, when the blade W passes the part H_b of H, contributes to the integral. We next consider a contour ℓ(figure (28.1) which connects the two sides of H_b for some point (ξ,η). Then first before the blade has arrived at that point

$$[\Phi(\xi,\eta)]^+_- = \Phi^+(\xi,\eta) - \Phi^-(\xi,\eta) = 0, \tag{29.6}$$

where by $[f]^+_-$ we denote the jump across H of any quantity f and $\Phi(\xi,\eta)$ denotes the value of $\Phi(x,y,z)$ at the point (ξ,η) of H. When the blade has passed entirely we have

$$[\Phi(\xi,\eta)]^+_- = -\int_{-\infty}^{+\infty}\Gamma(\xi,\eta,t)\,V(\xi,\eta,t)dt\,. \tag{29.7}$$

Hence we can rewrite (29.5) as

$$+\frac{\mu}{\tau}\iint_{H_b}[\Phi(\xi,\eta)]^+_-\cos_{n,x}(\xi,\eta)\,dS = T, \tag{29.8}$$

where the integration over H_b has to be carried out when the wing has passed H_b.

Formula (29.8) represents a constraint on the admitted potential functions $\Phi(x,y,z)$ with respect to the mean value of the thrust which has to be delivered by the blade. By replacing for instance the function $\cos_{nx}(\xi,\eta)$ by $\cos_{ny}(\xi,\eta)$ which is the cosine of the angle between the normal $\vec{n}$ and the positive y direction we can put a demand on $\Phi(x,y,z)$ so that a mean force in the y direction is delivered. More generally we can replace the $\cos_{nx}(\xi,\eta)$ by any function, then we obtain a number of constraints

$$\iint_{H_b}[\Phi(\xi,\eta)]^+_- g_i(\xi,\eta)dS - G_i = 0, \quad , \quad i = 1, \ldots, M \tag{29.9}$$

where $g_i(\xi,\eta)$ are prescribed functions and G_i prescribed constants.

Now we have to minimize E for a given function $\Phi_o(x,y,z)$ with respect to the unknown function $\Phi(x,y,z)$ which has to satisfy a number of constraints (29.9).

We have to be careful by demanding conditions (29.9), that they are not contradictory. For instance we can describe the thrust of a screw propeller to be T, while also we prescribe its moment about the x axis along which it is moving, to be M. This is not allowed because M is uniquely determined by T by means of the geometry of the screw blades. In fact the energy necessary for the useful work UT of the screw, where U is the velocity of advance, must be supplied by the torque hence

$$UT = \omega M, \tag{29.10}$$

where both quantities are $O(\varepsilon)$.

The same happens when we would prescribe both the thrust and lateral force acting on the sail of a sailing boat of which the course makes a finite angle with the direction of the relative wind.

We remark that (29.9) represents constraints which are related to mean values of force actions with respect to time. It is however also possible to consider constraints which prescribe force actions at each moment of time. We refer for this to [22].

Exercises.

1) Discuss the relation between the potential jump $[\Phi]^+_-$ at H when the wing has passed, and the free vorticity shed by the wing.
2) Formulate the variational problem in case there are more reference surfaces $H_1 \ldots H_N$.
3) Discuss the function $g_i(\xi,\eta)$ (29.9) which belongs to a prescribed mean value of the moment exerted by a lifting surface about the x axis.

30. Necessary condition for the optimum

In this section we minimize E (29.1) under the constraints (29.9). Suppose the function $\Phi(x,y,z)$ is the optimum potential we are looking for. We change it by $\delta\Phi(x,y,z)$, which has to be a periodic function with period b in the x direction. Then the first variation of E has to be zero,

$$\delta E = \mu \int_{-\infty}^{+\infty}\int_{0}^{b} \{\frac{\partial}{\partial x}(\Phi_o + \Phi).\frac{\partial}{\partial x}\delta\Phi + \frac{\partial}{\partial y}(\Phi_o + \Phi)\frac{\partial}{\partial y}\delta\Phi + \frac{\partial}{\partial z}(\Phi_o + \Phi)\frac{\partial}{\partial z}\delta\Phi\}\, dxdydz = 0. \tag{30.1}$$

We carry out partial integrations of the three terms in the integrand in (30.1) with respect to x, y and z respectively. Consider the first term

$$\mu \int_{-\infty}^{+\infty}\int_{0}^{b} \frac{\partial}{\partial x}(\Phi_o + \Phi)\frac{\partial}{\partial x}\delta\Phi\, dxdydz = \mu \int_{-\infty}^{+\infty}\int_{0}^{b} \frac{\partial}{\partial x}(\Phi_o + \Phi)\, d\delta\Phi dydz =$$

$$= \mu \int_{-\infty}^{+\infty}\int [\frac{\partial}{\partial x}(\Phi_o + \Phi).\delta\Phi \Big|_{x=o}^{b} - \int_{o}^{b} \delta\Phi.\frac{\partial^2(\Phi_o + \Phi)}{\partial x^2}dx]dydz - \mu \int_{H_b}\int [\frac{\partial}{\partial x}(\Phi_o + \Phi)\delta\Phi]_{-}^{+}dydz. \tag{30.2}$$

The second term can be rewritten as follows

$$\mu \int_{-\infty}^{+\infty}\int_{0}^{b} \frac{\partial}{\partial y}(\Phi_o + \Phi)\frac{\partial}{\partial y}\delta\Phi dxdydz = \mu \int_{-\infty}^{+\infty}\int_{0}^{b}\int_{-\infty}^{+\infty} \frac{\partial}{\partial y}(\Phi_o + \Phi)\, d\delta\Phi dxdz =$$

$$= \mu \int_{-\infty}^{+\infty}\int_{0}^{b} [\frac{\partial}{\partial y}(\Phi_o + \Phi).\delta\Phi \Big|_{y=-\infty}^{+\infty} - \int_{-\infty}^{+\infty} \delta\Phi \frac{\partial^2(\Phi_o + \Phi)}{\partial y^2}dy]dxdz - \mu \int_{H_b}\int [\frac{\partial}{\partial y}(\Phi_o + \Phi).\delta\Phi]_{+}^{-}$$

$$\cdot dxdz. \tag{30.3}$$

The third term becomes

$$\mu \int_{-\infty}^{+\infty}\int_{0}^{b} [\frac{\partial}{\partial z}(\Phi_o + \Phi).\delta\Phi \Big|_{z=-\infty}^{+\infty} - \int_{-\infty}^{+\infty} \delta\Phi \frac{\partial^2(\Phi_o + \Phi)}{\partial z^2}dz]dxdy - \mu \int_{H_b}\int [\frac{\partial}{\partial z}(\Phi_o + \Phi)\delta\Phi]_{+}^{-}dxdy. \tag{30.4}$$

We have to add (30.2), (30.3) and (30.4) and make use of the fact that both Φ_o and Φ are potential functions and that Φ_o, Φ and $\delta\Phi$ tend to zero for $y^2 + z^2 \to \infty$. Also we know that Φ_o, Φ and $\delta\Phi$ are periodic functions of period b in the x direction. Then a number of terms cancel each other in the sum, we find

$$\delta E = -\mu \int_{H_b}\int \frac{\partial}{\partial n}(\Phi_o + \Phi).[\delta\Phi]_{-}^{+}\, dS = 0. \tag{30.5}$$

By the continuity of $\frac{\partial}{\partial n}(\Phi_o + \Phi)$ across any surface in space, we are allowed to put this expression out of the square brackets.

The jump $[\delta\Phi]^+_-$ can be chosen zero everywhere with the exception of the neighbourhood of some arbitrary point P at H_b. This is most easily effectuated by placing on H_b, around P a slightly distributed closed vortex ring $\delta\gamma$. Then $[\delta\Phi]^+_-$ is zero for (ξ,η)outside this ring and has non zero values inside this ring (figure 30.1). However we have to satisfy M constraints (29.9).

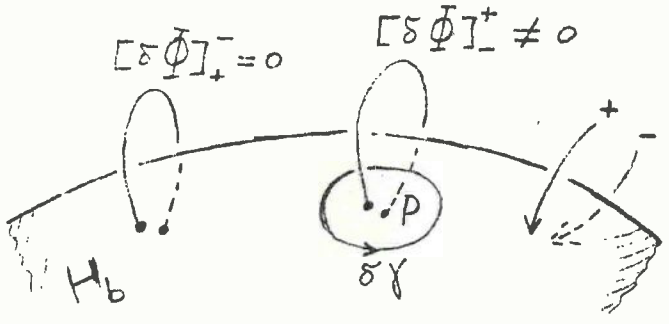

Fig. 30.1. The disturbance potential $\delta\Phi$.

In order to handle these we consider a disturbance $[\delta\Phi]^+_-$ which is non zero in the neighbourhood of M + 1 points $P_1, \ldots, P_{M+1}$ at H_b. The integral over the disturbance $[\delta\Phi]^+_-$ at point P_ℓ over the small region where it is non zero will be denoted by $\delta\Phi_\ell$, then we can replace (30.5) by

$$\frac{1}{\mu}\delta E = -\sum_{\ell=1}^{M+1} \frac{\partial}{\partial n}\{\Phi_o(P_\ell) + \Phi(P_\ell)\}\delta\Phi_\ell = 0. \tag{30.6}$$

For these disturbances the constraints (29.9) are written as

$$\sum_{\ell=1}^{M+1} g_i(P_\ell)\,\delta\Phi_\ell = 0 \qquad , i = 1, \ldots, M. \tag{30.7}$$

By equation (30.7) we can express $\delta\Phi_1, \ldots, \delta\Phi_M$ into $\delta\Phi_{M+1}$. We introduce the following determinants

$$D = \left| g_i(P_\ell) \right| \quad , \quad i,\ell = 1, \ldots, M, \tag{30.8}$$

$$D_k = \begin{vmatrix} g_1(P_1) & \cdots & g_1(P_{k-1}) & g_1(P_{M+1}) & g_1(P_{k+1}) & \cdots & g_1(P_M) \\ \vdots & & \vdots & \vdots & \vdots & & \vdots \\ g_M(P_1) & & g_M(P_{k-1}) & g_M(P_{M+1}) & g_M(P_{k+1}) & & g_M(P_M) \end{vmatrix}, \tag{30.9}$$

where $k = 1, \ldots, M$. Then we find by Cramer's rule

$$\delta\Phi_k = -D^{-1} \cdot D_k \, \delta\Phi_{M+1}. \tag{30.10}$$

Substituting this result in (30.6) and dividing by $\delta\Phi_{M+1}$ yields

$$-D^{-1} \sum_{\ell=1}^{M} \frac{\partial}{\partial n} (\Phi_o(P_\ell) + \Phi(P_\ell)) \, D_\ell = \frac{\partial}{\partial n} (\Phi_o(P_{M+1}) + \Phi(P_{M+1})). \tag{30.11}$$

Next we assume the points $P_1, \ldots, P_M$ to be chosen at fixed places at H_b, while the point P_{M+1} is allowed to move freely over H_b. This latter point will be denoted by P. Hence we find from (30.11) by expanding the determinants D_ℓ (30.9) with respect to the column which contains $P_{M+1} = P$

$$\frac{\partial}{\partial n} \Phi(P) = -\frac{\partial}{\partial n} \Phi_o(P) + \sum_{i=1}^{M} \lambda_i \, g_i(P), \quad P \in H, \tag{30.12}$$

where λ_i are unknown constants. This relation is a necessary condition for the normal component $\frac{\partial \Phi}{\partial n}$ of the velocity induced at H at an arbitrary point P by the free vorticity sheet left behind by the optimum wing at H. Herewith we have found for the optimum potential Φ a necessary condition in the form of a Neumann problem. This has to be solved while the λ_i are still unknown, afterwards the λ_i, $i = 1, \ldots, M$, can be determined by the M constraints (29.9).

Condition (30.12) follows also from the demand that the linear homogeneous equations (30.6) and (30.7), for the unknowns $\delta\Phi_\ell$, $\ell = 1, \ldots, M + 1$, would possess a non trivial solution.

Exercise.

Discuss the optimization condition (30.12) in case there are more reference surfaces $H_1, \ldots, H_N$.

31. Optimum ducted screw propellers

We consider a screw propeller with m blades placed in a shroud of zero thickness, which is in the neighbourhood of a circular reference cylinder of finite length and of radius r_s. The blades of radius r_o are connected to a two sided infinitely long hub of radius r_i. In section 39 we return to this model of a hub and discuss its limitation. The propeller rotates with an angular velocity ω and is placed in a parallel flow with velocity U in the negative x direction:

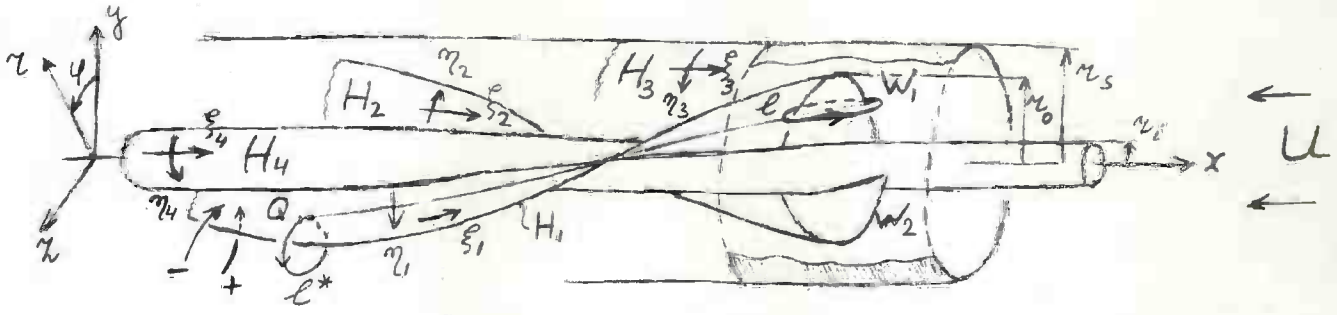

Fig. 31.1. Two bladed screw propeller within a shroud (partly removed).

It has to deliver a prescribed thrust T in the positive x direction.

In the optimum case the free vorticity shed by the blades and the shroud is determined by the optimization theory. The bound vorticity on shroud and blades in turn is determined by this free vorticity. Because the free vorticity behind the shroud is not rotationally symmetric as a consequence of the presence of the helicoidal vortex sheets behind the blades, also the circulation around the shroud will not be constant in circumferential direction. Therefore the shroud must have profiles which vary along its circumference. It is clear that the vortex configurations both on the screw as well as on the shroud are stationary with respect to a system of axes which rotates with the screw. In order to have also a stationary vortex configuration and local angles of incidence with respect to the shroud, we can assume that the shroud rotates with the same angular velocity as the screw. The profiles of the shroud are defined as the intersections of the shroud and the helicoidal surfaces

$$\varphi + ax = \text{const.} \tag{31.1}$$

It has been remarked already in section 20 that a shroud can be favourable with respect to efficiency by the interaction of the vorticity flowing from its trailing edge and the vorticity shed by the blades. The influence of the type of shroud described here will be optimal. This means that when a shroud of this type has not much influence, a rotationally symmetric conventional shroud when it has the same diameter cannot have more influence, irrespectively of its length. In the case of zero clearance ($r_o = r_s$) we have an optimum ring propeller of which the ring is not rotationally symmetric. For ring propellers with rotationally symmetric rings, we refer to [8]. The meaning of the schematization we use here will be discussed more extensively in section 35.

The reference surfaces H_k of the previous section are in our case the following. First, the H_j $j = 1, \ldots, m$, are the stationary helicoidal surfaces along which the m blades of the propeller are moving when the fluid is put to rest and the screw has the velocity U in the positive x direction, which is of course the same problem. The surface H_{m+1} is the surface along which the shroud is moving and H_{m+2} is the two-sided infinite shaft. On these surfaces we can introduce orthogonal length coordinates (ξ_k, η_k), $k = 1, \ldots, m+2$, as follows. On H_j, $j = 1, \ldots, m$ we choose as η_j the distance of a point of H_j to the x axis, hence $\eta_j = (y^2 + z^2)^{\frac{1}{2}} = r$; $(x,y,z) \in H_j$. We take for ξ_j the length coordinate along lines $\eta_j = r = \text{const}$. The positive direction of η_j is chosen in the direction of increasing r values. We can also introduce on H_j the non-length coordinate $x = \xi_j(1 + a^2r^2)^{-\frac{1}{2}}$. At H_{m+1} we take $\xi_{m+1} = x$ and $\eta_{m+1} = r_s\varphi$ analogously at H_{m+2}, $\xi_{m+2} = x$ and $\eta_{m+2} = r_i\varphi$.

In this case we assume that the incoming fluid is homogeneous, this means that for the problem of the advancing screw, the fluid is not disturbed before, hence $\Phi_o \equiv 0$. We have only one force condition (M = 1, (30.12)). The function $g_1(\xi,\eta)$ (29.9) becomes, as has already been discussed (29.8)

$$g_1(\xi,\eta) = \frac{\mu}{\tau} \cos_{(n,x)}(\xi,\eta), \tag{31.2}$$

where now (ξ,η) is any point on $H_1, \ldots, H_{m+2}$. Then the necessary condition for an optimum becomes

$$\frac{\partial}{\partial n}\Phi(\xi,\eta) = \lambda_1 \cos_{(n,x)}(\xi,\eta), \tag{31.3}$$

where we have absorbed the constant μ/τ in the still unknown constant λ_1.

The meaning of (31.3) is the following. Consider the m helicoidal surfaces $H_1, \ldots, H_m$ and the two circular cylinders H_{m+1} and H_{m+2}, all two sided infinite, to be rigid and impermeable. Then the potential $\Phi(x,y,z)$ belongs to the fluid motion which arises by translating these surfaces in the positive x direction with a velocity λ_1. First we will discuss this potential problem.

Introduce a helicoidal coordinate system (ζ,ρ,σ) by

$$\zeta = \varphi + ax \ , \ \rho = ar = a\,(y^2 + z^2)^{\frac{1}{2}} \ , \ \sigma = \varphi \ , \quad a = \omega/U. \tag{31.4}$$

The potential equation for the function φ becomes

$$a^2\{\frac{\partial^2}{\partial\zeta^2} + \frac{1}{\rho}\ \frac{\partial}{\partial\rho}\,\rho\,\frac{\partial}{\partial\rho} + \frac{1}{\rho^2}\ (\frac{\partial^2}{\partial\zeta^2} + 2\frac{\partial^2}{\partial\zeta\partial\sigma} + \frac{\partial^2}{\partial\sigma^2})\}\ \Phi(\zeta,\rho,\sigma) = 0. \tag{31.5}$$

We first show that this potential is independent of σ. This is clear from the statement of the problem for the velocities, however because the potential arises from these by means of integration, this is not evident for Φ itself. Suppose Φ is given in a point ζ_0, ρ_0, σ_0 and we calculate the potential in a general point ζ_1, ρ_1, σ_1. Then by figure 31.3

$$\Phi(\zeta_1,\rho_1,\sigma_1) = \Phi(\zeta_0,\rho_0,\sigma_0) + |\vec{v}(\zeta_0,\rho_0)|\ \cos\alpha \int_{\zeta_0,\rho_0,\sigma_0}^{\zeta_0,\rho_0,\sigma_1} ds +$$

$$+ \int_{\zeta_0,\rho_0,\sigma_1}^{\zeta_0,\rho_1,\sigma_1} \vec{v}(\zeta_0,\rho)\,.\,d\vec{s} + \int_{\zeta_0,\rho_1,\sigma_1}^{\zeta_1,\rho_1,\sigma_1} \vec{v}\ (\zeta,\rho_1)\ d\vec{s}\ , \tag{31.6}$$

where $\alpha = \alpha(\zeta_0,\sigma_0)$ is the angle between the velocity $\vec{v}$ and the helicoidal line through $(\zeta_0,\rho_0,\sigma_0)$ and $d\vec{s}$ is an "infinitesimal length" vector.

The first integral in (31.6) is along a helicoidal line, the second along a radius and the third in the x direction. From (31.6) it follows that we can

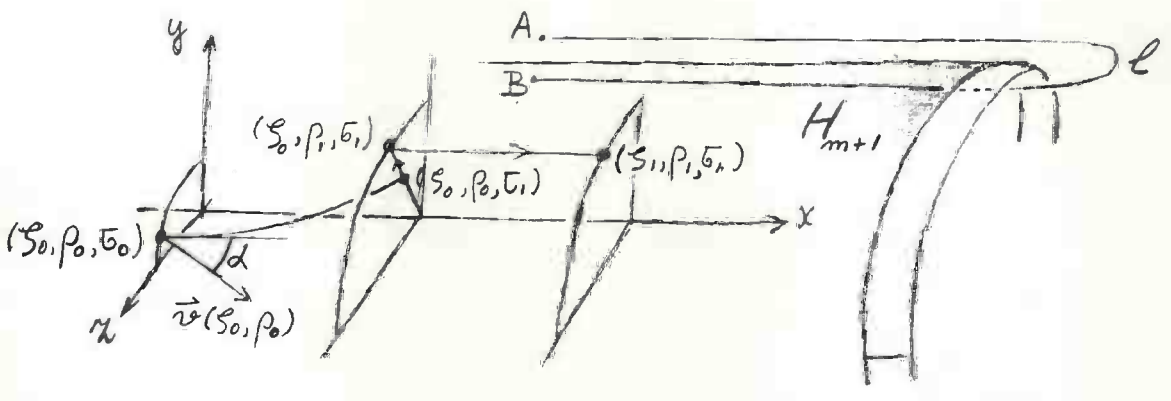

Fig. 31.2. The path of integration $(\zeta_0,\rho_0,\sigma_0) \to (\zeta_1,\rho_1,\sigma_1)$.

write the potential at the point $(\zeta_1,\rho_1,\sigma_1)$ in the form

$$\Phi(\zeta_1,\rho_1,\sigma_1) = \Phi(\zeta_o,\rho_o,\sigma_o) + (\sigma_1 - \sigma_o)k(\zeta_o,\rho_o)\cos\alpha + F(\zeta_1,\rho_1), \tag{31.7}$$

where $k(\zeta_o,\rho_o)$ is a non zero constant and F is a function independent of σ_1.

Formula (31.7) shows that when $\cos\alpha \neq 0$, we have a term which is linear in $(\sigma_1 - \sigma_o)$, hence the potential will increase indefinitely with σ_1, by fixed ζ_1 and ρ_1. Connect a point A outside H_{m+1} with a point B inside H_{m+1} by means of a long slender contour ℓ(figure 31.2) around the "beginning" of H_{m+1}. Then the potential difference between A and B equals the enclosed vorticity at H_{m+1}. However the vorticity at H_{m+1} is a periodic function of x with zero mean value hence the potential difference between A and B has to remain finite. This yields a contradiction when $\cos\alpha \neq 0$ and the fact that outside of H_{m+1} the disturbance velocity is zero. Hence $\cos\alpha = 0$ or $\alpha = \pi/2$ radians which means that the velocity field induced by the translation of the helicoidal surfaces $H_1, \ldots, H_m$ and the cylinder H_{m+1}, is perpendicular to the helicoidal lines $\zeta = \zeta_o$, $\rho = \rho_o < r_s$. Then

$$\Phi = \Phi(\zeta,\rho). \tag{31.8}$$

32. The boundary value problem for the potential

We consider the m helicoidal free vortex sheets far behind the propeller blades. Also we imagine m bisector helicoidal surfaces, exactly in between them. These two types of surfaces can be generated by straight lines perpendicular to the x axis, which move along this axis with the appropriate angular velocity.

Now we take such a line g generating a bisector plane consider it in a fixed position and rotate the whole system of vortex sheets and bisector surfaces about g over an angle of π radians After that each surface coincide with one or another surface of its own type of the original configuration. When we multiply next the vorticity on the vortex sheets and on the cylinder behind the shroud by -1, we obtain again the original velocity field.

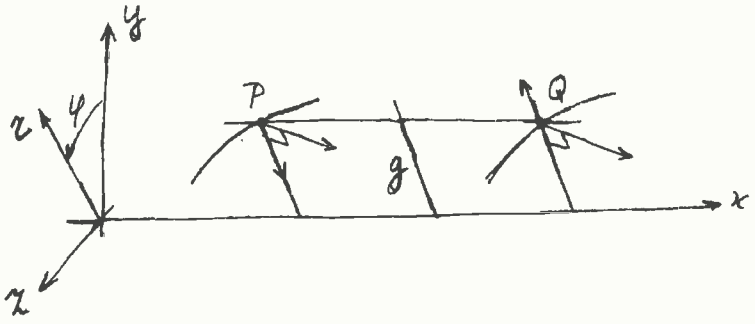

Fig. 32.1. Velocities in two points, symmetrically placed with respect to a bisector surface.

Consider an arbitrary pair of points P and Q, which have equal values of φ and r and which changed position after the rotation mentioned above. It follows that the velocities in P and Q possess the symmetry relation drawn in figure 32.1. The velocity components perpendicular to the r direction have to be parallel and of equal magnitude while the components in the r direction are of the same magnitude however opposite in sense.

When P and Q tend to each other and hence to the bisector plane, we see that the components of the velocity in the r direction have to vanish. This means that, because we found already that $\alpha = \pi/2$ radians in figure 31.2, the whole bisector surface has a constant potential, say $\Phi = 0$. Then however each bisector plane has the potential zero. This can be seen as follows, suppose the potential difference between two neighbouring bisector surfaces is Δ. Then we have $m\Delta = 0$, because after m steps we are again the same bisector surface, hence $\Delta = 0$.

An analogous reasoning can be given for two points which change position when we rotate the whole system overπ radiansabout a generating line of a helicoidal surface H_j, $j = 1, \ldots, m$. The only difference is that here the velocity components in the r direction do not have to vanish when both points tend to the free vortex sheet H_j, because by the presence of the vorticity on the sheet a discontinuity can be tolerated. However on the extensions of the H_j, $j = 1, \ldots, m$, to H_{m+1} the r component has to be zero, hence there the potential is constant. It can be seen that first all these extensions have the same potential and second that this value is zero. From these results it follows for the potential $\Phi(\zeta,\rho) = -\Phi(2\tilde{\zeta} - \zeta,\rho)$ when $\tilde{\zeta}$ belongs to a point on a bisector surface or on a vorticity sheet H_j, $j = 1, \ldots, m$.

We now discuss the boundary condition on the rigid and impermeable vorticity sheets H_j, which translate in the positive x direction with the velocity λ_1 (31.3). The equation of these surfaces in cylindrical coordinates is

$$G = \varphi + a(x - \lambda_1 t) - \frac{2\pi j}{m} = 0 \quad , \quad j = 0,1, \ldots, m-1. \tag{32.1}$$

The boundary condition (15.3) yields

$$-a\,\lambda_1 + a\,\frac{\partial\Phi}{\partial x} + \frac{1}{r^2}\,\frac{\partial\Phi}{\partial\varphi} = 0 \,, \tag{32.2}$$

or in helicoidal coordinates

$$\frac{\partial\Phi}{\partial\zeta} = \frac{\lambda_1}{a}\,\frac{\rho^2}{1+\rho^2} \,. \tag{32.3}$$

From this and the symmetry relations we find that the potential Φ has to satisfy the boundary conditions denoted in figure 30.2. Because $\Phi(\zeta,\rho)$ does

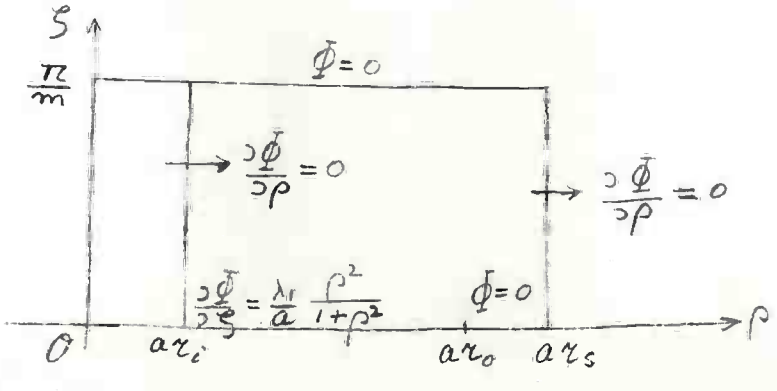

Fig. 32.2. The boundary conditions for the potential $\Phi(\zeta,\rho)$.

not depend on σ, (31.5) simplifies to

$$\left\{\rho \frac{\partial}{\partial \rho} \rho \frac{\partial}{\partial \rho} + (1 + \rho^2) \frac{\partial^2}{\partial \zeta^2}\right\} \Phi(\zeta,\rho) = 0. \tag{32.4}$$

This boundary value problem has to be solved by numerical means. In the case $\frac{\lambda_1}{a} = 1$, we denote the solution by $\Phi_1(\zeta,\rho)$.

When we have a screw propeller without a shroud we have to take in figure 32.2, $r_s = \infty$, hence we have to solve the boundary value problem for a semi infinite strip.

Exercises.

1. Show that the effect of the infinitely long cylindrical hub of figure 31.1 is, in the optimum case, the same as an "inner shroud".
2. Show that when we have no hub in this problem then we have instead of figure 32.2, the following boundary conditions.

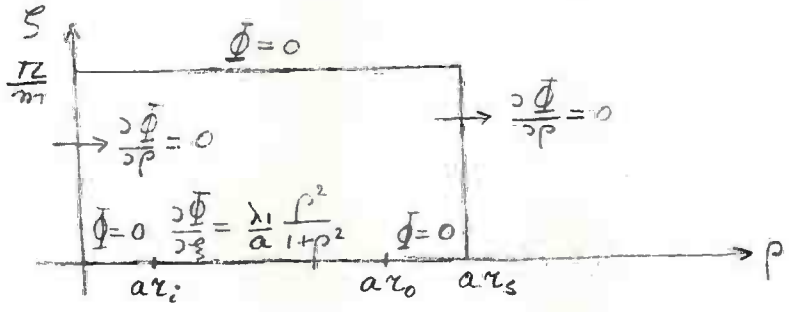

Fig. 32.3. Boundary conditions when hub is neglected.

33. Bound vorticity on blades and shroud

At a certain value of $\eta_1 = r$ we place a contour ℓ around the blade W_1 (figure 31.1) by which we define the circulation $\Gamma(r)$ around W_1. This circulation is reckoned positive when it is coupled with a right hand screw to the positive r direction. The total amount of free vorticity shed by the blade between the place r and the tip equals this value. We reckon the free vorticity, which lies along the ξ_1 coordinate line, positive when it is coupled with a right hand screw to the positive ξ_1 direction. Next we consider far behind the propeller the point Q on H_1 and the contour ℓ^* which connects the -side and the +side of H_1 at Q. Then we find

$$\Gamma(r) = -[\Phi(Q)]^+_- = 2\,\Phi(0,ar) = \frac{2\lambda_1}{a}\,\Phi_1(0,\rho)\ ,\ \rho = ar, \tag{33.1}$$

where Φ_1 is the potential which follows from the boundary value problem of figure 32.2 for $\frac{\lambda_1}{a} = 1$. We remark that contour ℓ^* can be obtained from contour ℓ by a continuous deformation without cutting vorticity lines hence without a change of enclosed vorticity.

Next we have to determine the unknown constant λ_1 by means of condition (29.9) which in this case has the special form (29.8) We can take

$$\tau = 2\pi/\omega \quad , \quad b = U\tau = \frac{2\pi}{a} \quad , \quad \left(a = \frac{\omega}{U}\right) , \tag{33.2}$$

hence because we have m blades (29.8) becomes

$$\frac{\mu\omega m}{2\pi} \iint_{H_b} [\Phi(\xi,\eta)]^+_- \cos_{n,x}(\xi,\eta)\, dS = \frac{\mu\omega m}{2\pi} \int_0^{\frac{2\pi U}{\omega}} \int_{r_i}^{r_o} [\Phi(r)]^+_- \frac{ar\ \ dr}{(1+a^2r^2)^{\frac{1}{2}}} \cdot$$

$$\cdot \sqrt{1+a^2r^2}\, dx = \mu\,\omega\, m \int_{r_i}^{r_o} [\Phi(r)]^+_- \ rdr = -\mu\,\omega\, m \int_{r_i}^{r_o} r\,\Gamma(r)\, dr = T. \tag{33.3}$$

In (3.13) we used the fact that behind the propeller blade $[\Phi]^+_-$ depends only on $\eta_1 = r$ where r is the distance of a point to the x axis. We remark that by the choice of the helicoidal surfaces (31.1) $\omega = -\frac{d\varphi}{dt}$. Substitution of (33.1) into (33.3) yields

$$\lambda_1 = \frac{-\omega^2 T}{2\mu m U^3} \left\{ \int_{ar_i}^{ar_o} \rho\,\Phi_1(0,\rho)\, d\rho \right\}^{-1} \underline{\underline{\text{def}}}\ \frac{\omega^2 T}{2\mu m U^3}\ J^{-1}(ar_i, ar_o, ar_s, m). \tag{33.4}$$

where we introduced the quantity J.

Next we direct our attention to the circulation Γ_s around the shroud. Around the shroud we take a narrow contour ABCD (figure 33.1).

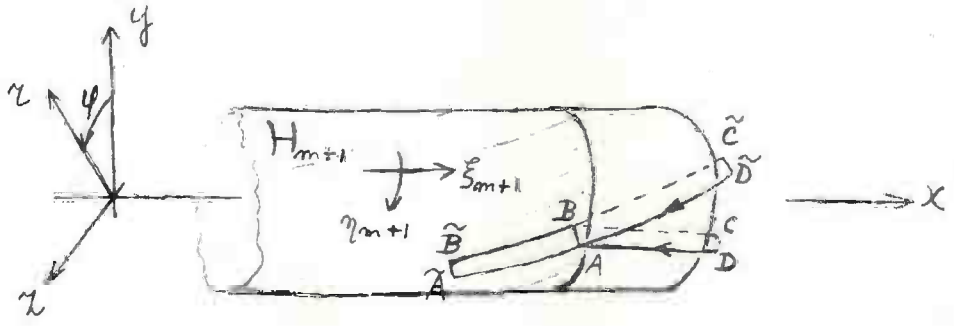

Fig. 33.1. On the circulation around the shroud.

This circulation is reckoned positive when it is coupled with a right hand screw to the direction of increasing φ on the shroud. First we observe that Γ_s is to a certain extent independent of the shape of ABCD. This contour may be deformed continuously, however when doing this it may not cut through vortex lines. Hence another more natural choice is to let it lie on a helicoidal plane $ax + \varphi = \zeta = \text{const.}$ $(\tilde{A},\tilde{B},\tilde{C},\tilde{D})$ around a profile (31.1) of the shroud. Next we let $\tilde{A}$ and $\tilde{B}$ tend along $\zeta = \text{const.}$ to a place far behind the propeller. Then it follows that

$$\Gamma_s(\zeta) = \Phi(\tilde{A}) - \Phi(\tilde{B}) \ , \tag{33.5}$$

where $\tilde{A}$ is just outside H_{m+1} and $\tilde{B}$ just inside it. Then we find

$$\Gamma_s(\zeta) = \Phi(\tilde{A}) - \frac{\lambda_1}{a} \Phi_1(\zeta, ar_s) \ . \tag{33.6}$$

The potential $\Phi(\tilde{A})$ is not fixed because only the normal derivative $\frac{\partial \Phi}{\partial n}$ is prescribed at the surfaces H_j, $j = 1, \ldots, m+2$, and H_{m+1} shields the outer region from the inside. This means that outside we can take any constant "function" as potential. From this it follows that we can add a constant value to the circulation of the shroud. This added constant circulation does not shed any vorticity, it increases or decreases the fluid velocity at the place of the screw.

The question remains how we have to find the shape of the blades and of the shroud which induces the optimum bound vorticity. First we consider the blades and assume the planform of them to be given. The known circulation has to be distributed in some way in chordwise direction. The way in which this is done is of no importance for the free vorticity left behind in our linearized theory. For instance we can take the bound vorticity constant along each chord, then we have along each chord a constant pressure jump which varies with r. By this the loading (15.17) of the blade becomes

$$Q(x,r) = \mu(U^2 + \omega^2 r^2)^{\frac{1}{2}} \Gamma(r)/b(r) \quad , \tag{33.7}$$

where $b(r)$ is the length of the chord. From this loading follows by considerations about the strength of the blade, its thickness distribution. For instance consider the case that no shroud is present ($r_s = \infty$) and that the influence of the hub is neglected. This means that in our previous formulas we have to use the potential which belongs to the boundary values of figure 32.3. Then by the lifting surface theory of sections 14-19, we can determine the shape of the blades in this optimum case.

When a shroud is present we have to discuss both blades and shroud together in one lifting surface theory. This is not more difficult in essence than the theory for the blades alone, however being rather complicated we will not discuss it here.

We still shortly discuss the interesting case that the clearance between blade tip and shroud is zero ($r_o = r_s$). Then it follows from numerical calculations that the bound vorticity on the blades does not tend to zero for $\rho \to ar_o$. Hence a concentrated free vortex of strength $\frac{2\lambda 1}{a} \Phi_1(0,ar_o)$ (33.1) leaves the tip of the blade. Next the vorticity on the shroud is odd with respect to the blades and discontinuous at the blades. Hence a jump in its vorticity exists by which a concentrated free vortex is shed, which is by (33.6) of the same strength as the tip vortex however of opposite sign so that they cancel each other.

In the case of a small clearance no concentrated free vortices arise, however the principle remains the same, a strong free vortex shed by the shroud interferes favourably with a strong free tip vortex.

Exercise.

Derive the last equality of equation (33.3) directly by means of the law of Joukowski for a force on a bound vortex.

34. The efficiency of optimum ducted propellers

In this section we will calculate the kinetic energy E left behind by the optimum directed propeller per unit of time. From this energy follows the efficiency of the propulsion system. We do not use formula (29.1), but a well known form which results by partial integration from it. The kinetic energy within a closed surface S, can be written as

$$E = -\tfrac{1}{2}\mu \iint_S \Phi \frac{\partial \Phi}{\partial n}\, dS, \tag{34.1}$$

where the normal derivative is with respect to the inward normal and dS is a surface element.

In our case we have to consider the kinetic energy in a part of space far behind the propeller, bounded by the hub, the cylinder behind the shroud and two flat planes perpendicular to the x axis at a distance U of each other. When the screw has m blades this kinetic energy is 2 m times the kinetic energy between a helicoidal surface behind one of the blades, extend to the cylinder and a bisector surface. From figure 32.2 it follows that the only contribution to (34.1) comes from the helicoidal surface. The value of $\frac{\partial \Phi}{\partial n}$ is given in (31.3) by the optimization condition

$$\frac{\partial \Phi}{\partial n} = \lambda_1 \frac{ar}{(1 + a^2 r^2)^{\frac{1}{2}}} . \tag{34.2}$$

Hence we find for (34.1)

$$E = -\frac{\mu m \lambda_1^2 U}{a^2} \int_{ar_i}^{ar_o} \rho\, \Phi_1\,(0,\rho)\, d\rho = \frac{\mu m \lambda_1^2 U}{a^2}\, J , \tag{34.3}$$

where we used the symbol J introduced in (33.4). Using (33.4) we can write the efficiency η as

$$\eta = \frac{TU}{TU + E} = \left(1 + \frac{\omega^2 T}{4\mu m U^4 J}\right)^{-1} . \tag{34.4}$$

From (34.4) it follows that the efficiency of the optimum directed propeller increases with the number J From the boundary values prescribed in figure 32.2 it seems reasonable that this happens when $r_s \to r_o$, because then the influence of the values $\Phi = 0$ at $\zeta = 0$, $ar_o \leq \rho \leq ar_s$ becomes less.

This follows by interpreting the values of Φ as the small deviation of a membrane from its neutral position, it will be confirmed by the numerical results of next section. Hence the clearance between blades and shroud must be as small as possible.

For convenience we will compare the kinetic energy left behind by the ducted propeller with the kinetic energy left behind by the actuator disk with a constant normal load, same total thrust, same working area and same velocity of advance. The quotient of the kinetic energy E_i shed per unit of time by the disk (11.12) and E becomes

$$q = \frac{E_i}{E} = \frac{2mU^2J}{A\omega^2} \tag{34.5}$$

where A is the working area of the disk. Using this coefficient we can write the efficiency (34.4) as

$$\eta = \left(1 + \frac{T}{2q\mu U^2 A}\right)^{-1} . \tag{34.6}$$

This efficiency equals for $q = 1$ the efficiency of the ideal propeller, as the actuator disk was named in section 11. We will call q the quality factor and prove lateron that

$$q \leq 1. \tag{34.7}$$

We remark that the quality factor and the efficiency are each other supplementing informations about a propeller. If under general conditions the efficiency of a propeller is in the neighbourhood of one, we can say the propeller is a good one, and it makes no sense to improve it. However when a propeller has to have prescribed dimensions and when it has to deliver a certain thrust it can happen that its efficiency is bad. Then we can test by considering its quality factor if this bad efficiency could be raised . When the quality factor is in the neighbourhood of one this is not possible and we have to say that even then it is a good propeller, under the conditions it has to satisfy.

In order to give numerical data for q we have to determine the working area A of the ducted propeller. In section 28 it was defined as the cross section of the most narrow cylinder with its axis along the direction of advance of the propeller which encloses all the vorticity belonging to the propulsion system. This means here that we have to enclose the free vorticity behind the shroud and behind the blades. Hence the cross section of the cylinder consists of a circle with radius r_i which has zero area and the area between the two circles with radius r_o and r_i. Hence we can take for the working region $A = \pi(r_o^2 - r_i^2)$. However because we consider in the next sections different values for r_i it seems more appropriate to choose

$$A = \pi r_o^2, \tag{34.8}$$

35. Numerical data, quality factor

We consider here numerical results with respect to optimum ducted propellers as described in section 31. Hence we have an infinitely long cylindrical hub of radius r_i, on which a number m of blades are mounted of tip radius r_o and around which there is a duct of radius r_s which is not rotationally symmetric but which rotates with the blades. We have solved equation (32.4) numerically for the potential Φ under the boundary conditions of figure 32.2.

First we show the influence of the clearance between shroud and the blade tips on the quality factor q (34.5). This will be given for a special choice of the parameters as is denoted in table 35.1. As working area we choose πr_o^2 as has been discussed in the previous section (34.8). In the first column we give two values of (ar_o). The second column gives for each of these values two values of the number of blades m. In the first row are given the values of r_s/r_o, which is a measure for the width of the clearance.

ar_o	m	1	1,025	1,05	1,075	1,1	∞	r_s/r_o
2	2	.558	.363	.331	.317	.308	.290	
	5	.581	.448	.433	.427	.424	.416	
5	2	.856	.685	.656	.644	.638	.631	
	5	.858	.761	.754	.753	.752	.749	

Table 35.1. Influence of the clearance on q , $r_i/r_o = 0,2$.

The whole table is valid for a constant ratio of hub and blade radius, $(ar_i)/(ar_o) = 0,2$. We see from this table that already a small slit of about 5% causes a sharp decrease of the value of q, especially for smaller values of r_o and m.

Next we give a more general survey of the influence of the parameters on the quality coefficient q. The grouping of the results in table 35.2 will be clear. From the numerical values it follows that the case of zero clearance $r_s/r_o = 1$, is substantially better than the case in which the shroud is absent $r_s/r_o = \infty$. This is especially true for a small number of blades.

These tables can possibly be used to judge if it will be appropriate from the viewpoint of efficiency, to apply a shroud. When in given circumstances the difference of q for the case with and without a shroud is small, then the losses by viscosity effects will nullify the gain in efficiency predicted by potential theory.

ar_o	r_i/r_o	r_s/r_o	1	2	3	4	5	m
2	0,1	1	.509	.539	.560	.572	.579	
		∞	.190	.285	.345	.387	.417	
	0,2	1	.544	.558	.568	.576	.581	
		∞	.190	.290	.350	.390	.419	
	0,3	1	.558	.563	.568	.572	.575	
		∞	.179	.282	.344	.384	.412	
3	0,1	1	.691	.713	.726	.732	.736	
		∞	.304	.438	.512	.558	.589	
	0,2	1	.713	.722	.728	.731	.733	
		∞	.302	.441	.513	.557	.586	
	0,3	1	.709	.712	.715	.717	.718	
		∞	.283	.425	.498	.542	.570	
4	0,1	1	.793	.806	.813	.816	.818	
		∞	.402	.553	.626	.668	.692	
	0,2	1	.802	.807	.810	.811	.812	
		∞	.397	.551	.622	.662	.686	
	0,3	1	.784	.786	.787	.788	.788	
		∞	.371	.527	.599	.639	.662	
5	0,1	1	.855	.862	.864	.866	.867	
		∞	.514	.647	.706	.738	.759	
	0,2	1	.853	.856	.856	.856	.858	
		∞	.504	.631	.697	.729	.749	
	0,3	1	.826	.826	.826	.827	.827	
		∞	.472	.609	.667	.699	.719	

Table 35.2. Survey of values of q.

Finally we give two examples of optimum circulation distributions on the blades and on the shroud. These follow from (33.1) and (33.6) respectively. In fact we discuss only the circulation of the shroud, for which the constant $\Phi(\tilde{A})$ in (33.6) is zero, hence the part which actually increases efficiency in potential theory by the favourable vortex interaction.

The two cases are, zero clearance $ar_o = ar_s = 2,5$ (figure 35.1) and a small clearance $ar_o = 2,5$ and $r_s = 1,04\ r_o$ (figure 35.2). We have a propeller with

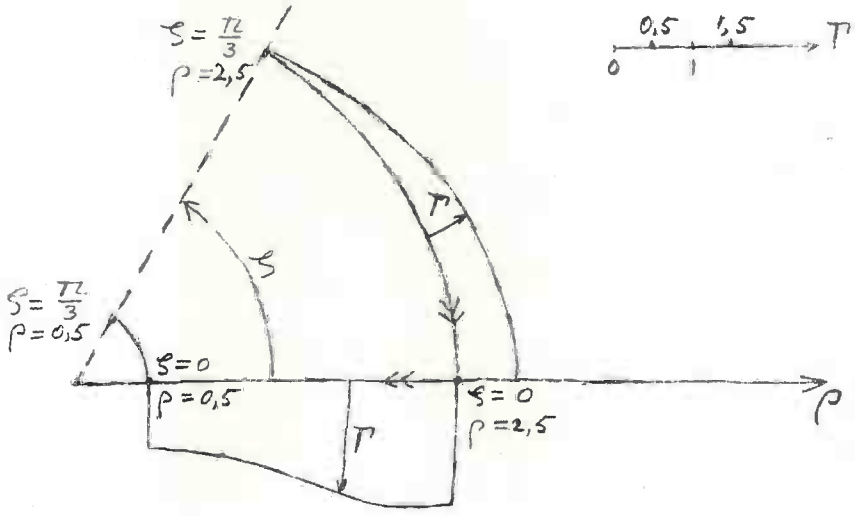

Fig. 35.1. The optimum circulation distribution on the blade and on part of the shroud, $ar_i = 0,5$, $ar_o = ar_s = 2,5$ and $m = 3$.

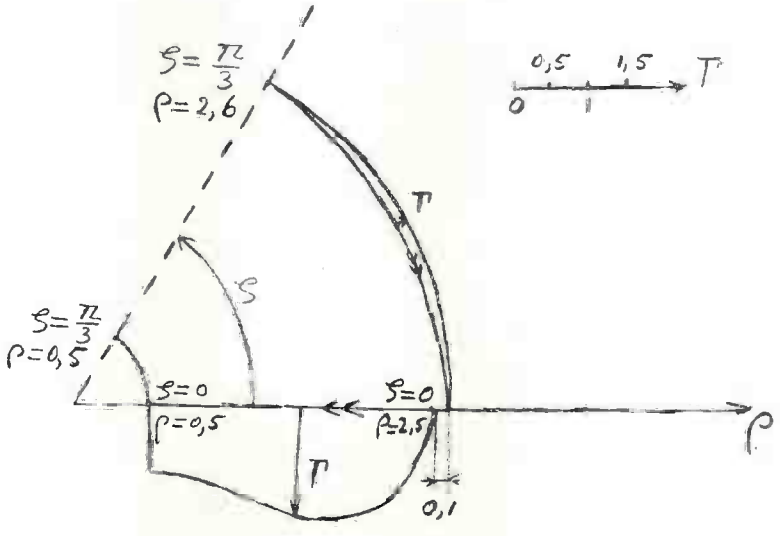

Fig. 35.2. The optimum circulation distribution on the blade and on part of the shroud, $ar_i = 0,5$, $ar_o = 2,5$, $ar_s = 2,6$ and $m = 3$.

three blades, m = 3. In both figures the blade is represented by the line from (ρ = 0,5; ζ = 0) towards (ρ = 2,5; ζ = 0), the shroud by the circle and the dashed line is a bisector plane. Both cases are calculated for $\frac{\lambda_1}{a}$ = 1, hence the potential used is $\Phi_1(\zeta,\rho)$ (figure 32.2). This does not mean that the thrust of both propellers is equal, however we can read from the figures the relative strength of the circulation on the blades and on the shroud.

Because the circulation on the shroud is odd with respect to the blade there is, in the case of zero clearance (figure 35.1) a finite jump in the circulation of the shroud which cause a concentrated free trailing vortex. This vortex has the same strength as the concentrated vortex shed by the blade tip, however, with opposite sign. Therefore they cancel each other. This can be seen in figure 35.1, where at the end of the blade the circulation has the strength 1,64 and the circulation on the shroud exhibits a jump of 2.0,82 = 1,64. The directions of the circulation on the blade and on the shroud are denoted by a double arrow (right-hand screw).

The case of finite clearance is given in figure 35.2. There we have the same parameters as in figure 35.1 only ar_s is different, we take ar_s = 2,6. The circulation at the blade tip now becomes zero and also at the shroud just opposite the tip.

36. The optimization of a sail of a yacht

We will give in this section a second application of the optimization theory and discuss a simple case of the optimization of a sail. We assume that the sail is represented by a lifting line OA of length ℓ, this is in the linearized theory not a restriction of generality. The line OA is assumed to be perpendicular to the water surface which coincides with the (z,x) plane and lies along the y axis. Also we assume that there is no gap between sail and water surface. In order to simulate the boundary between air and water we consider as usual the image OB of the lifting line with respect to the plane y = 0, then it is allowed to

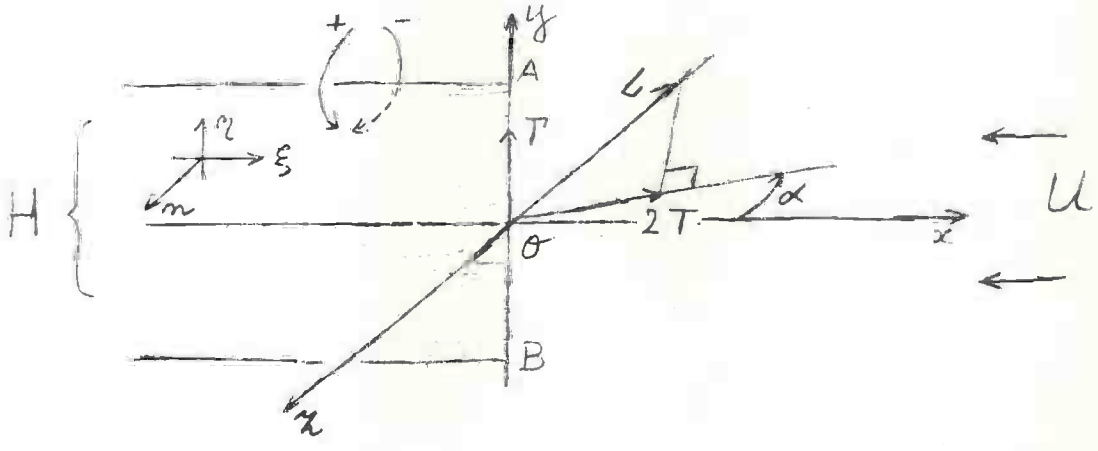

Fig. 36.1. The lifting line OA and its image OB.

consider the whole space to be filled with air. This air has a velocity of magnitude U with respect to the yacht. The x axis of the coordinate system is chosen so that the relative velocity of the air is in the negative x direction. The thrust of the sails has to be in a direction which, as denoted in figure 36.1, makes an angle α with the positive x axis. In this flow we now have a lifting line of length 2ℓ. In accordance with the terminology of the optimization theory we can state that this lifting line moves with respect to the air along a reference surface H which is the strip $-\infty \leq x \leq +\infty$, $|y| < \ell$, $z = 0$. As coordinates on H we could choose $\xi = (x - Ut)$ and $\eta = y$.

Now we will impose two conditions on the force action of the lifting line. First the thrust of the sails will have the magnitude $T(0(\varepsilon))$. Because the lifting line has become two times as long by means of the mirroring, we demand a lift for the total line $L = 2T/\cos\alpha$. Hence for the disturbance potential far behind the sail we have the constraint (29.9)

$$-\mu\, U \int_{-\ell}^{+\ell} [\Phi]_-^+ \, dy = \mu\, U \int_{-\ell}^{+\ell} \Gamma(y)\, dy = 2T/\cos\alpha, \tag{36.1}$$

where $\Gamma(y)$ is the circulation around the sail, reckoned positive with a right hand screw in the positive y direction. Second we prescribe the heeling moment of the sail

$$-\mu\, U \int_{-\ell}^{+\ell} [\Phi]_-^+ \, |y|\, dy = \mu\, U \int_{-\ell}^{+\ell} \Gamma(y)\, |y|\, dy = 2M, \tag{36.2}$$

where M is the moment exerted by the sail about the x axis, this moment is reckoned positive with a right hand screw in the negative x direction.

By (36.1) and (36.2) and because $\Phi_o = 0$, we find for the necessary condition (30.12) for minimum energy losses or what is the same for minimum induced resistance

$$\frac{\partial}{\partial n}\Phi(y,z) = \lambda_1 + \lambda_2 |y| \quad , \quad |y| \leq \ell \ , \ z = 0, \tag{36.3}$$

where we absorbed some constants in the still unknown λ_1 and λ_2. This is a two dimensional Neumann problem, the x coordinate does not enter into the problem because far behind the sail the disturbance velocities are independent of x. We introduce the potential functions $\Phi_1(y,z)$ and $\Phi_2(y,z)$ by

$$\frac{\partial \Phi_1}{\partial n}(y,z) = 1 \quad , \quad \frac{\partial \Phi_2(y,z)}{\partial n} = |y| \quad , \quad |y| \leq \ell \ , \ z = 0. \tag{36.4}$$

Then

$$\Phi(y,z) = \lambda_1\, \Phi_1(y,z) + \lambda_2 \Phi_2(y,z). \tag{36.5}$$

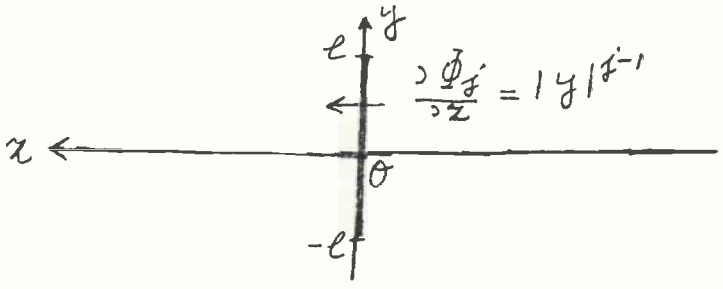

Fig. 36.2. The Neumann problem for Φ_j , $\dfrac{\partial^2 \Phi_j}{\partial y^2} + \dfrac{\partial^2 \Phi_j}{\partial z^2} = 0$, $j = 1,2$.

We have to determine λ_1 and λ_2 by the two conditions (36.1) and (36.2), this yields

$$\lambda_1 I_{10} + \lambda_2 I_{20} = \frac{-2\,T}{\mu\, U \cos\alpha} \overset{\text{def}}{=\!=} A_1, \tag{36.6}$$

$$\lambda_1 I_{11} + \lambda_2 I_{21} = \frac{-2\,M}{\mu U} \overset{\text{def}}{=\!=} A_2, \tag{36.7}$$

where

$$I_{kj} = \int_{-\ell}^{+\ell} [\Phi_k]_-^+ \, |y|^j \, dy \quad , \quad k = 1,2 \; ; \; j = 0,1, \tag{36.8}$$

we remark that $I_{11} = I_{20}$, see the exercise at the end of this section.

When we have no constraint on the heeling moment we can neglect condition (36.2) and put $\lambda_2 = 0$ in (36.3). Then we find by (36.6)

$$\tilde{\lambda}_1 = A_1 / I_{10} \, , \tag{36.9}$$

where by a "~" we denote in the following that the quantity belongs to the case of no constraint on M. Then from (36.7) it follows that the moment becomes

$$\tilde{M} = -\frac{\mu}{2} \, U \, A_1 \, \frac{I_{11}}{I_{10}} \, . \tag{36.10}$$

The constraint on the moment M will now be put in the form

$$M = \nu \, \tilde{M} \tag{36.11}$$

where ν denotes the fraction of the moment in the unrestricted case, which is tolerated, so in practice $\nu \leq 1$. Hence by (36.7) and (36.10),

$$A_2 = \nu \, A_1 \, \frac{I_{11}}{I_{10}} \, . \tag{36.12}$$

Next we calculate the kinetic energy per unit of length in the x direction, this is equal to the induced resistance R_i of the sail hence

$$R_i = \frac{\mu}{2} \int_{-\ell}^{+\ell} \frac{\partial \Phi}{\partial n} \, [\Phi]_-^+ \, dy. \tag{36.13}$$

Substitution of (36.5) in (36.13) and expressing λ_1 and λ_2 by means of (36.6) and (36.7) into A_1 and A_2, where A_2 in turn can be expressed in ν by (36.12) yields after an elementary reduction,

$$R_i = \frac{\mu}{2} \frac{A_1^2}{I_{10}} \{1 + \frac{I_{11}^2}{D} (1 - \nu)^2\}, \qquad (36.14)$$

where $D = (I_{10} I_{21} - I_{11}^2)$. The induced resistance $\tilde{R}_i$ for no constraint on M is found from (36.14) by putting $\nu = 1$. In this way we find

$$R_i = \tilde{R}_i \cdot \{1 + \frac{I_{11}^2}{D} (1 - \nu)^2\}. \qquad (36.15)$$

The dimensionless factor of $(1 - \nu)^2$ can be found by a numerical computation and becomes $I_{11}^2/D = 8{,}07$. Formula (36.15) shows explicitly by which factor the induced resistance increases by putting a constraint on the heeling moment M of the sail.

In figure 36.3 we have given numerical results for the circulation distribution $\Gamma(y)$ around the sail for some prescribed thrust. This has been done for several constraints on the heeling moment $M = \nu \tilde{M}$, first $\nu = 1$ hence no constraint, second $\nu = 0{,}4$ and third $\nu = 0$ hence the heeling moment is zero.

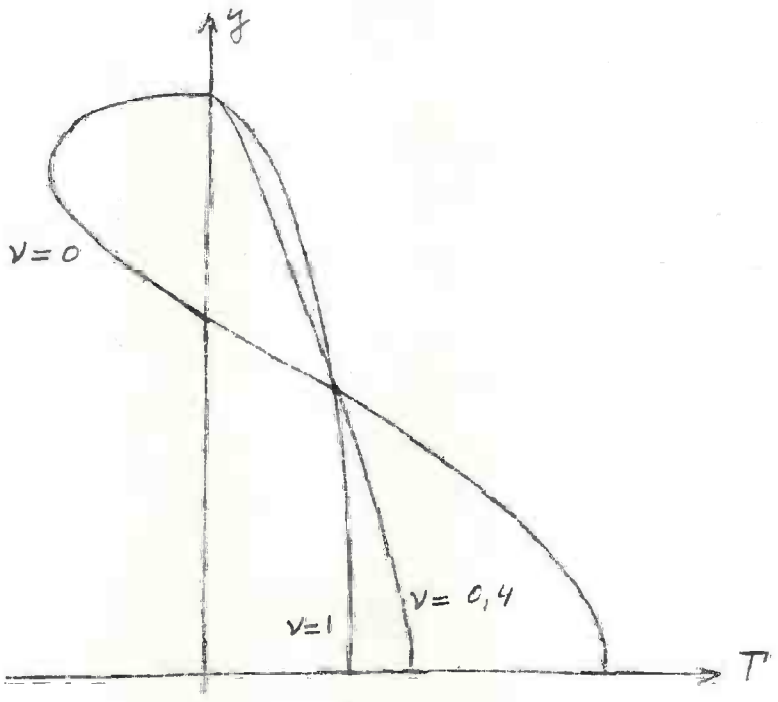

Fig. 36.3. Some circulation distributions $\Gamma(y) = -[\Phi]^+_-$ around the sail, for a fixed thrust T and different constraints on the heeling moment $M = \nu \tilde{M}$.

We remark that when we consider a more realistic theory for a sail of a yacht, we have to consider sail and keel in their reciprocal relation. This means that the constraint on the heeling moment of the sail is determined

by the action of the keel. In the case of sailing close to wind the theory becomes, although not essentially, somewhat different because the thrust T can be only of $O(\varepsilon^2)$. We refer for more general information for instance to [13], [14] and specifically for optimization problems to [27].

Exercise.

Consider two Neumann problems of the type described by figure 36.2, for the potential functions $\Psi_i(y,z)$ $i = 1,2$, with boundary conditions

$$\frac{\partial \Psi_i}{\partial z} = h_i(y) \quad , \quad |y| \leq \ell \ , \ z = 0. \tag{36.16}$$

Proof that the functions Ψ_1 and Ψ_2 satisfy the relations

$$\int_{-\ell}^{+\ell} [\Psi_1]_-^+ h_2(y)\, dy = \int_{-\ell}^{+\ell} [\Psi_2]_-^+ h_1(y) dy. \tag{36.17}$$

37. Classes of lifting surface systems

Up to now we have introduced lifting surface systems and have discussed their optimization. The reference surfaces H_i were given and we had to determine the circulation distribution of the wings W_i moving along them in such a way that certain constraints were satisfied and the kinetic energy left behind per unit of time is minimum. Next we will give more freedom to the admitted lifting surface systems, to this end we first introduce classes of these systems. We use the notations of section 28.

A class of periodically moving systems consists of all those which meet a certain number of conditions. We have two principal conditions which systems belonging to one class have to satisfy always. First, they have to have the same mean velocity of advance and second they have to have the same working area, as it was defined at the end of section 28. Besides these conditions we have to prescribe which force actions have to be delivered by the system. This can be done in exactly the same way as in section 29 where we introduced constraints by (29.9), of course the same caution has to be taken that these conditions are not contradictory.

Additional conditions, with respect to the geometry of the reference surfaces H which are admitted in the working area, can be imposed. For instance we can impose the constraint that the normal on these surfaces makes an angle with the x axis which is smaller than or equal to a prescribed value. This means that the surfaces H are not allowed to be too steep.

We now define the concept of an optimum wing system with respect to a class. This is a system which leaves behind the greatest lower bound of the kinetic energy losses of the systems of that class.

Not each class has optimum wing systems. When we consider for instance the class of screw propellers with prescribed diameter D, velocity of advance U, thrust T, number of blades m and a not prescribed but finite rotational velocity, this will happen. The reason is, as we will see later on, that the kinetic energy can always be lowered when it is possible to increase the rotational velocity. Hence no finite rotational velocity can appear as the result of an optimization process and hence there is no optimum propeller in this class. Of course the foregoing only holds in our linearized theory when viscosity and or cavitation is neglected.

We next consider a class of lifting systems for which the period of the motion is prescribed, its working area, mean velocity of advance and the mean value of the force action. No other conditions are imposed on this class

which will be denoted by C. Suppose we choose a set of reference surfaces H_k which are compatible with C, this means they are within the working area A and have the right period. Then we can find an optimum wing system W for those H_k by the methods described before. This system belongs to C. It is not necessary that W is an optimum system for C because in general we will need other surfaces H_k for that. Choose another set $\tilde{H}_k$, which is also compatible with C and look at the combined set of surfaces H_k and $\tilde{H}_k$. Again we can find an optimum wing system W^* by our previous method which now belongs to H_k and $\tilde{H}_k$. This system also belongs to C and again it need not to be optimum with respect to C.

Now we have the following important criterion. When for each combination of a fixed set H_k with other $\tilde{H}_k$ no free vorticity is needed in the optimum case on the set $\tilde{H}_k$, it is clear that the set H_k itself is able to yield an optimum wing system of the class C.

Blade systems which are optimum with respect to a class C of the type discussed above, will be called ideal. The reason is that, given their mean velocity of advance, their working area and their mean force action, there are no systems which have a higher efficiency. Hence they are the best that can be constructed, any how in the realm of a linearized potential theory. In the next section we will apply these considerations and especially the above mentioned criterion to the actuator disk with a constant pressure jump or force field and prove that indeed it is ideal.

38. The ideal propeller

Consider in the (y,z) plane the circular region $y^2 + z^2 \leq R^2$. This area is assumed to be the working area of a class of lifting surface systems C as discussed in the previous section. The lifting surface system has a velocity of advance U and has to deliver a mean value of thrust T. We will construct an ideal propeller for this class C.

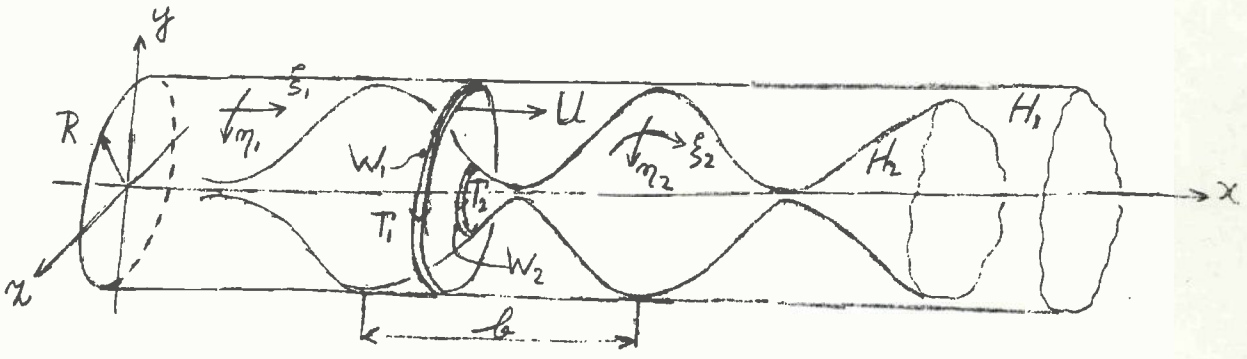

Fig. 38.1. A possible "realization" of an ideal thrust producing system.

A set of two reference surfaces H_1 and H_2 can be used for this purpose. The surface H_1 is the cylinder which is the boundary of the working region

$$H_1(x,y,z) = y^2 + z^2 - R^2 = 0. \tag{38.1}$$

The surface H_2 is more complicated. First it is periodic in the x direction with period b and rotationally symmetric around the x axis. Second it contracts up to the x axis, then expands up to the surface H_1, then contracts again and so on.

The condition for the perturbation potential $\Phi(x,y,z)$ far behind this propeller is in accordance with (30.12), because $\Phi_o \equiv 0$ and we have only to deliver a thrust,

$$\frac{\partial}{\partial n} \Phi(\xi,\eta) = \lambda_1 \cos_{(n,x)}(\xi,\eta), \tag{38.2}$$

where (ξ,η) is any point on H_1 or H_2. As before this potential can be created by translating the two reference surfaces H_1 and H_2, as rigid and impermeable surfaces with the velocity λ_1 in the positive x direction or what is the same by placing them in a parallel flow of velocity λ_1 in the negative x direction. The vorticity needed on H_1 and H_2 then is the free vorticity left behind by the optimum propeller. The constant λ_1 follows again from the condition that the mean value of the thrust has to be T.

It is clear that when H_1 and H_2 are placed in a flow parallel with the x axis, no velocity inside H_1, hence inside the working region will occur. This means that H_2 will not carry any free vorticity. Outside H_1 we have the undisturbed parallel flow, hence the vorticity on H_1 is constant and perpendicular to the x axis.

We now consider two circular wings W_1 and W_2 of variable diameter moving in the neighbourhood of H_1 and H_2 respectively. Assuming without restricting generality, that their chord lengths are very small, we represent them by two circular bound vortices Γ_1 and Γ_2. For simplicity we assume that the velocity of Γ_1 is U and that the velocity of Γ_2 along H_2 is such that it remains in the plane of Γ_1. This bound vortex system is not unique at all, however we choose some realization.

The thrust is entirely delivered by Γ_2 because Γ_1 cannot produce a force in the x direction. The working is as follows. Γ_1 increases linearly with time, hence it sheds the optimum vorticity which is constant at H_1. This however cannot go on indefinitely because then the strangth of Γ_1 would increase beyond all bounds and the propulsion system would not be periodic. It is here that Γ_2 appears on the stage. First it may not leave behind any vorticity inside H_1. Hence its strength has to be constant at parts of H_2 which are not at the x axis or at H_1. However when Γ_2 has to deliver a thrust it must have opposite signs at the different slopes which H_2 forms with the x axis. When Γ_2 arrives at the contact circle of H_2 with H_1, it changes sign instantaneously and leaves behind a concentrated free vortex at H_1. However when Γ_1 changes magnitude at exactly the same place it can cancel this concentrated free vortex. By this change however Γ_1 need not to grow beyond all bounds. The bound vorticity Γ_2 can also change sign at the points where H_2 touches the x axis because there its length is zero and hence no concentrated free vorticity is left behind. In figure 38.2 we have drawn the strength of Γ_1 and Γ_2 as a function of x. We note that never we may leave behind concentrated free vorticity, because the kinetic energy around a concentrated vortex is infinite. Hence the efficiency would be zero.

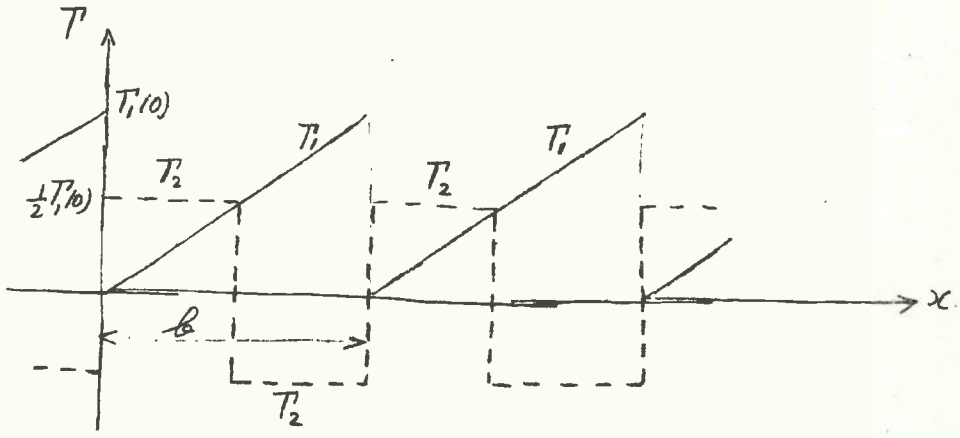

Fig. 38.2. Bound vorticity Γ_1 and Γ_2 as a function of x.

From the construction it follows that this propulsion device is ideal in the sense of the previous section. When any other reference surface H_3 is added inside H_1, it will not get any vorticity on it by the optimization procedure. Hence the free vorticity behind the supplemented propeller will be the same as before. This means that the efficiency of the original one cannot be raised. We remark that the surface H_2 is not unique at all, each surface which divides the interior of H_1 into disconnected parts could be used.

When we look at the free vorticity which is left behind by our ideal propeller, we see that it is exactly the same vorticity as is left behind by the actuator disk with a constant load, described by a linear theory(section 11). This means that both systems must have the same efficiency. However the system described here has the highest possible efficiency in comparison with each system of lifting surfaces with the same thrust, mean velocity of advance and working area. Hence also the efficiency (11.8) of the actuator disk yields an upperbound for any conceivable propeller of the class C under consideration. It is also the smallest upperbound because, as is discussed in this section, it yields the efficiency of some admitted bound vortex system.

Exercises

1. Consider the class C of the previous section for wings which have to deliver a lift force L in the y direction (figure 38.1), have a velocity of advance U and have the working region of which the boundary is given by (38.13). Determine explicitly the circulation distribution for an ideal ring wing of this class.

2. Consider the case of a working region defined by $-\infty < x < +\infty$, $|y| \leq a$, $|z| \leq b$. Discuss an ideal propeller in this case, consisting of a number of concentrated straight bound vortex lines of finite length. Describe a possible motion of these vortex lines and in which way their strength has to vary.

39. On a semi-linear optimization theory

In this section we discuss the optimization of lifting surface systems again acting in an unbounded, incompressible and inviscid fluid. The difference with the previous theory is that now the disturbance velocities induced by the devices are finite ($0(\varepsilon^0)$), however we assume that the free vorticity shed by them is small of $0(\varepsilon)$. This means that we can split the motion, which is also in this case assumed to be periodic, into two parts. First a periodic base motion which will be such that no free vorticity is shed. This motion may induce velocities of $0(\varepsilon^0)$, which have to be determined by numerical means and are assumed to be known. Second, an "added motion" with the same periodicity as the base motion and superimposed on it, which induces added disturbance velocities of $0(\varepsilon)$ and causes free vorticity of $0(\varepsilon)$ to be shed. Because the base motion cannot be described by a linear theory we use the term semi-linear optimization theory.

We consider a system of possible flexible lifting surfaces and bodies moving together periodically through the fluid. The mean direction of the motion is in the positive x direction of a Cartesian coordinate system which is at rest with respect to the undisturbed fluid. The spatial period along the x axis is b. We make the restriction that one of the following cases occurs; either the system has finite dimensions or all the lifting surfaces and bodies are cylinders with generators parallel to the y axis, so that a two dimensional problem is at hand.

Further we restrict ourselves for the three dimensional case to a prescribed mean value, with respect to time of the force exerted by the system on the fluid or to the mean value of its moment around the x axis. For the two dimensional case we restrict ourselves to the mean value with respect to time of the force per unit of length of span. These force actions are assumed to be $0(\varepsilon)$.

First consider the system under consideration moving without shedding vorticity. This means that it carries out the base motion. We keep in view the fluid particles which have passed the trailing edges of the lifting surfaces, these lie on surfaces H_k, which belong to the lifting surface W_k. When we look in the neighbourhood of the W_k the shape of these surfaces will be influenced strongly by the base motion. However when the W_k advance further in the x direction, the H_k will become more periodic and ultimately when the W_k are at infinity they are periodic with period b in the x direction.

Now we introduce the added motion and suppose, for the time being, that it is already the optimum one. We have free vorticity shed of $0(\varepsilon)$, which by the linearity of the theory will stay at the H_k and ultimately become periodic with period b in the x direction when the W_k are sufficiently far away.

Next we put at the surfaces H_k, far behind the wings W_k, bound vorticity of strength $-\Gamma_k(\xi_k,\eta_\xi,t)$ $(0(\varepsilon))$ where ξ_ξ and η_k are again suitable coordinates on the H_k. This vorticity moves along the H_k with the same mean velocity in the positive x direction as the W_k. Its strength will be such a function of time and position that the free vorticity it leaves behind annihilates the free vorticity shed by the W_k. This means that the system consisting of the W_k and the $-\Gamma_k$ does not leave behind free vorticity, hence we can apply the results of section 2.

Consider for instance in the three dimensional case the mean value of the thrust in the x direction to be prescribed. From the statement under formula (2.3) it follows that bound vorticity of strength $+\Gamma_k(\xi_\xi,\eta_\xi,t)$, moving in the same way as the aforementioned bound vorticity $-\Gamma_k(\xi_k,\eta_k t)$, hence far behind the wing system exerts the same mean force with respect to time on the fluid as the original system and leaves behind the same free vorticity.

We assume that the propulsive system W_k is connected to a large body which has to be propelled and which moves with uniform velocity U. The possibly time dependent thrust T(t) of the system delivers per period an amount of useful work equal to

$$U \int_0^{b/U} T(t)\, dt. \tag{39.1}$$

However because the concentrated bound vortex system $+\Gamma_k(\xi_\xi,\eta_\xi,t)$, has the same mean value of the thrust with respect to time, it yields the same amount of useful work per period. This means that, because both systems leave behind the same free vorticity and hence the same kinetic energy, their efficiencies are equal. In this way the vorticity $+\Gamma_\xi(\xi_\xi,\eta_\xi,t)$ is equivalent to the original system.

By the foregoing we arrive at the important result that instead of the original system we can optimize the system of bound vortices moving along periodical surfaces H_k under the constraint of a prescribed value of the mean thrust. This is however a special case of the problems discussed in sections 28 - 30.

For the three dimensional case we can treat equally well conditions for a mean force in the y or z direction, or for a moment about the x axis. A non zero mean force of $0(\varepsilon)$ per unit of span in the y or z direction for the two dimensional case is without interest. This can always be obtained without energy losses by a constant circulation around the cylinders.

From what has been discussed it is clear that we can calculate the energy losses of the wing system by looking at the ultimately periodic surfaces H_k far behind the wing system, which in some cases are not difficult to calculate by numerical means. This facilitates calculations to a high extent.

It is not possible in general in our case to calculate the energy losses by looking at the pressure distribution around the wing system. An apparent way would seem to calculate by means of the pressure distribution at the wing system the energy supplied to it and subtract the useful work. Now the induced velocities are accurate up to and including $0(\varepsilon)$ and hence also the pressures have the same accuracy. Because the amplitude of the motion is finite, there is an inaccuracy in the power of $0(\varepsilon^2)$. However the kinetic energy left behind per unit of time is also of $0(\varepsilon^2)$. Hence no correct answer can be expected by such a computation.

Exercise.

Discuss how from the optimum free vorticity far behind in the wake, the vorticity on the wing system itself can be calculated.

40. Two examples

a) First we consider as an example of the method of the previous section, a periodically moving rigid profile of finite chord length which is described as regime ii in section 21. We use the notations of that section and consider the special case of an infinitely thin and flat profile.

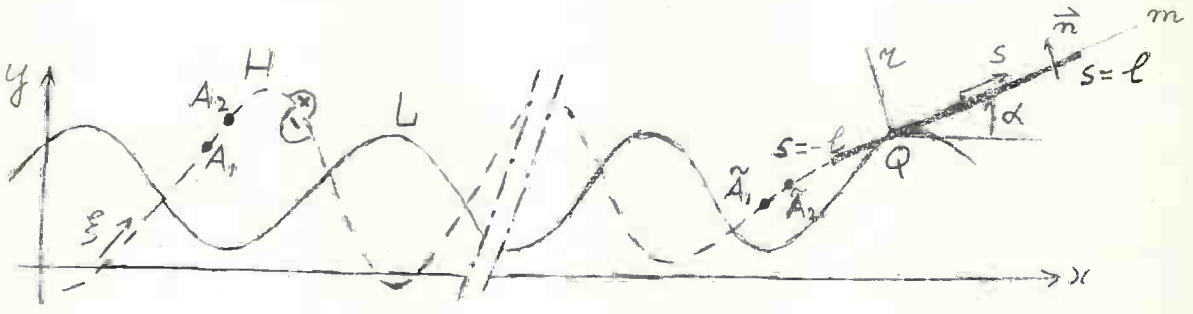

Fig. 40.1. Flat profile moving along L.

Along the flat profile we have a length parameter s (figure 40.1) which is zero at the midpoint of the profile, at the leading edge $s = \ell$ and at the trailing edge $s = -\ell$. The direction m is of course the direction of the profile itself. Now we have to determine one point Q (figure 21.2) of the line r. We look for a point Q lying on the profile and denote its parameter value s by a. When we rotate the profile around Q with rotational velocity ω, the velocities of the points of the profile are in the direction of the normal $\vec{n}$ and amount to

$$v_n(s) = \omega(s - a). \tag{40.1}$$

The vorticity $\Gamma(s)$, needed on the profile in order that the fluid flows along it, satisfies

$$v_n(s) = \frac{1}{2\pi} \oint_{-\ell}^{+\ell} \frac{\Gamma(\sigma)}{(s - \sigma)}\, d\sigma. \tag{40.2}$$

The solution of this equation which satisfies the Kutta condition at the trailing edge $s = -\ell$, is

$$\Gamma(s) = 2\omega(a + \ell - s)\sqrt{\frac{\ell + s}{\ell - s}}. \tag{40.3}$$

The condition that the total circulation is zero yields

$$\int_{-\ell}^{+\ell} \Gamma(s)\, ds = \pi\omega\, \ell\, (\ell + 2a) = 0, \tag{40.4}$$

hence

$$a = -\ell/2. \tag{40.5}$$

This means that Q is the well-known three quarter chord point. Hence when a flat profile moves with its three quarter chord point along an arbitrary line L and is tangent to L, then its total circulation is zero while its vorticity has the form

$$\Gamma(s,t) = \dot{\alpha}(t)\ (\ell - 2s)\sqrt{\frac{\ell + s}{\ell - s}}\ . \tag{40.6}$$

When the periodic line L is prescribed and also the periodic velocity with which the plate moves along L, at each moment we can calculate $\dot{\alpha}(t)$ and hence $\Gamma(s,t)$. Then by the law of Biot and Savart for the two dimensional case we can calculate the velocity of each fluid particle, we find

$$\dot{x}(t) = -\frac{\dot{\alpha}}{2\pi} \int_{-\ell}^{+\ell} \frac{(\ell - 2s)\sqrt{\frac{\ell + s}{\ell - s}}\ \{y - y_Q - (s + \ell/2)\sin\alpha\}}{R^2}\, ds, \tag{40.7}$$

$$\dot{y}(t) = +\frac{\dot{\alpha}}{2\pi} \int_{-\ell}^{+\ell} \frac{(\ell - 2s)\sqrt{\frac{\ell + s}{\ell - s}}\ \{x - x_Q - (s + \ell/2)\cos\alpha\}}{R^2}\, ds, \tag{40.8}$$

where

$$R^2 = \{x - x_Q - (s + \ell/2)\cos\alpha\}^2 + \{y - y_Q - (s + \ell/2)\sin\alpha\}^2, \tag{40.9}$$

and $x_Q(t)$ and $y_Q(t)$ are the coordinates of the point Q. This is a system of two coupled ordinary differential equations for the path $x = x(t)$, $y = y(t)$ of a fluid particle.

We now define the motion of the wake H of our profile. A point $\bar{x}$, $\bar{y}$ belongs to the wake if there exists a solution of (40.7), (40.8) with

$$\bar{x} = \bar{x}(\bar{t})\ ,\ \bar{y} = \bar{y}(\bar{t}) \tag{40.10}$$

and if there exists a $t' \leq \bar{t}$ such that $\bar{x}(t')$ and $\bar{y}(t')$ are the coordinates of the trailing edge at the moment t'. In words, the wake consists of all those fluid particles which once have been in contact with the profile and hence have left it at the trailing edge.

It is not difficult to solve by numerical means the equations (40.7) and

(40.8) for a particle which at $t = t_j$, leaves the trailing edge. By doing this for a large number of t_j, $j = 1, \ldots, N$, regularly distributed over one time period of the motion the wake H (figure 40.1) can be calculated. For the motion of the profile which has zero circulation and which is the base motion as discussed in section 21 and the previous section, this wake has no relevant physical meaning. When the profile has to deliver a nonzero mean value of the thrust, however, its added motion sheds free vorticity of $0(\varepsilon)$ which is assumed to be situated at the wake as defined.

Next the optimization of the free vorticity at the wake can be carried out as discussed in the previous section hence using condition (30.12) with respect to the thrust

$$\frac{\partial \Phi(\xi)}{\partial n} = \lambda_1 \cos_{(n,x)}(\xi), \tag{40.11}$$

where ξ is a length coordinate along the wake H (figure 40.1). Having solved numerically this Neumann problem for $\lambda_1 = 1$, we have to determine λ_1, by (29.8). Then we know the optimum free vorticity infinitely far behind the profile.

The next step is to calculate numerically the density of the vorticity behind the profile at any place. This can be done as follows. Consider far behind the profile two points A_1 and A_2 close together at H. Suppose the density of the free vorticity at that place is

$$\gamma(\xi) = \frac{\partial \Phi^+}{\partial \xi}(\xi) - \frac{\partial \Phi^-(\xi)}{\partial \xi}, \tag{40.12}$$

where $\gamma(\xi)$ is reckoned positive with a right hand screw in the direction of a rotation of the y axis to the x axis. The points A_1 and A_2 can be traced backwards to a time they were still at a finite distance behind the trailing edge $\tilde{A}_1$, $\tilde{A}_2$. Then the free vorticity at that place becomes

$$\tilde{\gamma} = \frac{|A_1, A_2|}{|\tilde{A}_1, \tilde{A}_2|} \cdot \gamma, \tag{40.13}$$

where $|\ ,\ |$ is the distance between the denoted points.

The last step is to determine the added motion which can be defined by the angle $\beta(t)$ which is $0(\varepsilon)$, which has to be added to $\alpha(t)$. We denote the normal component of the velocity induced by the wake by $\tilde{v}_n(s,t)$, where s is the parameter on the profile. This is by our optimization process and by the calculation of the free vorticity at a finite distance behind the profile a known function of s and t. Then when $\tilde{\Gamma}(\sigma,t)$ is the vorticity at the plate we have the following two equations

$$\{\tilde{v}_n(s,t) + \dot{\alpha}(t)(s-a)\} + \beta(t)\,U(t) + \dot{\beta}(t)(s-a) = \frac{1}{2\pi}\int_{-\ell}^{+\ell} \frac{\tilde{\Gamma}(\sigma,t)}{(s-\sigma)}\,d\sigma, \qquad (40.14)$$

$$\frac{d}{dt}\int_{-\ell}^{+\ell} \tilde{\Gamma}(\sigma,t)\,d\sigma = U(t)\,\tilde{\tilde{\gamma}}(t), \qquad (40.15)$$

where $\tilde{\tilde{\gamma}}$ is the density of the free vorticity at the trailing edge and U(t) the velocity of Q along H. Equation (40.15) states that the circulation along a contour which surrounds the profile and floats with the fluid has to be constant. From these equations we have to solve $\beta(t)$ and $\tilde{\Gamma}(\sigma,t)$, then our semilinear optimization problem is solved. We remark that in the last two equations we can subtract from $\tilde{\Gamma}(\sigma,t)$ the $0(\varepsilon^0)$ part (40.6) when we neglect in (40.14) at the left hand side the term $\dot{\alpha}(t)\,(s-a)$.

b) As a second example we consider the large hub propeller, which is also discussed in [1] from a more practical point of view. We assume that the hub induces disturbance velocities of $0(\varepsilon^0)$ and that the prescribed thrust T to be delivered by the blades is $0(\varepsilon)$. For simplicity these blades are assumed to be infinitely thin. The base motion of this system is a rotation around

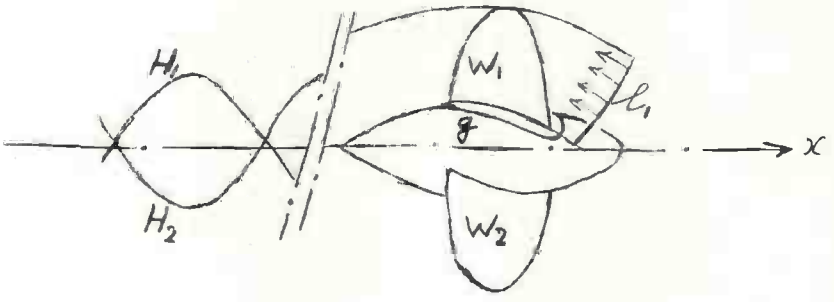

Fig. 40.3. The two bladed, large hub propeller.

the x-axis with a constant angular velocity ω, while it moves forward with a constant velocity U. We suppose that in the base motion the blades do not disturb the flow around the hub. This can easily be achieved. Choose some line ℓ_1, which is not necessarily straight, connected to the hub, which moves with the hub and remains in the same relative position. The paths of the particles of fluid which cut the line ℓ_1 form a more or less helicoidal surface H_1. When the blade W_1 is part of this surface, then it does not disturb the fluid flow around the hub. In the same way the other blades can be formed.

As the base motion plus the added motion we define the motion of a large-hub propeller with the same rotational velocity and velocity of advance as before, which however deviates geometrically as well for the blades as possibly for the hub, from the original one by $0(\varepsilon)$.

Now the theory of the previous section says that the free vorticity shed by the optimum propeller can be found by optimizing bound vorticity far behind the propeller, moving along the surfaces H_i (figure 40.3) which are formed by the particles that have passed along the blades. As we have seen the optimum free vorticity on the H_i can be found by translating them as rigid and impermeable surfaces in the x direction with some velocity λ_1 (31.3). The unknown factor λ_1 follows again from the prescribed total thrust T.

It is clear that no concentrated vortex exists at the x axis which is the line in common of the surfaces H_i, otherwise the efficiency of the system would be zero. From this follows the important conclusion that in the optimum case the circulation around the blades along some contour g (figure 40.3) is zero at their roots.

We draw the attention to the essential difference between this hub of finite length and the infinitely long cylindrical hub of section 3.1. There the vorticity shed by the root of the blade at the cylinder never enters freely the fluid and hence the circulation at the root of the blades need not to be zero. Hence from this point of view an infinitely long hub is rather poor approximation which conceals some interesting phenomenas.

Exercises.

1. Calculate the total force and the total moment acting on the flat profile in the base motion, when the vorticity is given by (40.6). For the suction force at the leading edge use (23.20).

2. Show that the added motion in the case of the profile is not unique to realize the optimum propulsion, discuss another possibility which is also optimum.

3. Discuss in the case of the large hub propeller, in which way the profiles of the blades follow from the known optimum free vorticity far behind the propeller. This can be done most easily by also changing the shape of the hub by deformations of $0(\varepsilon)$, by which the hub is no longer rotationally symmetric. When the hub is kept rotationally symmetric it will induce velocities on the blades because the normal component of the velocity at its surface has to remain zero.

4. Give an analogous reasoning for the large hub propeller for the case that the blades have finite thickness ($0(\varepsilon^0)$), however possess a sharp trailing edge. Again the thrust T is assumed to be of $0(\varepsilon)$.

41. Existence of optimum propellers

Questions of existence of optimum propulsion systems are rather delicate. We confine ourselves to the three regimes described in section 21, which we will discuss successively. These discussions will not at all be exhaustive because several of the problems connected with them have not been solved up to now.

We start with regime i. In order not to get lost into too much generality we will consider the case of only one lifting surface W which has to deliver a prescribed mean value T of the thrust.

When the reference surface H is prescribed the calculation of the optimum free vorticity is not difficult by numerical means. We have to solve a Neumann problem of which the solution from the point of view of applied mathematics can be found for instance by finite difference methods, then the existence seems to be assured.

A more complicated situation arises when the reference surface H is not fixed, hence when we consider a class of lifting surfaces. For instance we assume a working region $-\infty < x < +\infty$, $|y| \leq a$, $|z| \leq \ell$ and because we want

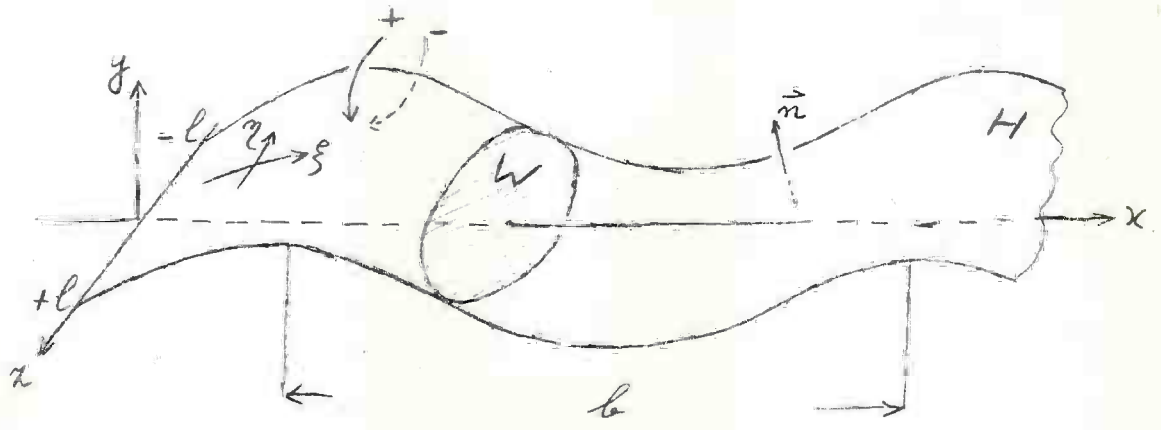

Fig. 41.1. Large amplitude flexible wing, regime i.

to have some more or less technically realizable reference surface we put constraints on the slope, curvature and some higher order partial derivatives. The spatial period will be b in the x direction. We consider a space of admissable reference surfaces H of the representation

$$y = g(x,z) \quad , \quad |z| \leq a. \tag{41.1}$$

The space of all such continuous functions with continuous partial derivatives upto and including the second order, will be denoted by G. As a norm we introduce

$$\|g\| = \max_{\substack{0 \le x \le b \\ |z| \le \ell}} (|g|, |g_x|, |g_z|, |g_{xx}|, |g_{xz}|, |g_{zz}|) \tag{41.2}$$

This space is complete which means that for each Cauchy sequence $\{g_m\} \in G$ there consists a $g \in G$ with

$$\lim_{m\to\infty} \|g_m - g\| \to 0. \tag{41.3}$$

Next consider the subset $F \subset G$ consisting of elements $g \in G$ which have continuous third order partial derivatives with

$$|g| \le A_1,\ |g_x| \le A_2,\ |g_z| \le A_3,\ \ldots,\ |g_{xzz}| \le A_9,\ |g_{zzz}| \le A_{10}. \tag{41.4}$$

Then it can be shown that F is relatively compact, by which is meant that the closure $\bar{F}$ of F is compact.

On F we define the functional E which is the kinetic energy left behind per period b in the x direction when the lifting surface W moves along some H ($y = g(x,z)$) in an optimum way and delivers a mean thrust T, This functional can be expressed as follows.

Denote by $\Phi_1 = \Phi_1(x,y,z)$ the velocity potential which belongs to the Neumann problem

$$\frac{\partial \Phi_1}{\partial n}(\xi,\eta) = \cos_{(nx)}(\xi,\eta), \tag{41.5}$$

where (ξ,η) is a point at H. Suppose $\Phi = \lambda_1 \Phi_1$ belongs to the optimum wing when W delivers the mean thrust T. Hence (33.3)

$$\frac{\mu U}{b}\ \lambda_1 \int_{H_b}\int [\Phi_1(\xi,\eta)]^+_-\ \cos_{(nx)}(\xi,\eta)\,d\sigma = T. \tag{41.6}$$

The lost kinetic energy E can by (41.5) and (41.6) be written as

$$E = \tfrac{1}{2}\mu\ \lambda_1^2 \int_{H_b}\int [\Phi_1]^+_-\ \frac{\partial \Phi_1}{\partial n}\,d\sigma = \frac{b^2T^2}{2\mu U^2}\ \left\{\int_{H_b}\int [\Phi_1(\xi,\eta)]^+_-\ \cos_{(nx)}(\xi,\eta)\,d\sigma\right\}^{-1}. \tag{41.7}$$

From the point of view of applied mathematics there seems to be little doubt that the integral at the right hand side of (41.7) is a continuous functional for the norm (41.2) on G. In fact consider two surfaces H and $\tilde{H}$ represented by two equations $y = g(x,z)$ and $y = \tilde{g}(x,z)$, then to each of these surfaces belongs lost kinetic energy E and $\tilde{E}$ in the optimum case for the same T and mean velocity of advance U. Then it is acceptable that for fixed $g(x,z)$ and variable $\tilde{g}(x,z)$ for each ε a $\delta(\varepsilon)$ exists such that, when

$$||g(x,z) - \tilde{g}(x,z)|| \leq \delta(\varepsilon), \tag{41.8}$$

then

$$|E - \tilde{E}| < \varepsilon. \tag{41.9}$$

A rigorous proof for this statement is rather complicated and should be given for a good foundation of the theory.

Assuming this for granted we have a continuous functional E on a relatively compact subset $F \subset G$. Such a functional assumes its extremes hence also its minimum at the closure $\bar{F}$ of F. Hence G being complete this minimum is assumed for some $y = g(x,z) \in G$. This means there exists an optimum reference surface H with continuous and bounded slopes and curvatures which satisfy (41.4) upto and including A_6.

Next we shortly consider the two dimensional case of regime ii. Suppose the only condition on the line L (figure 40.2), along which the rigid profile is moving, is that it can be described by a one valued function of x and has to remain within the strip $|y| < a$. Then it is proved in [23] that we can construct a series of rather complicated lines L by which the wake, which was defined in section 40, can be made wider and wider. Then by our semi linear theory the free vorticity shed by the added motion is transported over larger and larger distances at both sides of the mean direction of motion. From our optimization theory it follows that the efficiency of such a series of motions tends to one and it is seen that no optimum can exist (see the exercises).

When we demand that the lines L, hence the base motions, have to be sufficiently smooth, then it can be proved that the efficiency, under the condition of a prescribed mean thrust T and mean velocity of advance U, cannot approach one.

At last some remarks on regime iii. When the constraints on the flexible profile $y = h(x,t)$ (22.1) are chosen too loosely no optimum profile motion will exist. It can be shown , that then profile motions can be designed which have the possibility to wriggle with sharper and sharper bends, by which the efficiency increases (theoretically), such that in the limit there is no longer a decent profile. This happens when for instance we demand only

$$|h(x,t)| \leq B, \tag{41.10}$$

hence for bounded amplitudes. When we only admit motions which satisfy a sufficient number of constraints on their partial derivatives with respect to time and place it can be proved that optimum motions do exist.

Exercises.

1,a. Consider in the semi linear theory a series of base motions, for instance in the two dimensional case, by which the wake can be made wider than any given width. Discuss that then the efficiency of the propulsion tends to one for a fixed value of the prescribed thrust T of $0(\varepsilon)$.

1,b. Discuss that when a series of base motions of a profile can be constructed for which the efficiency tends to one for fixed T, no optimum base motion can exist in the semi linear theory.

REFERENCES

1. Andrews, J.B. and Cummings, D.E., A design procedure for large hub propellers, Journal of Ship Research, 1972.

2. Betz, A., Schraubenpropeller mit geringstem Energieverlust, Kgl. Ges. Wiss. Nachrichten, Math.-phys., Heft 2, 1919.

3. Cole, G H.A., Fluid dynamics, Methuen and Co. Ltd., London, 1962.

4. Doetsch, G., Theorie und Anwendung der Laplace Transformation, Dover publications, New York, 1943.

5. van Gent, W., On the use of lifting surface theory for moderately and heavily loaded ship propellers, Thesis Delft, 1977.

6. Greenberg, M.D., Non linear actuator disk theory, Zeitschrift für Flugwissenschaften, 20, Heft 3, 1972.

7. Gröbner, W. and Hofreiter, N., Integraltafel, Teil I, II, Springer Verlag, Wien, New York, 1965.

8. van Gunsteren, L.A., Ring propellers and their combination with a stator, Marine Technology, 1970.

9. Hess, F., Boomerangs, aerodynamics and motion, Thesis, University of Groningen, The Netherlands, 1975.

10. Hough, G.R. and Ordway, D.E., The generalized actuator disk. Developments in Theoretical and Applied Mechanics. Vol. II, Pergamon Press, Oxford/London/ New York/Paris, 1965.

11. Kellog, O.D., Foundations of potential theory, Springer Verlag, Berlin, 1929.

12. Kotschin, N.J., Kibel, J.A. and Rose, N.W., Theoretische Hydromechanik, Bd. I, Akademie Verlag, Berlin, 1954.

13. Marchaj, C.A., Sailing theory and practice, Dodd, Mead and Company, New York, 1964.

14. Milgram, J.H., The analytical design of yacht sails, Trans. S.N.A.M.E., 1968.

15. Mueller, F., Recent developments in the design and application of the vertical axis propeller, Trans. S.N.A.M.E , 1955.

16. Muskhelishvili, N.J., Singular integral equations, P. Noordhoff N.V., Groningen, Holland, 1953.

17. Oosterveld, M.W.C., Wake adapted ducted propellers, Thesis Delft, 1970.

18. Prandtl, L., Beitrag zur Theorie der tragende Fläche, Z.A.M.M. 16, 1936.

19. Proceedings of Third Cal/AVLABS Symposium on Aerodynamics of Rotary Wing and V/STOL Aircraft, Vol. 1, Buffalo, N.Y., 1969.

20. Proceedings symposium "On swimming and flying in nature", Plenum Publishing Corporation, 1975.

21. Schmidt, G.H. and Sparenberg, J.A., On the edge singularity of an actuator disk with large constant normal load, Journal of Ship Research, to be published.

22. Sparenberg, J.A., Some ideas about the optimization of unsteady propellers, O.N.R symposium, London, 1976.

23. Sparenberg, J.A. and Takens F., On the optimum finite amplitude motion of a thrust producing profile, Journal of Ship Research, 1975.

24. Uldrick, J.P. and Siekmann, J., On the swimming of a flexible plate of arbitrary finite thickness, Journal of Fluid Mechanics, 1964.

25. Verburgh, P.J., Unsteady lifting surface theory for ship screws, Interim report, Hydronautics-Europe, 1965.

26. Watson, G.N., A treatise on the theory of Bessel functions, Cambridge, 1922.

27. Wiersma, A.K., On the maximum thrust of a yacht by sailing close to wind, Journal of Engineering Mathematics, 1977.

28. Wu, T.Y., Flow through a heavily loaded actuator disk, Schiffstechnik, 1962.

29. Wu, T.Y., Hydromechanics of swimming propulsion, Journal of Fluid Mechanics, 1971.

30. Wu, T.Y., Hydromechanics of swimming of fishes and cetaceans, Advances in Applied Mechanics, Vol. 12, Academic Press, New York.